Defects in TRH signaling, not thyroid hormone transport, underlie IGSF1-deficiency syndrome

By

Tanya Silander

Department of the Integrated Program in Neuroscience

Faculty of Medicine

McGill University

Montréal, QC, Canada

October, 2015

A thesis submitted to McGill University in partial fulfillment of the requirements of the degree of Master's Science (MSc)

Dedicated to

My mom, ***Maryann McDermott***

May your laughter forever lilt upon the wind,
and your spirit dance among the stars.

While you may not be here to witness my accomplishments,
I know you would be proud.

and

My family*,*

For all of your love and support
I could not have done this without you.

Table of Contents

Abstract

Pathogenic mutations in the carboxyl-terminal domain (CTD) of immunoglobulin superfamily member 1 (IGSF1, formerly known as InhBP/p120) cause IGSF1-deficiency syndrome, a novel form of central hypothyroidism. IGSF1-deficient (*Igsf1*$^{\Delta ex1/y}$) mice have demonstrably upregulated levels of thyrotropin-releasing hormone (*Trh*) mRNA in the hypothalamus, which may reflect low circulating thyroid hormones (THs) and/or impaired TH transport into the hypothalamus. Delivery of THs to the hypothalamus requires their active transport across the blood-cerebrospinal fluid barrier (BCSFB) by TH transporters, the most notable of which is monocarboxylate transporter 8 (MCT8). Here we investigated the possibility that increased *Trh* expression in the hypothalamus of *Igsf1*$^{\Delta ex1/y}$ mice was reflective of impaired MCT8-mediated TH transport across the BCSFB. We demonstrate a novel interaction between IGSF1 and MCT8 that occurs at the plasma membrane, which is specific to MCT8 as IGSF1 does not interact with the closely related MCT10. With both IGSF1 and MCT8 expressed at the apical membrane of the choroid plexus (CP), which forms the BCSFB, of wild-type mice, we suspected that IGSF1 acted as an ancillary protein to MCT8, trafficking MCT8 to the apical membrane. However, MCT8 remains apically localized in the CP of *Igsf1*$^{\Delta ex1/y}$ mice, suggesting that IGSF1 is dispensable for MCT8 subcellular localization. Furthermore, we did not detect an effect of IGSF1 on TH influx *in vitro*, nor does impaired TH transport into the hypothalamus account for increased *Trh* expression in *Igsf1*$^{\Delta ex1/y}$ mice. However, *Igsf1*$^{\Delta ex1/y}$ mice had a significantly blunted thyroid-stimulating hormone (TSH) response to hypothyroidism and exogenous TRH administration, as well as low *Trhr* expression. These results suggest that TH transport is not affected by the loss of IGSF1 in the hypothalamus, and that downregulation of TRH receptor may directly impair TRH-mediated TSH secretion.

Résumé

Les mutations pathogéniques dans le domaine de la terminaison carboxyle (CTD) du membre de la superfamille des immunoglobulines 1 (IGSF1, auparavant connu sous le nom de InhBP/p120) cause un syndrome dû à une déficience en IGSF1, une nouvelle forme d'hypothyroïdie centrale. Les souris déficientes en IGSF1 (*Igsf1*$^{\Delta ex1/y}$) démontrent un niveau élevé d'ARNm de l'hormone thyréotrope (*Trh)* au niveau de l'hypothalamus, ce qui pourrait signifier une baisse des hormones thyroïdiennes (THs) dans la circulation et/ou un problème de transport des THs vers l'hypothalamus. Pour accéder à l'hypothalamus, les THs doivent être activement transportées au travers de la barrière sang-liquide céphalo-rachidien (BCSFB) par des transporteurs de TH, dont l'un des plus important est le transporteur monocarboxylate 8 (MCT8). Cette thèse examine la possibilité qu'une augmentation de l'ARNm de *Trh* au niveau de l'hypothalamus des souris *Igsf1*$^{\Delta ex1/y}$ reflète un trouble de transport des THs au travers de la BCSFB, qui est dépendent de MCT8. Nous avons démontré une nouvelle interaction entre MCT8 et IGSF1 à la surface de la membrane cellulaire. Cette interaction est spécifique pour MCT8 car IGSF1 n'interagie pas avec MCT10 un membre rapproché de MCT8. De plus, parce que IGSF1 et MCT8 interagissent à la membrane apicale du plexus choroïde (CP), qui forme la BCSFB chez les souris de type sauvage, nous croyons que IGSF1 pourrait diriger MCT8 vers la membrane apicale des cellules. Par contre, la localisation de MCT8 à la membrane apicale demeure la même dans le CP des souris *Igsf1*$^{\Delta ex1/y}$, ce qui suggère que IGSF1 n'est pas nécessaire à la localisation de MCT8 dans le CP. Selon nos expériences qui adressent la fonction de cette interaction *in vitro*, IGSF1 n'a aucun effet sur l'influx des THs. De plus, chez les souris *Igsf1*$^{\Delta ex1/y}$ un trouble de transport des THs vers l'hypothalamus ne semble pas être responsable pour l'augmentation de l'ARNm de *Trh*.

Par contre, les souris *Igsf1*$^{\Delta ex1/y}$ ont une réponse de l'hormone thyréostimuline (TSH) diminuée lorsque que l'axe est provoqué par des niveaux bas de THs ou une administration de TRH exogène, ainsi qu'un niveau d'ARNm de *Trhr* bas. Les résultats présentés ici suggèrent que le transport des THs n'est pas affecté par la perte d'expression de IGSF1 au niveau de l'hypothalamus, et que la réduction des récepteurs de TRH pourrait directement affecter la sécrétion de TSH par TRH.

Acknowledgements

This work was made possible through the invaluable support and encouragement of my supervisor Dr. Daniel Bernard. You have been incredibly patient and understanding throughout my graduate studies, and your hard work and dedication to your students and to science will forever be an inspiration. Thank you, I could not have had a better mentor.

A special thank you to my committee members, Dr. Terry Hébert, Dr. Florian Storch, and my graduate studies mentor, Dr. Kenneth Hastings. I am truly grateful for all your advice and support throughout the years.

I would especially like to thank Dr. Samuel Refetoff, who has been a wonderful collaborator over the years, and Xiao-Hui Liao, who measured the serum hormone levels discussed within this thesis. The contributions of Dr. Heike Heuer and Denica Doycheva in scientific conversations, and their co-operation on the *in situ* hybridization experiments have greatly furthered our understanding of IGSF1 function and we are extremely grateful for their involvement.

Lab members and colleagues, past and present that have guided me throughout my graduate studies, and selflessly offered their help and resources; to you I am forever grateful. In particular, I would like to thank Beata Bak, whose initial guidance and training in the lab prepared me for the rest of my graduate studies. Xiang Zhou, who is not only the most wonderful person I have ever met, is also very much to thank for assisting in practically all of the animal work presented in this thesis. Chirine Toufaily has not only been my wonderful little post-doc, but, along with Marc-Olivier Turgeon, has saved me the gruesome task of translating the abstract into French. I have greatly enjoyed having Marc-Olivier Turgeon in the lab and I confidently leave the future of this project in his capable hands. Shahriar Khan and David Cui thank you for

your input on this thesis, I really do owe you cupcakes this time, promise. I would also like to thank Jérôme Fortin, Stella Tran, Ying Wang, Yining Li, and Luisina Ongaro for being wonderful lab mates over the years and graciously helping me in both scientific endeavours as well as keeping me sane with your lovely personalities. Also, a huge shout-out to the Hébert lab, you have always been a wonderful group of people who have been great resources both for scientific advice and materials (seriously, you have saved some of my experiments, greatly appreciated).

I would also like to thank the staff of the Department of Pharmacology, although I was not a part of the department, you have never treated me otherwise. You have graciously offered your time and support, and made me feel as though I was a part of the family, and for that I am truly appreciative. I would also like to thank the staff of the Department of the Integrated Program in Neuroscience, you all work so tirelessly to keep up with such a large department, and I appreciate all your efforts.

Finally, I would like to thank my family. My daddy, Dale Silander, has always believed in my dreams and has supported all of my endeavours. My 'little' brother, Cody Silander, who is truly my best friend and biggest fan, I love you dearly. My sister and her family, those kids keep me young while making me feel old. My grandma, for loving me despite my sporadic phone calls. And my best friend, Emily Griffiths, without your support and encouragement during our daily phone calls I am not sure I would have made it through all of this. All of you have believed in me even when I could not believe in myself. I love you all and thank you.

Funding was generously provided by the Canadian Institute of Health Research (CIHR), and the Natural Sciences and Engineering Research Council (NSERC).

List of abbreviations

ACTB	β-actin
BCSFB	Brain-CSF barrier
BHB	Brain-hypothalamic-barrier
BMI	Body mass index
BRET	Bioluminescence resonance energy transfer
BSA	Bovine serum albumin
BTUB	β-tubulin
BW	Body weight
Cas9	Caspase 9
CGA	Chorionic gonadotropin alpha
CP	Choroid plexus
CRISPR	Clustered regularly interspaced short palindromic repeats
CRYM	Mu Crystallin
CSB	Cell surface biotinylation
CSF	cerebrospinal fluid
CTD	carboxyl-terminal domain
DIO	deiodinase
EndoH	Endoglycosidase H
ER	Endoplasmic reticulum
FT4	Free T4
GFP	Green fluorescent protein
HA	Hemagluttinen
HDAC	Histone deacetylase
HEK293	Human embryonic kidney
HPT	Hypothalamic-pituitary-thyroid
HRP	Horse radish peroxidase
IF	Immunofluorescence
Ig	Immunoglobulin
IGSF	Immunoglobulin superfamily
***Igsf1*$^{+/y}$**	*Igsf1*-wild-type mice
***Igsf1*$^{\Delta ex1}$**	*Igsf1*-deficient mice
IHC	Immunohistochemistry
IP	Immunoprecipitation
i.p.	Intraperitoneal
ISH	*In situ* hybridization
KO	Knock-out (*Igsf1*$^{\Delta ex1/y}$)
LAT	L-amino acid transporter
LoI/PTU	Low iodine/propylthiouracil

MCT	Monocarboxylate transporter
miRNA	Micro RNA
NIS	Sodium/Iodine symporter
NTD	Amino-terminal domain
OATP	Organic anion transporter protein
OSCAR	Osteoclast-associated receptor
PBS	Phosphate buffered saline
PEI	Polyethylenimine
PNGaseF	Peptide -*N*-Glycosidase F
PRL	Prolactin
PVN	Paraventricular nucleus
RRE	Retinoid X receptor response element
RXR	Retinoid X receptor
SP	Signal peptidase
SPP	Signal peptide peptidase
T3	Triiodothyronine
T4	Thyroxine
TBG	Thyroxine-binding globulin
Tg	Thyroglobulin
TH	Thyroid hormone
THR	Thyroid hormone receptor
THT	Thyroid hormone transporter
TMD	Transmembrane domain
TPO	Thyroid peroxidase
TRE	Thyroid hormone receptor response element
TRH	Thyrotropin-releasing hormone
TSH	Thyroid-stimulating hormone
TSHβ	Thyroid-stimulating hormone beta
TSI	Thyroid-stimulating immunoglobulin
WT	Wild-type (*Igsf1*$^{+/y}$)

Contribution of Authors

The work in this thesis was made possible by collaborators at the University of Chicago and the Fritz-Lipmann Institute – Leibniz Institute for Age Research.

Dr. Samuel Refetoff and Xiao-Hui Liao measured serum hormone levels (Figures 3.5, 3.7 and 3.10).

Dr. Heike Heuer and Denica Doycheva conducted *in situ* hybridization of *Trh* (Figure 3.11f).

The author of this thesis performed all biological experiments and manuscript writing under the supervision of Dr. Daniel Bernard.

Manuscripts published

1. Joustra SD, Wehkalampi K, Oostdijk W, Biermasz NR, Howard S, **Silander TL**, Bernard DJ, Wit JM, Dunkel L, Losekoot M (2014). IGSF1 variants in boys with familial delayed puberty. European Journal of Pediatrics 174(5):687-692.
2. Nakamura A, Bak B, **Silander TL**, Lam J, Hotsubo T, Yorifuji T, Ishizu K, Bernard DJ, Tajima T (2013). Three novel IGSF1 mutations in four Japanese patients with X-linked congenital central hypothyroidism. Journal of Clinical Endocrinology and Metabolism 98(10):E1682-91.

Chapter 1: General Introduction

1.1. Hypothalamic-pituitary-thyroid (HPT) axis

Thyroid hormones (THs) regulate brain development[1,2], increase metabolism[3], and act as potent stimulators of cellular differentiation[4,5]. Circulating THs are tightly regulated by the HPT axis (Figure 1.1)[6–9]. Hypophysiotropic thyrotropin-releasing hormone (TRH)-expressing neurons are located in the parvocellular region of the paraventricular nucleus (PVN) of the hypothalamus and project to the median eminence[10,11]. In response to low circulating THs, TRH is produced and released into the hypophysial portal system and binds TRH receptors (TRHR) on thyrotrope cells of the anterior pituitary gland[12–16]. TRH binding to TRHR initiates a signaling cascade that induces activating post-translational modifications of thyroid-stimulating hormone (TSH) and its calcium-dependent release into the general circulation[17–23]. TSH binds the TSH receptor (TSHR) on epithelial cells of the thyroid gland, stimulating the production and release of the biologically active TH, triiodothyronine (T3) and the pro-hormone thyroxine (T4)[24–34]. THs are released from the thyroid into the circulation and are actively transported into target tissues by TH transporters (THTs)[35–44]. Within cells, T4 is deiodinated by 5' iodinases (deiodinases) into the biologically active T3, which then binds nuclear TH receptors (THRs)[45–48]. THRs translocate into the nucleus and bind DNA to regulate transcription of target genes[49–57]. THs negatively regulate their own production through negative feedback at the levels of the hypothalamus and pituitary. In response to TH, transcription of *TRH/Trh* and biosynthesis of TRH are downregulated in the hypothalamus[13,14]. In the pituitary, TH inhibits transcription of the alpha and beta subunits of TSH, *TSHB/Tshb* and *CGA/Cga*[49,58–60]. Diminished TRH secretion leads to reduced TSH activation and release, resulting in decreased TH production in the thyroid gland[17–20,61]. Regulation of general and intracellular levels of TH is crucial for proper development and

metabolic responses in animals and humans. Below, we discuss the major determinants of TH availability and intracellular action in more detail.

1.1.1. TRH/TRHR signaling

TRH is synthesized in the hypothalamus as a preprohormone encoded by the *TRH/Trh* gene, and is extensively processed to produce multiple copies of the TRH tripeptide (pyro-Glu-His-Pro-NH_2)[62–64]. Human prepro-TRH contains six copies of the progenitor TRH sequence[65], Lys-Arg-Gln-His-Pro-Gly-Arg-Lys/Arg, while the murine[63] and rat[66] prepro-TRHs contain five, each of which is flanked by basic Lys-Lys or Lys-Arg residues and linked by connecting peptides[62,64]. Prepro-TRH contains an N-terminal signal peptide, directing its co-translational translocation into the endoplasmic reticulum (ER), where signal peptidase cleaves the signal peptide to produce pro-TRH[63,65,66]. Pro-TRH is then cleaved in the secretory granules by prohormone convertases 1/3 at all dibasic residues to produce multiple copies of the precursor TRH tripeptide (Glu-His-Pro) and TRH-free connecting peptides[67]. Further sequential processing by carboxypeptidase, peptidylglycine α-hydroxylating monooxygenase, and pyroglutamyl cyclase removes the C-terminal dibasic residues, amidates the proline residue and converts the glutamine residue to pyroglutamate, respectively[68]. Mature TRH and prepro-TRH derived peptides are stored in secretory granules in axon terminals located at the median eminence and exocytosed in response to calcium influx[69]. TRH is then secreted into the hypophysial portal vessels, and binds TRH receptor (TRHR)-expressing thyrotropes[70,71], lactotropes[70,71], and somatotropes[72] of the anterior pituitary to stimulate production and secretion of thyroid-stimulating hormone (TSH)[17,18,73,74], and prolactin (PRL)[17,74–76], and growth hormone (GH) mRNA expression[17,75,76], respectively.

The TRHR is a G-protein coupled receptor (GPCR), with an extracellular amino-terminus (N-terminal), seven transmembrane helices and an intracellular carboxyl-terminus (C-terminal)[66,75,77]. TRHR couples to the G-proteins $G_{\alpha q}$ and $G_{\alpha 11}$, which mobilize intracellular calcium through phospholipase C (PLC) activity [21,71] (Figure 1.10). Binding of TRH to the TRHR induces a conformational change allowing G_{α} to exchange guanine diphosphate (GDP) for guanine triphosphate (GTP), which phosphorylates PLC and leads to PLC-mediated hydrolysis of phosphatidylinositol 4,5-bisphosphate (PIP_2)[71,78]. Hydrolysis of PIP_2 forms the second messengers diacylglycerol (DAG) and inositol 1,4,5-trisphosphate (IP_3). IP_3 is then released into the cytosol and binds IP_3-sensitive calcium ion (Ca^{2+})-channels on the smooth endoplasmic reticulum (ER), rapidly increasing cytosolic Ca^{2+} levels and activating trafficking of secretory granules to the plasma membrane where they exocytose their cargo. DAG promotes protein kinase C (PKC) translocation from the cytosol to the plasma membrane, and together with Ca^{2+}, PKC phosphorylates the pituitary-specific transcription factor Pit-1[79]. The transcription factors *c-fos* and *c-jun* are also immediate early genes of TRH stimulation, which form Activator Protein-1 (AP-1) complexes[80]. Together with AP-1, Pit-1 binds specific response elements in the promoter regions of *Tshb* and *Cga*, stimulating their transcription[81,82]. Furthermore, TRH activation of PKC and Ca^{2+} negatively regulates expression of *Trhr*[83], potentially through the recruitment of repressor proteins to the *Trhr* promoter region by Pit-1[77].

Following TRH activation of PKC and elevation of Ca^{2+} through the $G_{\alpha q/11}$ pathway, the TRHR is rapidly desensitized and internalized[84]. Desensitization of the TRHR to TRH occurs at the plasma membrane, where PLC activity declines in the continuing presence of TRH due to receptor uncoupling. PLC uncouples from the TRHR in response to phosphorylation of serine and threonine (Ser/Thr) residues in the cytoplasmic tail of TRHR by GPCR kinase 2 (GRK2).

Dissociation of TRH from the TRHR allows dephosphorylation and resensitization of the receptor, allowing it to mount a maximal response after a refractory period[85]. Internalization of TRHRs requires arrestins 2 or 3, which bind to the TRHR C-terminal tail at specific phosphorylated Ser/Thr residues. Bound arrestins contribute to TRHR desensitization, and can induce endocytosis of the phosphorylated receptor into clathrin-coated vesicles. TRH is then degraded by the TRH degrading ectoenzyme (TRDE)[86], and protein phosphatase 1 is able to dephosphorylate TRHRs at the plasma membrane and in sorting endosomes[85]. Dephosphorylated TRHRs can then repopulate the plasma membrane from the pool of recycling endosomes. Desensitization and internalization of the TRHR allows pulsatile TRH signaling and redistribution of TRHRs on the plasma membrane, respectively.

While TRH is primarily considered a potent regulator TSH activation and secretion (See Section 1.1.2), TRH also regulates *Prl* and *Gh* transcription and stimulates release of PRL in lactating mice, as indicated by PRL deficiency in *Trh*-/- mice[73]. Presumably, the mechanism by which TRH regulates *Prl* and *Gh* transcription is similar to that of *Tshb* and *Cga* as their promoter regions contain Pit-1 binding elements[76], and both lactotropes and somatotropes express TRHR[70,72].

1.1.2. TSH/TSHR signaling

TSH is a glycoprotein hormone produced by thyrotrope cells of the anterior pituitary in response to TRH and low circulating TH levels[34,59]. It is released into the circulation and subsequently binds to TSH receptors (TSHR) on thyrocytes of the thyroid gland to stimulate the production and release of THs[26,32,34,87–90]. TSH is composed of two subunits, TSHβ and CGA, encoded by the *TSHB/Tshb* and *CGA/Cga* genes[91,92]. TSHβ and CGA are co-translationally

glycosylated with one or two asparagine (N)-linked carbohydrates, respectively, which promotes proper folding of the subunits in the endoplasmic reticulum (ER) and their dimerization in the Golgi apparatus[93–95]. These N-linked high mannose sugars are further modified in presecretory granules of the Golgi to form complex carbohydrates essential for TSH stability and biological activity[23,94,96,97]. As previously mentioned, *Tshb* and *Cga* transcription are positively regulated by low pituitary TH levels. TRH has little effect on translation of TSHβ or CGA; however, TRH promotes glucosamine incorporation in both TSHβ and CGA subunits, essential for dimerization of the two subunits as well as biological activity of TSH[18,97,98]. This is demonstrated by the phenotype of *Trhr*-/- and *Trh*-/- mice, where serum TSH levels are normal or elevated in the absence of TRH signaling, indicating that TRH is dispensable for TSH secretion in central hypothyroid mice[17,73]. However, biological activity of TSH is clearly reduced as circulating TH levels are low, despite normal TSH serum levels.

Glycosylated TSH released into the circulation binds TSHRs expressed in the thyroid gland, stimulating the production of T3 and T4[87]. THs are produced by thyrocytes of the thyroid gland from the precursor, thyroglobulin (Tg) following iodine organification. Briefly, iodine is actively transported into the thyrocyte by the sodium-iodine symporter (NIS) at the basolateral membrane and diffuses into the lumen by the exchanger pendrin at the apical membrane[99]. Tg produced in the ER of the thyrocyte is released into the lumen and iodine, oxidized by thyroperoxidase (TPO) and H_2O_2, is covalently bound to tyrosyl residues of the Tg macromolecule[100]. TPO also catalyzes coupling of two iodotyrosine residues producing the prohormone T4 and, to a lesser extent, T3. Iodinated Tg is then endocytosed by the thyrocyte into endosomes which fuse with lysosomes where THs are enzymatically cleaved from the Tg backbone. Finally, THs are secreted into the circulation through active transport via the basolaterally localized thyroid

hormone transporter, monocarboxylate transporter 8 (MCT8) and other as yet unidentified THTs[101].

1.1.3. TH transport and action

Circulating THs are bound to a variety of serum proteins, which increase their solubility and prevent aggregation, with a small portion of THs circulating in 'free' or unbound form[102]. Dissociation from TH binding proteins is required for their transport into peripheral tissues, and free circulating T4 (FT4) measurements are considered an accurate diagnostic tool to assess intracellular T4 levels in a clinical setting[103]. As zwitterionic tyrosine hormones, THs are incapable of passively diffusing across the plasma membrane, and active transport by thyroid hormone transporters (THTs) is required for their influx and efflux[39]. The major THTs identified are MCT8 (refer to section 1.1.3.1 MCT8) and MCT10, as well as some organic anion-transporting proteins (OATPs) and L-type amino acid transporters (LATs). T4 is the main circulating TH and is primarily bound by thyroxine binding globulin (TBG) from which it dissociates prior to transport into target tissues[104]. Intracellular T4 is deiodinated by the deiodinases DIO1 and DIO2 to produce the biologically active T3, which binds the nuclear TH receptors (THRs) and regulates gene transcription[46,105]. Ligand-bound and unbound THRs translocate into the nucleus and bind TH response elements in the promoter regions of target genes, where they are able to recruit repressive or activating protein complexes to inhibit or enhance transcription[49,52,55]. THRs also mediate T3-dependent repression of thyroid hormone production through interactions with promoter regions of the TH-sensitive genes of the pituitary and hypothalamus[57,106,107]. In the presence of T3, THRs bind promoter regions of *TRH/Trh*, *TRHR/Trhr, TSHβ/Tshb*, and *CGA/Cga* and recruits retinoid X receptor (RXR) to inhibit their transcription through recruitment of histone deacetylases (HDACs)[50,108–110]. When T3 is

inactivated to reverse T2 by DIO3-mediated deiodination, transcription of these genes is upregulated by recruitment of nuclear co-repressor (NCoR) which acts to activate transcription by recruiting histone acetyltransferases (HATs) and transcription factor II (TFIIB)[46,56,57,108,111]. Through TH-mediated negative feedback, circulating TH levels are kept within a narrow range, which can be rapidly adjusted in response to environmental cues.

1.1.3.1.Monocarboxylate transporter 8 (MCT8)

MCT8 is a specific transporter of T3 and T4, which exhibits widespread expression in tissues such as the pituitary, liver, heart, kidney, thyroid gland, skeletal muscle tissue and throughout the central nervous system (CNS)[37,112,113]. Within the CNS, *MCT8/Mct8* mRNA expression has been observed in distinct neuronal populations of the cerebral cortex, hippocampus and amygdala, as well as in hypothalamic neuroendocrine nuclei of the PVN[35,37,42,114–119]. Furthermore, *MCT8*/*Mct8* is expressed in brain capillary endothelial cells, CP, and tanycytes, which constitute the main barriers for TH influx into the CNS[37,42,114,116–118]. Expression of MCT8 in the CP and tanycytes is particularly interesting given their role in the formation of the blood-cerebrospinal fluid barrier (BCSFB) and the BCSF-hypothalamic barrier (BHB), respectively[120–122]. Briefly, circulating T4 is actively transported into the epithelial cells of the CP by the THT OATP1C1, which is localized at both the apical and basal membranes of CP epithelium (Figure 1.2)[123,124]. The apically (ventricle-facing) localized MCT8 then transports T4 into the ventricular CSF and MCT8-expressing tanycytes, which line the floor of the third ventricle, transport T4 into the PVN of the hypothalamus[123,124]. In the PVN, T4 is deiodinated by DIO2 into the biologically active T3, which acts to inhibit *Trh* transcription[123,124].

Mice and humans deficient in MCT8 exhibit deficiencies in TH-mediated neuronal migration and differentiation, as well as hypothalamic modulation of the HPT axis[125–127]. Indeed, mutations in MCT8 underlie Allan-Herndon-Dudley Syndrome (AHDS), a rare disorder affecting approximately 10% of patients with psychomotor retardation[128]. Patients with AHDS have severe mental retardation as well as muscle hypotonia and spastic paraplegia[126,127], resulting from impaired TH expression and transport. T4 efflux by the basolaterally localized MCT8 is greatly reduced in MCT8-deficient patients and mice, leading to increased circulating T3 and low circulating T4[101]. Furthermore, uptake of T3 is impaired in some tissues expressing MCT8, including the brain, and peripheral muscle tissue as exemplified by psychomotor impairments in patients with AHDS. Impaired hypothalamic TH influx is also observed, where *Trh* mRNA expression is increased in *Mct8*-ko mice leading to increased circulating TSH levels[101,114,118,129].

1.1.4. Diseases associated with HPT axis alterations

As mentioned, the HPT axis regulates circulating TH levels within a narrow physiological range through TH-mediated expression of *Trh* and *Tshb* and TRH-mediated post-translational modifications and release of TSH. This is crucial to the development and survival of the organism as THs are necessary for neuronal migration, growth and differentiation of cells and regulation of body temperature and energy consumption through metabolic activation. Therefore, impairment in the regulation of circulating TH levels and TH action in tissues has a number of consequences. Here, we will briefly discuss the HPT axis phenotypes and physiological consequences of primary hyperthyroidism, primary hypothyroidism, and central hypothyroidism.

1.1.4.1. Hyperthyroidism

Hyperthyroidism is characterized by low serum TSH levels with high TH levels, typically associated with the autoimmune disorder, Grave's disease, which occurs in approximately 1% of the population and accounts for the majority of hyperthyroid cases[130–133]. Grave's disease is caused by aberrant release of thyroid hormones in response to thyroid-stimulating immunoglobulins (TSIs), which act through the TSHRs on the thyroid gland in an agonistic manner[134,135]. TSIs act autonomously from HPT axis regulation, resulting in weight loss, an inability to control body temperature, and rapid heart rates due to an overactive metabolism[136]. Treatments directed at impeding TH production largely rely on destroying the thyroid gland with radioactive iodine as well as inhibiting TH production[131,132]. Endogenous TH production is then replaced with exogenous TH replacement therapy.

1.1.4.2. Hypothyroidism

Primary hypothyroidism is characterized by increased serum TSH with low circulating THs, indicating impaired TH output in response to TSHR-mediated signaling at the level of the thyroid gland[137–139]. The most common cause of low circulating TH is dietary iodine deficiency, with an estimated prevalence of more than 400 million worldwide[140]. Iodine deficiency directly impedes TH synthesis despite normal TSHR signaling (see section 1.1.2. on TSH/TSHR signaling). Therefore, upregulated TSH increases TSHR signaling and results in excessive proliferation of thyrocytes in the thyroid gland (goiter) without affecting TH levels[137–141]. Primary hypothyroidism may also be caused by the autoimmune disorder, Hashimoto's thyroiditis, with a prevalence of approximately 1:2,000 persons[142]. In Hashimoto's thyroiditis, the immune system attacks the thyroid gland and directs antibodies against TPO, necessary for TH production (see section 1.1.2 on TSH/TSHR signaling)[143,144]. Leukocyte invasion of the thyroid gland increases thyroid gland size and gradually destroys the follicles. Both TPO

inactivation and follicular damage directly impede the TH response to TSHR signaling. Finally, inactivating *TSHR* mutations in four unrelated families have been identified that impair TSHR signaling and subsequent TH production without increasing thyrocyte proliferation[88,145].

Patients with primary hypothyroidism have decreased metabolic energy expenditure, which reduces resting body temperatures and leads to increased weight. Furthermore, hypothyroidism in pregnant women is detrimental to fetal development, particularly neocorticogenesis, as the fetus is dependent on maternal THs during the first trimester. Given the deficiencies in dietary iodine and selenium (necessary for DIO production) worldwide and the important role THs play in fetal neocorticogenesis, primary hypothyroidism remains the most common cause of mental retardation[146].

1.1.4.3. Central hypothyroidism

Central hypothyroidism is characterized by reduced circulating THs secondary to insufficient TSH stimulation of an otherwise normal thyroid gland[137–139]. Circulating TSH levels may be low/normal despite low circulating TH, suggestive of decreased TSH bioactivity and a consequent inability of TSH to elicit an appropriate TH response. TRH signaling confers biological activity to TSH through post-translational modifications of TSH glycosylation[26,96,97]. In the absence of TRH signaling, TSH is secreted normally, yet has a reduced ability to stimulate TH production in the thyroid gland[147,148]. Therefore, low serum TH levels in the face of normal circulating TSH is associated with defects in TRH signaling, either as a result of impaired TRH release or TRH signaling through the TRHR. Central hypothyroidism is very rare, and affects approximately 1:20,000 to 1:80,000 people worldwide[149,150]. Congenital forms of isolated central hypothyroidism are caused by inactivating mutations in the *TRHR*, *TSHB*, and *IGSF1* genes.

Patients with pathogenic TRHR mutations have decreased serum T4 levels with normal TSH secretion, indicative of impaired TRH signaling resulting in TSH that is less biologically active. Mutations in the *TRHR* have been reported in two families and span only three different mutations[74,151]. Mutations in the *TSHB* subunit gene have severely decreased TH and TSH levels due to impaired TSH subunit dimerization and mutations have been described in 5 different families throughout the world[152–154]. Recently, pathogenic mutations in the X-linked gene, *IGSF1,* have been reported in over forty non-related families with an approximate prevalence of 1:100,000 persons worldwide[149]. These mutations cause central hypothyroidism, with normal circulating TSH and low FT4 serum levels (explored in more detail in section 1.2.2 on IGSF1-deficiency syndrome)[149,155–157]. IGSF1 does not currently have a defined role in the HPT axis; however pathogenic mutations in the IGSF1 protein impair its plasma membrane expression, and IGSF1-deficient mice appear to have impaired TRH signaling[157].

1.2. Immunoglobulin superfamily

The immunoglobulin superfamily (IGSF) is an expansive family of proteins containing one or more immunoglobulin (Ig) domains, which were originally described in antibodies and later identified in proteins not associated with the immune system[158–161]. The Ig domain possesses two β-sheets composed of anti-parallel β-strands and linked by a single disulfide bond[162]. There are three main subtypes of Ig domains based on their resemblance to the variable (V-type), or constant (C-type) Ig domains in antibodies, with C1-type domains more closely resembling the C-type Ig domains, and the C2-type domains being a hybrid between the V- and C-type.

IGSF members play diverse physiological roles, with Ig domains commonly associated with cell-cell communication and interaction[158–160,163,164]. Additionally, multiple functions may be

attributed to a single IGSF member under various physiological conditions and cell types, making it difficult to pinpoint specific functions of any given IGSF member[161,165,166].

1.2.1. Immunoglobulin superfamily member 1 (IGSF1)

IGSF1 (previously known as InhBP/p120) is a single-pass transmembrane glycoprotein encoded by the *IGSF1/Igsf1* gene located on the X-chromosome of humans and other mammalian species[167–169]. *IGSF1/Igsf1* is predicted to encode 12 C2-type Ig domains, an N-terminal signal peptide, a hydrophobic linker region containing two hydrophobic domains, and a C-terminal transmembrane domain (TMD) followed by a short C-terminal tail (Figure 1.3)[168]. However, cleavage of the hydrophobic linker region during co-translational translocation into the ER separates the protein into N-terminal domain (NTD) and C-terminal domain (CTD) with 5 and 7 Ig domains, respectively, a single-pass TMD, and a short intracellular C-terminal tail (Figure 1.3)[167]. During translation, high mannose sugars (immature sugars) are attached to the asparagine residues of both the IGSF1-NTD and –CTD, promoting proper folding. The CTD is then trafficked to the Golgi apparatus where high mannose residues are converted into complex carbohydrates (mature sugars), while the NTD appears to be trapped in the ER[157,167]. The CTD is then trafficked to the plasma membrane, where the Ig domains are oriented extracellularly, with the short C-tail oriented intracellularly (Figure 1.4). The CTD is expressed primarily by thyrotrope, somatotrope and lactotrope cells of the anterior pituitary, in the apical membrane of the CP, and in the fetal liver of the mouse and rat[157,170,171].

In addition, the *IGSF1/Igsf1* mRNA is alternatively spliced, giving rise to multiple isoforms (Figure 1.5 and 1.6), differentially expressed in various tissues[168–170,172]. The *IGSF1-1/Igsf1-1, IGSF1-3* and *IGSF1-4* isoforms encode the entirety of IGSF1 as described above. Additionally,

both mice and humans express the *IGSF1-2/Igsf1-2* and humans express the additional *IGSF1-5* isoform, which encode the N-terminal signal peptide and the first two Ig domains of the NTD. Lacking a TMD, this isoform is predicted to be secreted, and has been detected in human plasma[173]; however, the function of this protein remains unknown. Importantly, the murine *Igsf1-4* isoform encodes the entirety of the CTD, with its expression under the control of an internal promoter[172]. Interestingly, the *Igsf1-4* isoform appears to be expressed at lower levels than the *Igsf1-1* isoform (Bak, B, unpublished), indicating that the upstream promoter is more active and potentially differentially regulated compared with the internal promoter. The presence of an *IGSF1-2/Igsf1-2* isoform in addition to the more active promoter may explain the evolutionary retention of the NTD despite the absence of any obvious function.

We now know that pathogenic mutations in the *IGSF1* gene result in central hypothyroidism. These mutations impair or restrict IGSF1 expression at the plasma membrane, suggesting that IGSF1 must be expressed at the plasma membrane to fulfill its functional role in the HPT axis. Several point mutations, deletions, insertions, frameshift mutations and whole gene deletions have since been identified in patients with central hypothyroidism throughout the world (Figure 1.7)[149,156,157,174–176].

1.2.2. IGSF1-deficiency syndrome

IGSF1-deficiency syndrome is a novel X-linked disorder resulting from pathogenic mutations in the *IGSF1* gene, resulting in congenital central hypothyroidism and macroorchidism[149,156,157]. A fraction of patients also present with hypoprolactinemia, GH deficiency, delayed pubertal development, and an increased body mass index (BMI). In IGSF1-deficient patients, circulating FT4 levels are reduced with non-elevated TSH, consistent with

defective TRH signaling at the central level in the absence of IGSF1[155–157,174–176]. Given the role for TRH in PRL and, to a lesser extent, GH expression and secretion, a defect in TRHR signaling may account for the variable hypoprolactinemia and GH deficiency observed in patients with IGSF1-deficiency syndrome[147,148].

1.2.3. IGSF1-deficient mice

IGSF1-deficient mice were generated by deletion of the first exon (*Igsf1*$^{\Delta ex1}$), which abolishes expression of isoforms *Igsf1-1*, *Igsf1-2*, and *Igsf1-3*[172]. However, the *Igsf1-4* isoform, which encodes the entirety of the IGSF1-CTD, is controlled by an internal promoter and is retained in *Igsf1*$^{\Delta ex1}$ mice. Expression of IGSF1-4 does not appear to be upregulated in the pituitary or brain of *Igsf1*$^{\Delta ex1}$ mice (Beata Bak, unpublished), and does not appear to be capable of compensating for IGSF1-deficiency in these mice.

Igsf1$^{\Delta ex1/y}$ mice have central hypothyroidism, with low circulating TSH levels as well as low pituitary TSH content[157]. Circulating T3 levels were reduced, but to a lesser extent than one would expect in light of the reduced TSH levels. Furthermore, circulating T4 levels were normal on average, in spite of low circulating TSH. Pituitary *Tshb* mRNA levels were also normal, indicating that TH feedback at the level of the pituitary was not affected. These results are consistent with central hypothyroidism, where serum TSH levels are inappropriately low in response to low TH serum levels. Interestingly, *Trh* mRNA expression was upregulated in the hypothalamus of IGSF1-deficient mice, while *Trhr* mRNA expression in the pituitary was downregulated[157]. Provided this is reflective of the protein expression, this is suggestive of a TRH signaling defect in *Igsf1*$^{\Delta ex1/y}$ mice, where TRH is incapable of upregulating TSH pituitary content and serum levels. Hypothalamic *Trh* mRNA expression is regulated by TH binding to

THRs in TRH-expressing neurons of the PVN, where TH influx into the PVN is largely mediated by MCT8 transport of T4 across the BCSFB into the hypothalamus (see section 1.1.3.1 Monocarboxylate transporter 8). Given that circulating TH levels were variably low, the uniform increase in *Trh* mRNA expression may be reflective of low T3 influx into the hypothalamus by MCT8. This would theoretically result in increased TRH release, and increased TSH secretion. However, low pituitary expression of *Trhr* mRNA expression suggests that the pituitary is impaired in TRHR signaling despite increased TRH secretion. Furthermore, it is unclear whether the decreased serum TSH levels are the result of decreased TSH pituitary content and/or a consequence of ineffective TRH-regulated release of TSH.

Hypothalamic *Trh* mRNA expression appeared inappropriately high in *Igsf1*$^{\Delta ex1/y}$ mice given their relatively mild reduction in circulating T3 levels and normal T4 levels. Therefore, it is possible that, in addition to a pituitary defect, these mice may also experience impaired TH transport into the hypothalamus. As described above (see section 1.1.3.1 Monocarboxylate transporter 8), MCT8 is required for T3 transport across the BCSFB, where it is transported into the hypothalamus and affects *Trh* transcription in TRH-expressing neurons of the PVN. MCT8 is apically localized in the murine CP, and polarized expression of some MCT family members is dependent on IGSF chaperones (Figure 1.8)[177,178]. Indeed, the structurally similar IGSF member, CD147 (basigin), interacts with members of the MCT family and affects both their plasma membrane trafficking and membrane localization in polarized cells (Figures 1.8 and 1.9)[178,179]. IGSF1 is also expressed at the apical membrane of the CP, and given CD147's role in plasma membrane sorting of MCT family members, we hypothesized that IGSF1 might similarly affect MCT8 subcellular localization in the choroid plexus. This thesis focuses on the effect of IGSF1-deficiency on the murine HPT axis, with a particular focus on a potential role for IGSF1 in

MCT8-mediated T3 transport into the hypothalamus. In order to elucidate the potential role of IGSF1 on MCT8-mediated T3 transport into the hypothalamus, we first defined an interaction between IGSF1 and MCT8 *in vitro*, and characterized the functional significance of this interaction on MCT8 influx of THs *in vitro* and *in vivo*. We then observed the effects of IGSF1-deficiency on MCT8-mediated influx of TH *in vivo* and further characterized the effect of IGSF1-deficiency on TRH signaling in the absence of TH and in the presence of exogenous TRH. We found that IGSF1 does not affect MCT8-mediated transport of T3 *in vitro*, nor does IGSF1-deficiency affect TH transport into the hypothalamus. However, loss of TH elicits a significantly blunted TSH response in *Igsf1*$^{\Delta ex1/y}$ mice compared to *Igsf1*$^{+/y}$ mice. Furthermore, exogenous TRH stimulation of TSH is also incapable of increasing TSH secretion in *Igsf1*$^{\Delta ex1}$ mice to the same extent as *Igsf1*$^{+/y}$ mice. These results indicate that IGSF1 does not affect MCT8-mediated transport of TH in the hypothalamus, and that the TRH signaling defect observed in *Igsf1*$^{\Delta ex1}$ mice is mainly the result of a pituitary defect.

Figure Legends

Figure 1.1 – Components of the hypothalamic-pituitary-thyroid (HPT)-axis. *Trh* mRNA is transcribed in neurons of the PVN in response to reduced TH influx. TRH is released from axon terminals localized at the median eminence where it travels through portal vessels and binds TRHRs on thyrotropes to induce post-translational glycosylation of TSH and its release into the peripheral circulation. TSH then binds TSHRs on thyrocytes of the thyroid gland and stimulates production and release of the THs T3 and T4 into the circulation where they are taken up by target tissues through active transport by THTs and affect gene transcription. THs also negatively regulate their own production by inhibiting transcription of *Trh* and *Tshb* in the hypothalamus and pituitary, respectively.

Figure 1.2 – Hypothesis of the mechanism for TH transport across the BCSFB. THs are synthesized in the thyroid gland and secreted into the circulation where they bind thyroid distributor proteins (THDPs, here they show albumin (Alb), transthyretin (TTR), thyroxine-binding globulin (TBG)). T4 dissociates from THDPs and is actively transported across the CP by OATP1C1. Some T4 binds TTR produced in the CP epithelial cell and diffuses into the CSF. The majority of T4 is unbound and is effluxed into the CSF by MCT8. Modified from Richardson, S.J., et al (2015) - Transport of thyroid hormones via the choroid plexus into the brain: the roles of transthyretin and thyroid hormone transmembrane transporters. *Frontiers in Neuroscience*. **9**:1-8.

Figure 1.3 – IGSF1 is sequentially cleaved at an internal signal peptide by signal peptidase and signal peptide peptidase. IGSF1 is a 12 Ig domain containing protein with an N-terminal signal peptide, an internal hydrophobic linker region, containing a TMD and a signal peptide, and a C-terminal TMD. The N-terminal signal peptide directs IGSF1 co-translational translocation into the ER. Within the ER the N-terminal signal peptide is co-translationally cleaved by signal peptidase (SP), the first five Ig domains are translated and the first TMD is inserted in the ER membrane. A short luminal C-terminal tail is translated followed by the internal signal peptide. The internal signal peptide is co-translationally cleaved from the C-terminal portion of the NTD by SP. Translation of the C-terminal portion of IGSF1 continues into the lumen of the ER, where the next seven Ig domains are translated prior to insertion of the C-terminal TMD into the membrane followed by translation of the short luminal C-terminal tail of the IGSF1-CTD protein. Signal peptide peptidase (SPP) then degrades the internal signal peptide, releasing the CTD from the membrane at the N-terminus. This process results in two distinct IGSF1 proteins, the IGSF1-NTD and IGSF1-CTD.

Figure 1.4 – IGSF1-CTD is a membrane glycoprotein. IGSF1-CTD obtains mature glycosylation in the ER prior to trafficking to the plasma membrane. The single-pass TMD is inserted into the plasma membrane with the 7 glycosylated Ig domains oriented extracellularly and with a short cytoplasmic C-tail.

Figure 1.5 – Human *IGSF1* mRNA isoforms and corresponding protein products. *IGSFI* is alternatively spliced to produce five different isoforms in human. *IGSF1-1*, *IGSF1-3,* and *IGSF1-4* encodes the full-length IGSF1 protein, with minor differences in the 5'UTR. The *IGSF1-1, IGSF1-3* and *IGSF1-4* isoforms produce the entirety of the IGSF1 protein, while the *IGSF1-2* and *IGSF1-5* isoforms produce a soluble form of IGSF1 which contains the first two Ig domains and lacks a TMD and is secreted in human plasma. (Modified from Beata Bak, unpublished)

Figure 1.6 – Murine *Igsf1* mRNA isoforms and corresponding protein products. Murine *Igsf1* is alternatively spliced to give rise to four different isoforms, only one of which encodes the entirety of the IGSF1 protein (*Igsf1-1*). *Igsf1-2* is orthologous to the human *IGSF1-2* and *IGSF1-5* isoforms, and produces the short protein product containing the first two Ig domains and lacks a TMD, and is presumably secreted. The *Igsf1-3* isoform encodes the entirety of the NTD as well as the first two Ig domains of the CTD, lacking the TMD of the CTD. Therefore, the entirety of the NTD is intact and is presumably retained in the ER, while the first two Ig domains of the CTD may also be secreted. Additionally, the entirety of the CTD is encoded by *Igsf1-4* which is transcribed through an internal promoter. (Modified from Beata Bak, unpublished).

Figure 1.7 – Pathogenic mutations identified in human patients with IGSF1-deficiency syndrome. Pathogenic mutations of deletion, nonsense, missense and insertion subtypes have been identified in patients from the Netherlands, the United Kingdom, Japan, Ireland, and Italy. The majority of mutations identified to date are located in the CTD of IGSF1. Diagram modified from Daniel Bernard, unpublished.

Figure 1.8 – CD147 is an ancillary protein of MCT1 required for plasma membrane expression and subcellular localization. CD147 is an IGSF protein composed of two C2-type Ig domains and a single-pass transmembrane domain containing a negatively charged amino acid. Its Ig domains are oriented extracellularly while its short C-terminal tail is cytoplasmic. CD147 binds MCT1 and directs expression of MCT1 to the basolateral membrane of some polarized cell types. (Modified from Halestrap, Andrew P. and Meredith, David (2004). The SLC16 gene family - From monocarboxylate transporters (MCTs) to aromatic amino acid transporters and beyond. *European Journal of Physiology*. **447**(5): 619-628).

Figure 1.9 – CD147 and IGSF1 share structural similarity. Both IGSF1 and CD147 are composed of extracellular C2-type Ig domains, a single-pass transmembrane domain and a short cytoplasmic C-terminal tail. CD147 contains a negatively charged amino acid in its TMD, while IGSF1 contains a positively charged amino acid.

Figure 1.10 – Intracellular signaling upon binding of TRH to the TRHR. Upon binding of TRH to the TRHR, TRHR then couples to the G-proteins $G_{\alpha q}$ and $G_{\alpha 11}$, which mobilize intracellular calcium through phospholipase C (PLC) activity. Binding of TRH to the TRHR induces a conformational change allowing G_{α} to exchange guanine diphosphate (GDP) for guanine triphosphate (GTP), which phosphorylates PLC and leads to PLC-mediated hydrolysis of phosphatidylinositol 4,5-bisphosphate (PIP_2). Hydrolysis of PIP_2 forms the second messengers diacylglycerol (DAG) and inositol 1,4,5-trisphosphate (IP_3). IP_3 is then released into the cytosol and binds IP_3-sensitive calcium ion (Ca^{2+})-channels on the smooth endoplasmic reticulum (ER), rapidly increasing cytosolic Ca^{2+} levels and activating trafficking of secretory granules to the plasma membrane where they exocytose their cargo. DAG promotes protein kinase C (PKC) translocation from the cytosol to the plasma membrane, and together with Ca^{2+}, PKC phosphorylates the pituitary-specific transcription factor Pit-1. The transcription factors *c-fos* and *c-jun* are also immediate early genes of TRH stimulation. Following TRH activation of PKC and elevation of Ca^{2+} through the $G_{\alpha q/11}$ pathway, the TRHR is rapidly desensitized and internalized.

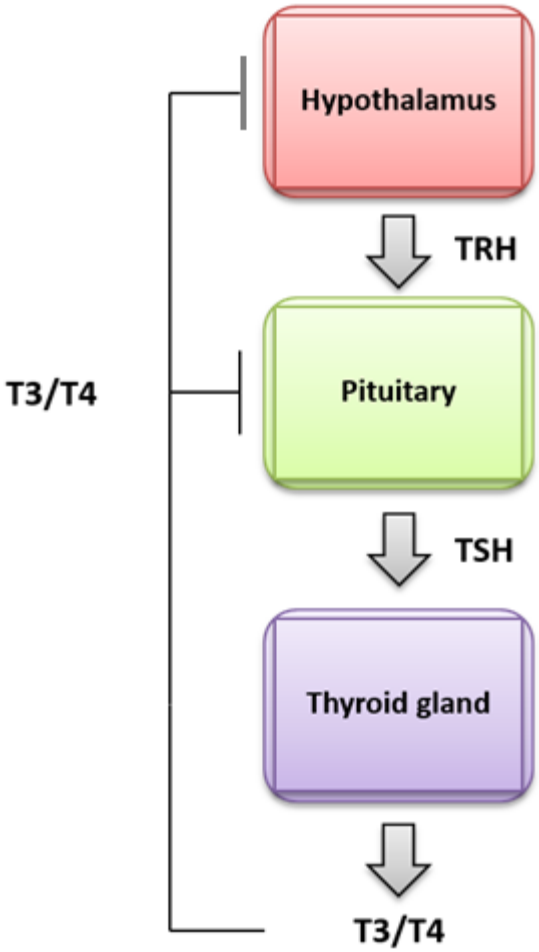

Figure 1.1

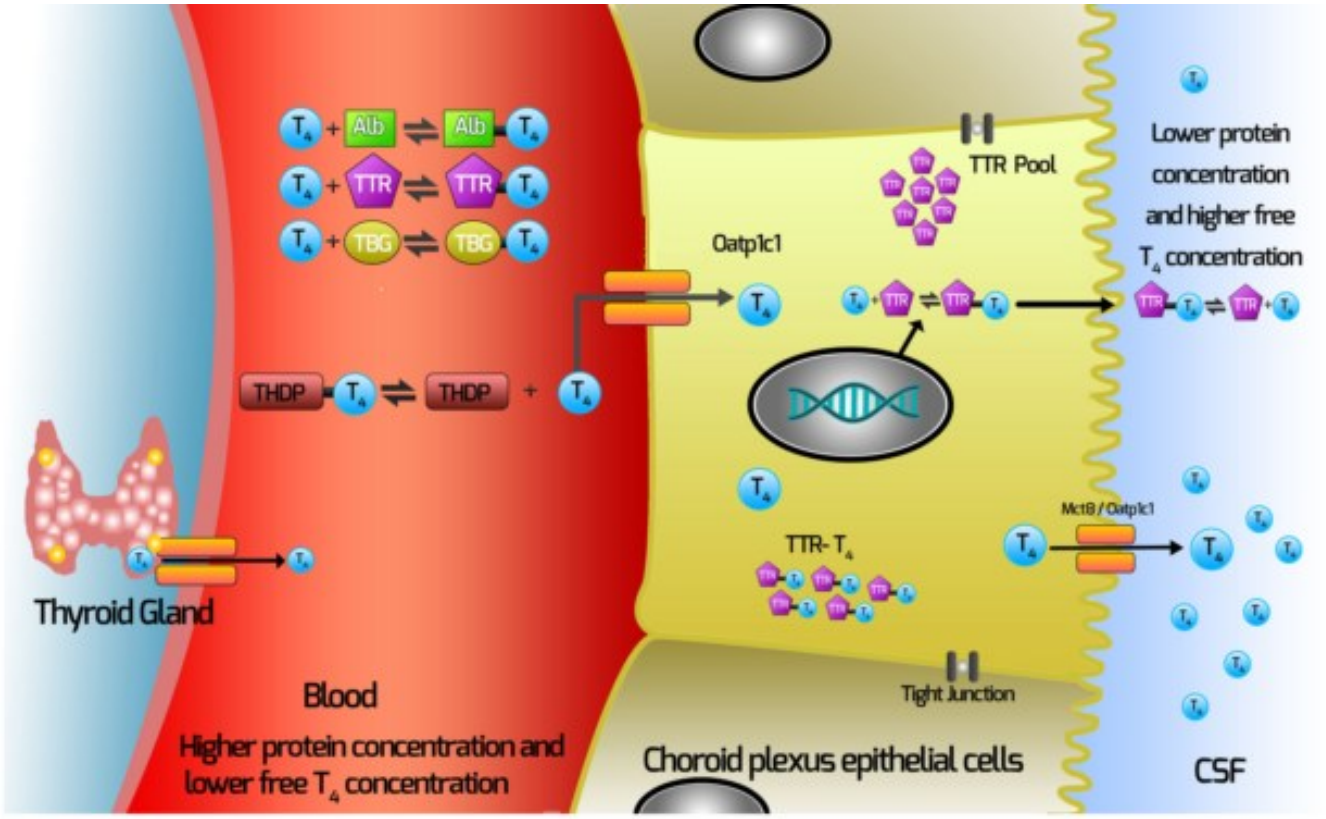
Alb
TTR
TBG
THDP
Oatp1c1
TTR Pool
Lower protein concentration and higher free T_4 concentration
Mct8 / Oatp1c1
TTR- T_4
Tight Junction
Thyroid Gland
Blood
Higher protein concentration and lower free T_4 concentration
Choroid plexus epithelial cells
CSF

Figure 1.2

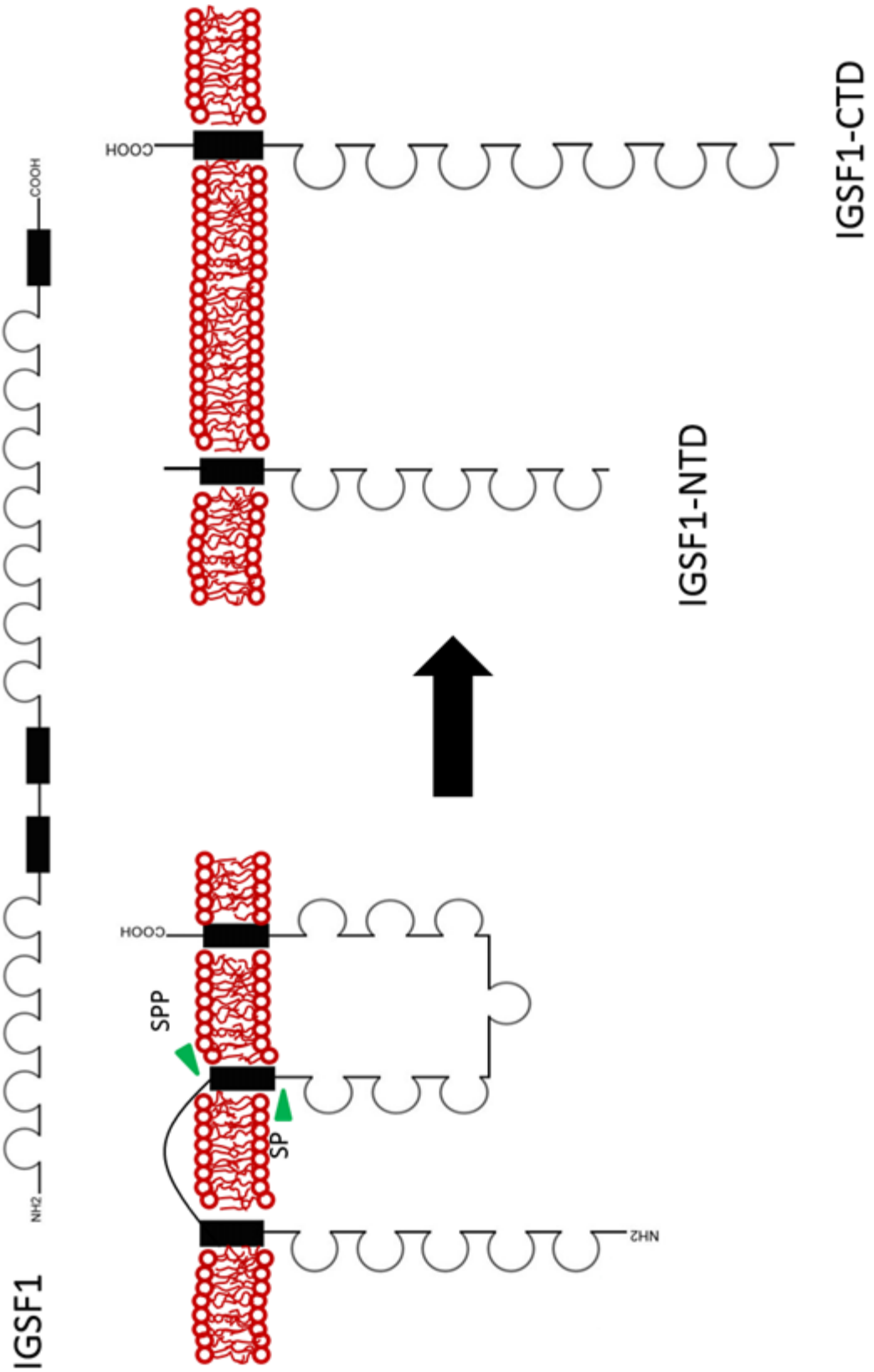

Figure 1.3

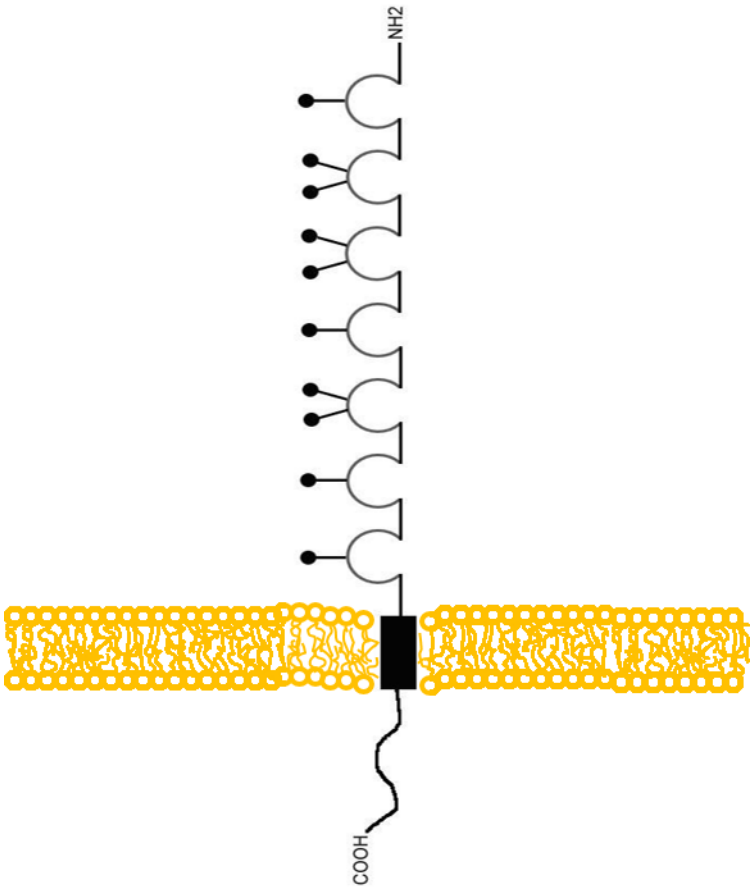

Figure 1.4

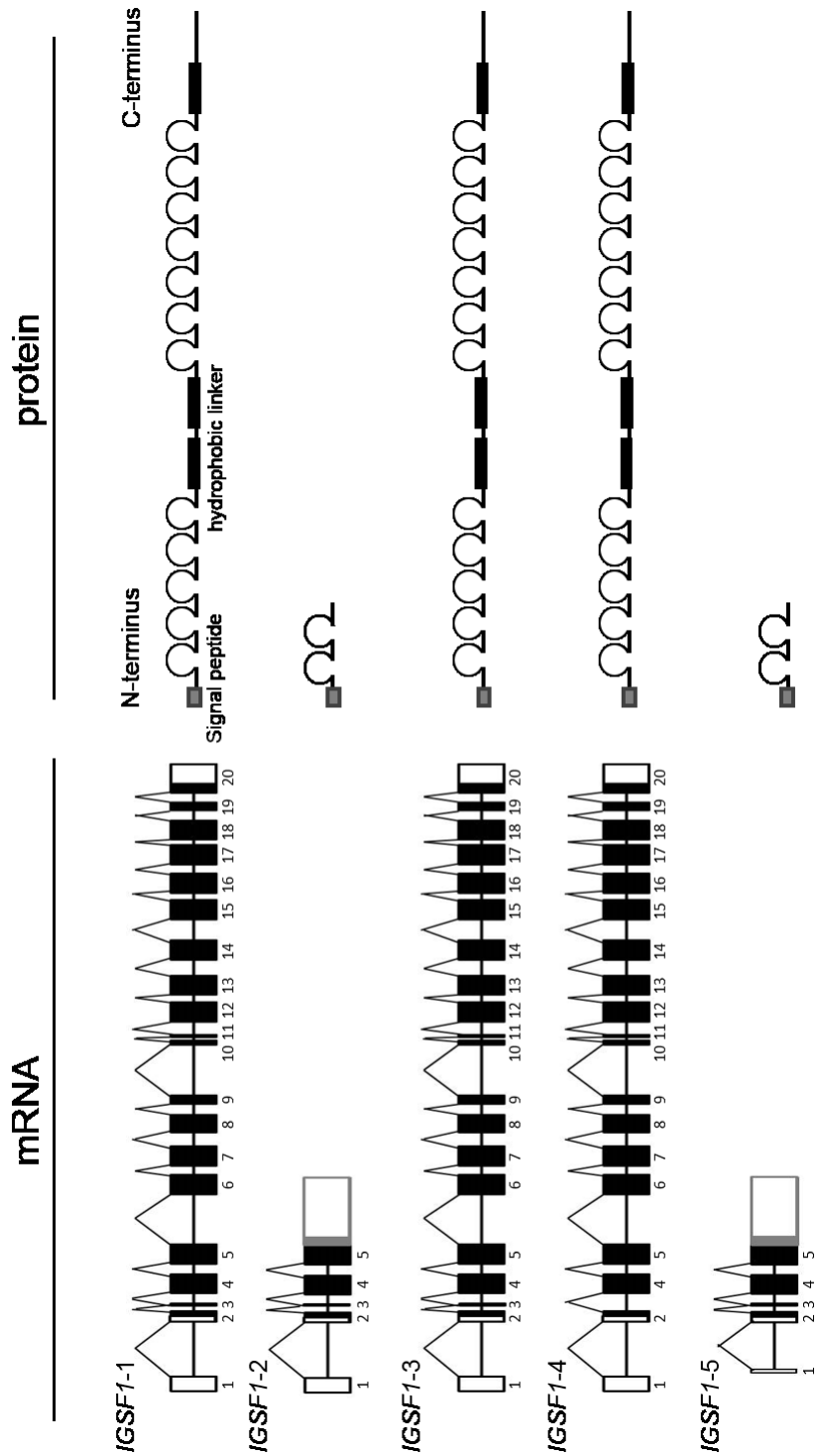
protein
mRNA
N-terminus
C-terminus
Signal peptide
hydrophobic linker
IGSF1-1
IGSF1-2
IGSF1-3
IGSF1-4
IGSF1-5

Figure 1.5

mRNA
protein
N-terminus
C-terminus
Signal peptide
hydrophobic linker
Igsf1-1
Igsf1-2
Igsf1-3
Igsf1-4
1 2 3 4 5 6 7 8 9 10 11 12 13 14 15 16 17 18 19 20
1 2 3 4 5
1 2 3 4 5 6 7 8 9 10 11 12 13 13b
10 11 12 13 14 15 16 17 18 19 20

Figure 1.6

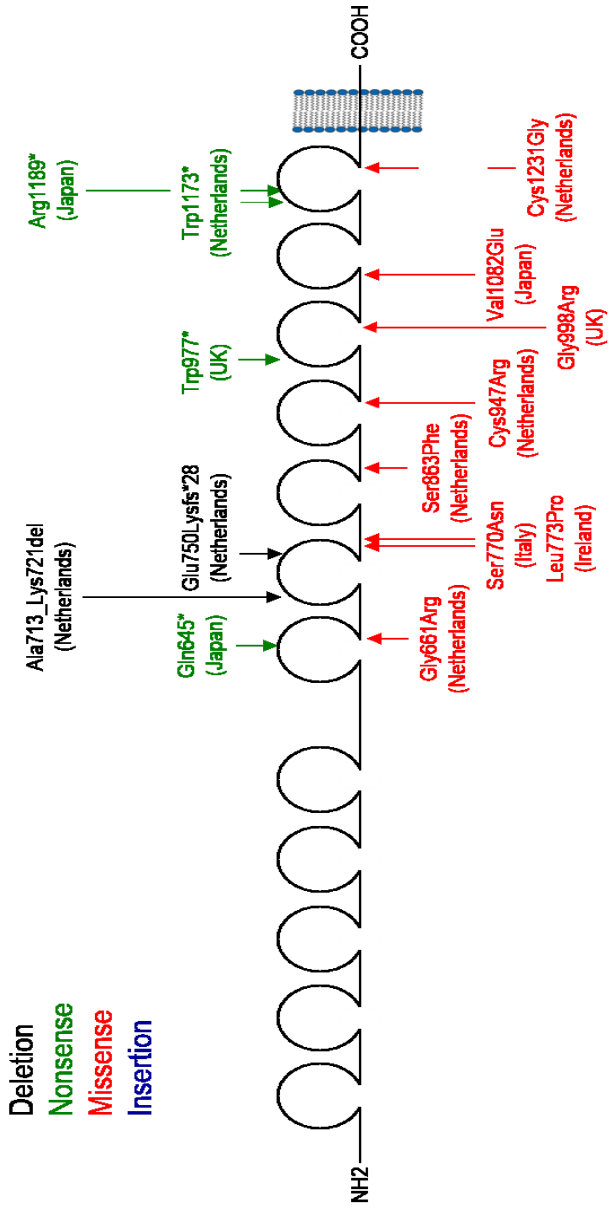
Deletion
Nonsense
Missense
Insertion
NH2
COOH
Arg1189*
(Japan)
Ala713_Lys721del
(Netherlands)
Gln645*
(Japan)
Glu750Lysfs*28
(Netherlands)
Trp977*
(UK)
Trp1173*
(Netherlands)
Gly661Arg
(Netherlands)
Ser863Phe
(Netherlands)
Ser770Asn
(Italy)
Cys947Arg
(Netherlands)
Leu773Pro
(Ireland)
Val1082Glu
(Japan)
Gly998Arg
(UK)
Cys1231Gly
(Netherlands)

Figure 1.7

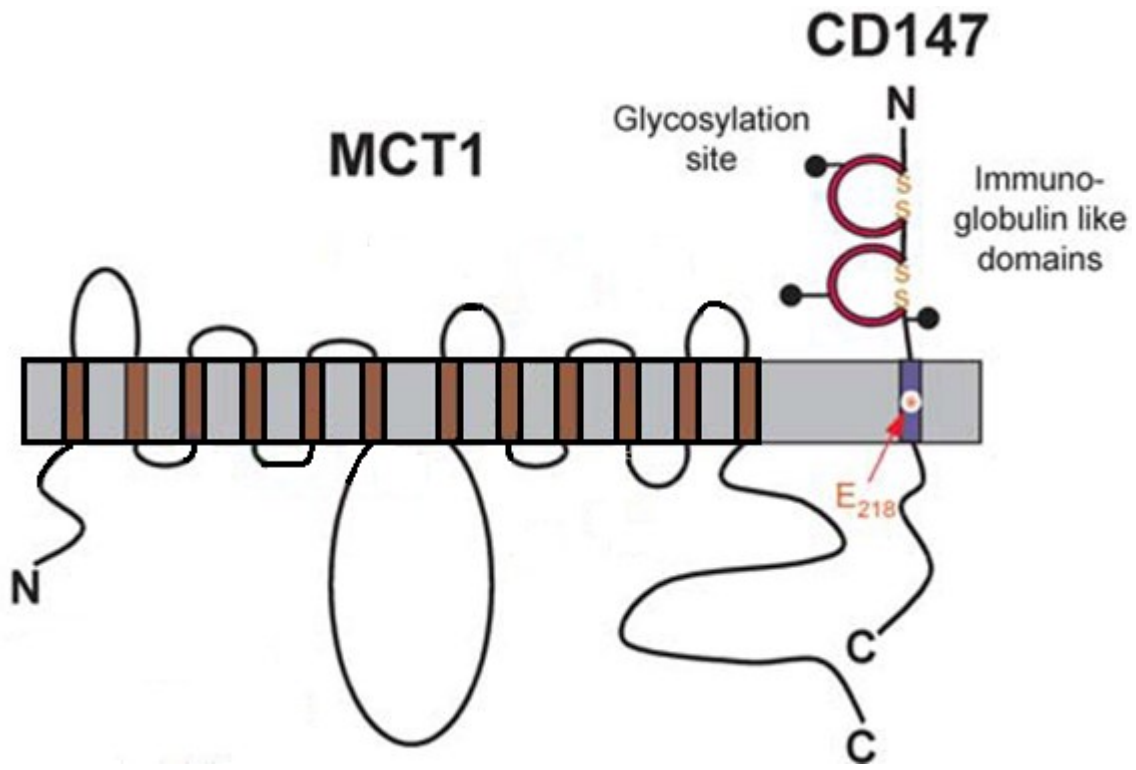
CD147
MCT1
Glycosylation site
N
Immuno-globulin like domains
S
S
S
S
E218
N
C
C

Figure 1.8

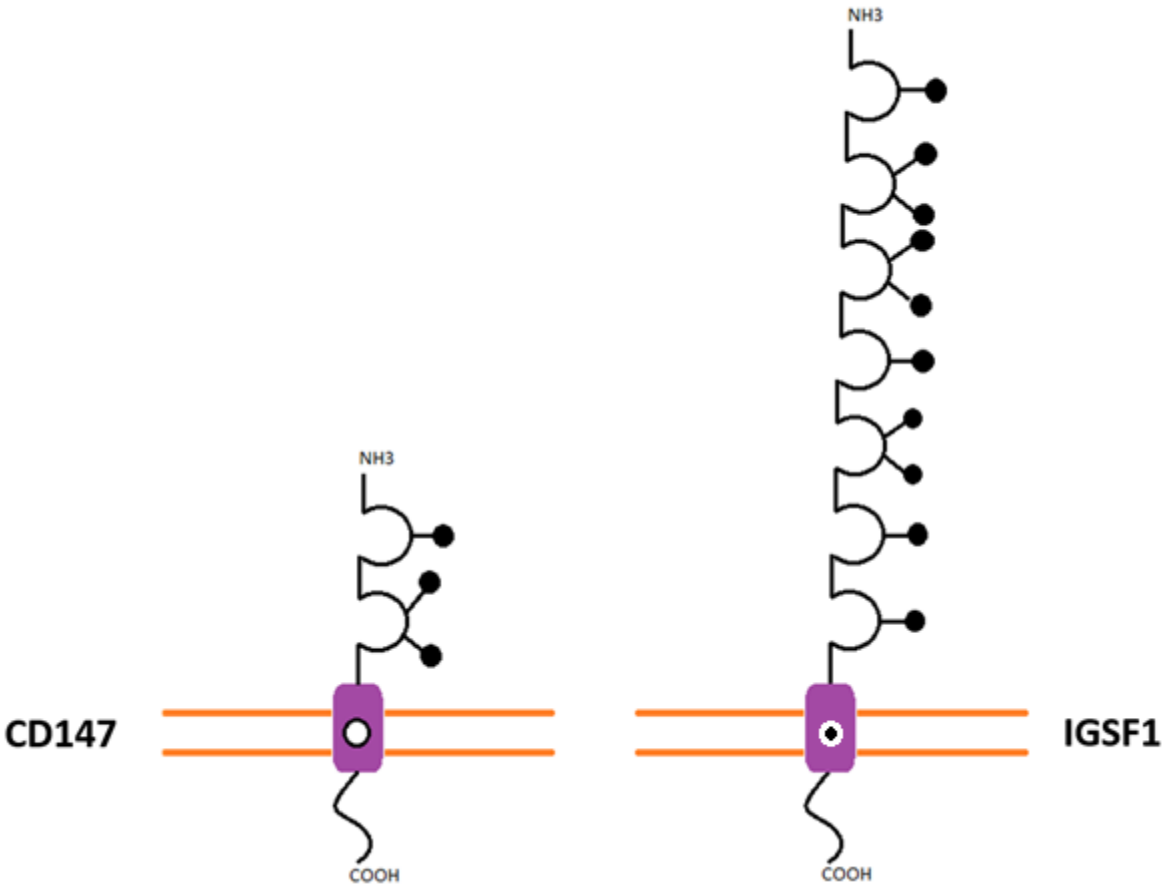

Figure 1.9

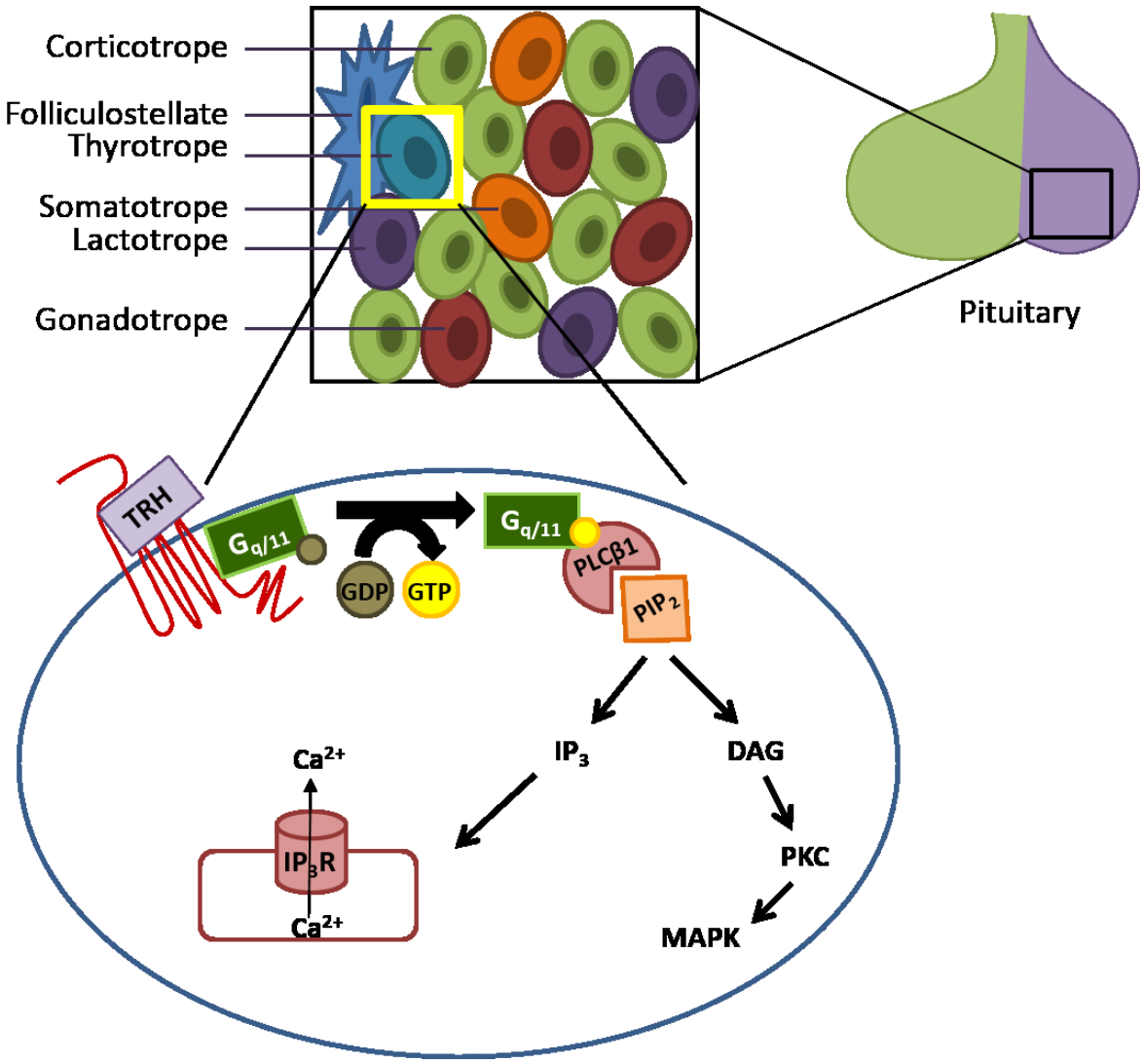
Corticotrope
Folliculostellate
Thyrotrope
Somatotrope
Lactotrope
Gonadotrope
Pituitary
TRH
$G_{q/11}$
GDP
GTP
$G_{q/11}$
PLCβ1
PIP_2
IP_3
DAG
Ca^{2+}
IP_3R
Ca^{2+}
PKC
MAPK

Figure 1.10

Chapter 2: Materials and Methods

Reagent list

Rabbit antiserum against murine IGSF1-CTD was generated and provided by Dr. Peter Scheiffele[167]. Affinity purified rabbit antibody against MCT8 was provided by Dr. Ezra Tai (XenoPort, Santa Clara, California)[37]. Mouse monoclonal antibodies against HA (H9658) and β-actin (A5441), EZview Red anti-HA affinity gel (E6779), and L-T3 (T2752) and L-T4 (T2376) were obtained from Sigma Aldrich (St. Louis, Missouri, USA). Secondary antibodies for western blotting (goat anti-mouse 170-6516 and goat anti-rabbit 170-6515) were obtained from BioRad (Mississauga, Ontario, Canada). Monoclonal goat anti-rabbit Alexa 488 (A-11008), monoclonal rabbit anti-GFP (G10362), TRIzol reagent (15596-026) and Pro-Long Gold anti-fade reagent with DAPI (P36935) were obtained from Invitrogen (Burlington, Ontario, Canada). DME/F12 (12500-039) was obtained from Gibco, Life Technologies (Burlington, ON, Canada). *Pfu*Ultra-HF (600380) was obtained from Agilent Technologies (Santa Clara, CA, USA). *Hind*III (R0104S) and *Cla*I (R0197S), 1X glycoprotein denaturing buffer (B0701S), PNGaseF (P0704S), and EndoH (P0702S) were obtained from New England BioLabs (NEB; Whitby, Ontario, Canada). Gel purification kit (BS353) was obtained from BioBasic (Markham, ON, Canada). T4 DNA ligase (M1801), MMLV-RT (M1701), and RQ1 DNase (M6101) were obtained from Promega (Madison WI, USA). Normal goat serum (053-110), D-PBS (311-425-CL), DMEM (319-005), and FBS (081-105) were obtained from Wisent (Saint-Jean-Baptiste, QC, Canada). PEI (23966) was obtained from Polysciences Inc. (Warrington, PA, USA). BCA assay kit (23227) and EZ-link-sulfo-NHS-LC-biotin (21327) were obtained from ThermoScientific (Waltham, Massachusetts, USA). Vectastain ABC kit (PK6100) was obtained from Vector laboratories (Burlingame, CA, USA). ECL Western Lightning Plus (NEL105001EA),

nitrocellulose membranes (NBA083C001EA), [^{125}I]-T3 (NEX110X100UC), and [^{125}I]-T4 (NEX111H100UC) were obtained from Perkin Elmer (Boston, MA, USA). HyBlot CL Autoradiography film (E3018) was obtained from Denville Scientific Inc. (Metuchen, NJ, USA). Proteinase K (PRK403) was obtained from BioShop (Burlington, Ontario, Canada). Optimum Cutting Temperature TissueTek (25608-930) was obtained from VWR (Mont Royal, QC, Canada). BSA (10735086001) was obtained from Roche (Mannheim, Germany). EvaGreen (Mastermix-S) was obtained from ABM (Richmond, BC, Canada). Iodine-deficient/0.15% PTU (LoI/PTU) diet was obtained from Harlan laboratories (Teklad TD.95125, Montreal, Quebec, Canada). [^{35}S]-UTP and [^{35}S]-CTP (1,000 Ci/mmol) and Hyperfilm β-max were obtained from Amersham (Braunschweig, Germany). RNase T_1 was a product of Boehringer Mannheim (Mannheim, Germany). NTB-2 nuclear emulsion and Rapid Fix were obtained from Kodak (Integra Bioscience, Fernwald, Germany). Coated-tube RIA kits were obtained from Siemens Medical Solutions Diagnostics (Los Angeles, CA, USA).

Constructs

A construct encoding the full-length human MCT8 containing an N-terminal GFP tag was a gift from Dr. Samuel Refetoff (University of Chicago, Chicago, Il, USA). A construct encoding the mouse IGSF1 isoform 4 was a gift from Dr. Peter Scheiffele. The mouse MCT10-HA construct was generated in-house through the amplification of mouse liver *Mct10* cDNA and its ligation into a pcDNA3 expression vector containing the HA coding sequence at the 3' end of the multiple cloning site using the primer set in Table 1.2 and the high-fidelity *Pfu*Ultra-HF polymerase. Briefly, an existing *Hind*III restriction site was first removed from *Mct10* using the primer set indicated in Table 1.3 and the QuikChange mutagenesis protocol (Stratagene) after which *Mct10* was amplified as described above. The *Mct10* amplicon, and pcDNA3.0-HA

plasmid grown in *Dam*- (SCS110) bacteria were then digested with 0.5 units of *Hind*III and *Cla*I at 37°C for 2 h. Digested products were gel purified using the BioBasic gel purification kit and ligated with 1 unit T4 DNA ligase at 4°C overnight. The mouse MCT8-HA construct was generated by amplifying *Mct8* from mouse liver cDNA using the primer set in Table 1.2 and *Pfu*Ultra. The pcDNA3.0-HA plasmid grown in *Dam*- (SCS110) bacteria, and the *Mct8* amplicon were digested using 0.5 units of *Hind*III and *Cla*Iand ligated with T4 DNA ligase as described above. The human IGSF1-1 construct, containing a myc-tag directly following the N-terminal signal peptide and a 3X HA tag at the C-terminus was a gift from Dr. Peter Scheiffele (Biozentrum, University of Basel, Switzerland). This construct was modified by Dr. Beata Bak (McGill University, Montreal, Quebec) to include an epitope for the mouse IGSF1-CTD antiserum[157]. The mouse CRYM vector was generated in house by amplifying *Crym* from murine brain using the primer set described in Table 1.2 and *Pfu*Ultra-HF polymerase. Amplification of *Crym* using these primer sets added an *Eco*RI restriction endonuclease site at the 5' end of the amplicon and an *Xho*I restriction site at the 3' end. The resultant 987 bp PCR product and the pcDNA3.0 vector were digested with *Eco*RI and *Xho*I, gel purified using the BioBasic gel purification kit and ligated using T4 ligase as described above.

Cell lines

Human embryonic kidney 293 (HEK293) cells (a gift from Dr. Terence Hébert, McGill University, Montréal, Québec, Canada) and HeLa cells (a gift from Dr. Jason Tanny, McGill University) were maintained in DMEM supplemented with 10% FBS. All cells were cultured at 37°C with 5% CO_2 in a water-jacketed incubator.

Cell culture and transfection

For cell surface biotinylation, HEK293 cells were seeded in 6-well plates at $4x10^4$ cells/well, respectively. Twenty-four hours post-plating, cells were transfected with 2 µg plasmid DNA and 6 µg polyethylenimine (PEI). Briefly, DNA and PEI were combined in 200 µl serum-free DMEM, and incubated at room temperature for 15 min. Cell culture media was replaced with 1 ml serum-free DMEM and 200 µl of the DNA:PEI mix was added to appropriate wells. Cells were incubated at 37°C for 2 h with the DNA:PEI mix after which the transfection medium was replaced with growth medium and incubated at 37°C overnight. For T3/T4 transport assays (described below), HeLa cells were plated in 12-well plates at $1x10^5$ cells/well and transfected with 1 µg DNA and 3 µg PEI 24 h post-plating as described above.

Cell surface biotinylation (CSB) and immunoprecipitation (IP)

HEK293 cells were grown in 6-well plates for 24 h prior to transfection with either pcDNA3, pcDNA3 + IGSF1-HA, pcDNA3 + MCT8-GFP, or IGSF1-HA + MCT8-GFP or pcDNA3, pcDNA3 + IGSF1-4, pcDNA3 + MCT8-HA, pcDNA3 + MCT10-HA, IGSF1-4 + MCT8-HA or IGSF1-4 + MCT10-HA (Figure 3.1 a and b, respectively) to a total of 2 µg DNA per well. Twenty-four hours post-transfection, cells were washed 3X with cold phosphate buffered saline (PBS; pH 7.4, 137 mM NaCl, 2.7 mM KCl, 10 mM Na_2HPO_4, 1.8 mM KH_2PO_4) and incubated in 1 ml 0.5 mg/ml EZ-link-sulfo-NHS-LC-biotin per well for 30 min at 4°C with gentle rotation to biotinylate cell surface proteins. Cells were then washed with cold 100 mM glycine in PBS 3X 5 min at 4°C with gentle rotation and harvested in 300 µl lysis buffer (50 mM Tris pH 7.5, 150 mM NaCl, 1 mM EDTA, 1% Triton X-100). Lysates were centrifuged at 16.1

rcf at 4°C for 20 min and supernatant collected for immunoprecipitation and analysis via western blot (below).

Immunoprecipitation was conducted using 20 µl EZview Red anti-HA affinity beads, which were washed 2X with lysis buffer prior to incubation with 250 µl of lysates at 4°C overnight with rotation. The next day, beads were washed 3X with lysis buffer and immunoprecipitated lysates were eluted by heating in 60 µl lysis buffer and 15 µl Laemmli buffer containing 2% 2-mercaptoethanol at 70°C. Immunoprecipitated lysates and total lysates were resolved by SDS-PAGE on 8% Tris-glycine gels and analyzed by western blotting (described below) using the primary antibodies rabbit anti-GFP (1:1000), mouse anti-HA (1:40,000), rabbit anti-IGSF1-CTD (1:1000) and mouse anti-ACTB (1:20,000) or anti-BTUB (1:20,000) diluted in blocking buffer to detect total and immunoprecipitated proteins. Detection of biotinylated proteins was conducted using the Vectastain ABC kit. Briefly, membranes were incubated in 5% BSA in TBST for 1 h prior to incubation with the Vectastain reagent. Two drops of reagent A and two drops of reagent B were diluted in 5 ml of 2.5% BSA in TBST and incubated at room temperature for 30 min. The membrane was then incubated in Vectastain reagent for 30 min, followed by 4X 10 min washes with TBST. Protein was visualized as described in the western blotting section below.

Western blotting

Protein lysates were heated to 70°C for 5 min in Laemmli buffer (50 mM Tris pH 6.8, 2% SDS, 10% glycerol, 0.04% Bromophenol Blue) containing 2% 2-mercaptoethanol, and resolved by SDS-PAGE on 8% Tris-glycine gels. Proteins were transferred to nitrocellulose membranes (30 V, 1 h) and the membranes blocked with 5% skim milk (primary antibodies) or bovine serum

albumin (BSA, for Vectastain) in Tris-buffered saline with Tween-20 (TBST; 0.05% Tween-20 in 10 mM Tris pH 8.0, 150 mM NaCl) for 1 h at room temperature with mild rocking. Membranes were incubated in primary antibody in blocking buffer overnight at 4°C with mild rocking. The next day, membranes were washed 4X 10 min in TBST and incubated in 1:3000 dilution of appropriate horseradish peroxidase (HRP)-conjugated secondary antibody in blocking buffer for 1 h at room temperature. Finally, membranes were washed 4X 10 min in TBST, incubated in ECL Plus reagent according to manufacturer's instructions, and exposed to HyBlot CL autoradiography film.

Animals

IGSF1-deficient (*Igsf1*$^{\Delta ex1}$) mice were described previously[157,172]. Mice were handled according to federal and institutional (McGill University) guidelines. The animals had access to water and standard or LoI/PTU chow *ad libitum*. An ambient temperature of 22°C and 12 h light, 12 h dark light cycle were maintained automatically. Wild-type (*Igsf1*$^{+/y}$) and hemizygous (*Igsf1*$^{\Delta ex1/y}$) male mice were generated by mating heterozygous female mice (*Igsf1*$^{\Delta ex1/+}$) to wild-type males. At specified ages, male mice were culled by CO_2 asphyxiation. Genomic DNA was extracted by digesting toe tissue collected at post-natal day 10 with 100 µg/ml proteinase K in tail digest buffer (100 mM Tris pH 8.0, 5 mM EDTA, 200 mM NaCl, 0.2% SDS) overnight at 55°C. Samples were centrifuged for 10 min at 16.1 rcf to pellet insoluble material and collect the supernatant. DNA was precipitated in 1 volume isopropanol and DNA dissolved in 20 µl Tris-EDTA buffer (TE, 10 mM Tris pH 8.0, 1 mM EDTA). Genotyping PCR to identify *Igsf1*$^{+/y}$ and *Igsf1*$^{\Delta ex1/y}$ males was performed using primers in Table 1.1. Briefly, the *Igsf1*$^{+}$ primers anneal to the first exon of *Igsf1* and amplify a 100 bp amplicon while the *Igsf1*$^{\Delta ex1}$ primers anneal to the Pgk-HPRT selection cassette, which replaced the first exon in *Igsf1*$^{\Delta ex1/y}$ mice during

homologous recombination of the targeting vector, and amplify a 200 bp amplicon[172]. Two µl of genomic DNA was subjected to PCR using 1X GoTaq buffer, 5 mM $MgCl_2$, 200 µM each dNTP, 0.4 mM *Igsf1*$^{+}$ forward and reverse primers, 0.8 mM *Igsf1*$^{\Delta ex1}$ forward and reverse primers and 1 unit of Taq polymerase. PCR cycling conditions were as follows: initial denaturation, 95ºC for 2 min followed by 18 cycles of denaturation at 95ºC for 15 sec, annealing at 50ºC for 30 sec, and extension at 68ºC for 1 min. Amplicons were run on a 1.75% agarose gel containing ethidium bromide and run at 120 V for 20 min.

Deglycosylation

Tissues from 8-week old *Igsf1*$^{+/y}$ and *Igsf1*$^{\Delta ex1/y}$ male mice were dissected and frozen on dry ice prior to protein extraction. Tissues were then suspended in 1 µl/µg tissue RIPA buffer (150 mM NaCl, 50 mM sodium fluoride, 10 mM $NaPO_4$, 2 mM EDTA, 1% NP-40, 1% sodium deoxycholate, 0.1% SDS) containing protease inhibitors (2 mg/ml aprotinin, 2 mg/ml leupeptin, 1 mg/ml pepstatin A, and 0.2 M PMSF) and allowed to thaw prior to homogenization with a hand-held homogenizer. Homogenized tissues were then centrifuged, and the concentration of the collected supernatant was determined by BCA assay. Ten to 20 µg of protein was denatured in 1X glycoprotein denaturing buffer for 10 min at 90°C followed by deglycosylation with 500 units of either endoglycosidase H (EndoH) or peptide-N-glycosidase F (PNGase F), following the manufacturer's instructions, overnight at 37°C. Proteins were resolved by SDS-PAGE on 8% Tris-glycine gels and analyzed by western blotting as described below.

Choroid plexus immunofluorescence

Brains were collected from 8-week old male wild-type (*Igsf1*$^{+/y}$) and *Igsf1*$^{\Delta ex1/y}$ mice and flash frozen in isopentane cooled to -30°C to -50°C. Brains were embedded in OCT medium

prior to cryosectioning with a cryostat (Leica). Ten μm sections from Bregma 0.14 mm and Bregma 0.02 mm were mounted on positively charged glass slides, dried, and stored at -80°C for immunofluorescence. Slides were warmed to room temperature and fixed using 4% paraformaldehyde (PFA) in Hank's Buffered Saline Solution (HBSS, 137 mM NaCl, 5.4 mM KCl, 0.25 mM Na_2HPO_4, 0.1 g glucose, 0.44 mM KH_2PO_4, 1.3 mM $CaCl_2$, 1.0 mM $MgSO_4$, 4.2 mM $NaHCO_3$) for 15 min. Sections were washed 3X with PBS and then blocked with 5% goat serum diluted in PBST (PBS + 0.1% Triton X-100) for 30 min at room temperature. Affinity purified rabbit anti-MCT8 or rabbit anti-IGSF1 were diluted to 1:100 or 1:500, respectively, in 5% goat serum in PBST and incubated for 2 h at room temperature. Sections were washed 3X 5 min at room temperature with PBST, and then incubated for 1 h at room temperature in 1:400 Alexa 488 goat anti-rabbit. Sections were washed as above and glass cover slips were mounted with ProLong Gold with DAPI. Slides were incubated overnight at room temperature in the dark and visualized using confocal microscopy. Confocal microscopy was conducted using a Leica SP8 microscope and HC PL APO CS2 63X/1.40 oil objective. The multiphoton laser was set to emit at 780 nm and emission detected at 721 nm to 774 nm for DAPI images, while the HPD laser was set to emit at 488 nm and emission detected at 406 nm to 480 nm for Alexa 488 with a numerical aperture of 1.40, a 1.0 zoom, and a pinhole of 600 μm. Images were taken sequentially and overlayed using LAS AF Lite.

T3/T4 in vitro transport assays[41]

HeLa cells were grown in 12-well plates, and transfected with either pcDNA + CRYM, CRYM + IGSF1 + pcDNA, CRYM + MCT8-GFP, or CRYM + IGSF1-HA + MCT8-GFP to a total of 3 μg total DNA, 24 hours post-plating. 24 hours post-transfection, cells were washed twice with 500 μl of Dulbecco's modified PBS (D-PBS) containing 0.1% BSA. For import

assays, cells were equilibrated in D-PBS + 0.1% BSA for 30 min at 37°C prior to addition of [^{125}I]-T3 or [^{125}I]-T4. Following equilibration, D-PBS + 0.1% BSA was removed and 1 nM [^{125}I]-T3 or [^{125}I]-T4 in 500 µl D-PBS + 0.1% BSA was first added to the 10 min time point and incubated at 37°C for 5 min. The process was then repeated for the 5 min time point, and finally the 0 min time point. All cells were then washed 2X with 500 µl D-PBS + 0.1% BSA and harvested with 300 µl 0.1 M NaOH + protease inhibitors. Iodinated ligand imported into cells was measured using a gamma counter. Data are presented as means +SEM of either two or three independent experiments, respectively, normalized to total [^{125}I] input and analyzed by linear regression.

Low-iodine propriothiouracil (LoI/PTU) diet

Eight-week old male *Igsf1*$^{+/y}$ and *Igsf1*$^{\Delta ex1/y}$ mice were fed a LoI/PTU diet *ad libitum* for 3 weeks to disrupt iodothyronine production and induce a severely hypothyroid state (n=10 per genotype, per condition). Mice were sacrificed by CO_2 asphyxiation for collection of blood, pituitaries, and brains. Blood was allowed to clot for 1-2 h at room temperature and serum collected following centrifuging at 3000 rpm for 10 min at room temperature for hormone analysis (described below). Pituitaries were frozen in TRIzol reagent on dry ice and stored at -80°C prior to RNA extraction and qPCR (described below) to analyze *Tshb*, *Trhr*, and *Cga* mRNA expression.

T3/T4 transport in vivo

Eight-week old male *Igsf1*$^{+/y}$ and *Igsf1*$^{\Delta ex1/y}$ mice (n=7 per genotype, per condition) were subjected to a LoI/PTU diet (as described above). During the last four days, mice were injected intraperitoneally (i.p.) with one of four treatments: D-PBS containing 0.002% BSA (control); 5

ng 3,3′,5-triiodo-L-thyronine (L-T3)/g body weight (BW) per day (low T3); 25 ng L-T3/g BW per day (high T3); or 100 ng L-thyroxine (L-T4)/g BW per day (T4). L-T3 and L-T4 were dissolved in 1 M NaOH:EtOH (1:10) at 1 mg/ml and diluted in D-PBS + 0.002% BSA for working concentrations of 1 μg/ml (low T3), 200 μg/ml (high T3), and 100 μg/ml (T4), allowing injection of approximately 200 μl per animal regardless of treatment. Twelve hours after the last injection, animals were sacrificed via CO_2 asphyxiation and blood collected via cardiac puncture. Blood was allowed to clot for 1-2 h at room temperature and then centrifuged at 3000 rpm for 10 min at room temperature and serum was collected for hormone measurement (described above). Brains and pituitaries were immediately dissected for *in situ* hybridization (below) and RT-qPCR analysis (below), respectively.

In situ hybridization (ISH)

All ISH experiments were kindly carried out on a collaborative basis by Dr. Heike Heuer and Denica Doycheva (Leibniz Institute for Age Research – Fritz Lipmann Institute, Jena, Germany) as previously described[180]. Briefly, brains dissected from 12-week old *Igsf1*$^{+/y}$ and *Igsf1*$^{\Delta ex1/y}$ male mice were flash frozen in isopentane cooled to -30°C to -50°C on dry ice and stored at -80°C. Coronal 20 μm slices were cut on a cryostat (Leica), thaw-mounted on silane-treated slides, and stored at -80°C until further processing. [^{35}S]-labeled *Trh* cRNA probes were generated from *Trh* cDNA subclones in Bluescript KSII+ plasmids using *in vitro* transcription, according to standard protocols, and [^{35}S]-UTP and [^{35}S]-CTP labeled nucleotides[181]. The resultant probe corresponds to nucleotides 103-870 of prepro-*Trh* cDNA. The [^{35}S]-labeled *Trh* probe was then diluted in 50 μl RNase-free water and subjected to mild alkaline hydrolysis with 50 μl sodium bicarbonate buffer (80 mM $NaHCO_3$, 120 mM Na_2CO_3; pH 10.2) at 60°C for 25 min. Frozen sections were fixed with 4% PFA in PBS for 60 min at room temperature and rinsed

2X with PBS. Sections were then treated with proteinase K (0.01 mg/ml) for 10 min at 37°C and re-fixed with 4% PFA for 10 min at room temperature. Following the second fixation, sections were incubated in 0.1 M triethanolamine, pH 8 + 0.25% v/v acetic anhydride for 10 minutes at room temperature and rinsed 3X with PBS. Sections were dehydrated with successive ethanol washes of increasing concentrations, followed by air-drying. [^{35}S]-labeled *Trh* cRNA probe was diluted in hybridization buffer (50% formamide, 10% dextran sulfate, 0.6 M NaCl, 10 mM Tris/HCl pH 7.4, 1X Denhardt's solution, 100 µg/ml sonicated salmon sperm DNA, 1 mM EDTA-di-Na and 10 mM dithiothreitol) to a final concentration of 5 x 10^4 dpm/µl and applied to sections. Coverslips were then applied and sections were incubated in a humidity chamber at 58°C for 16 h. Two times standard saline citrate (SSC; 0.3 M NaCl, 0.03 M sodium citrate, pH 7.0) was used to remove coverslips post-hybridization and sections were treated with RNase A (20 µg/ml) and RNase T_1 (1 U/ml) at 37°C for 30 min. Sections were then washed at room temperature with successive SSC concentrations (1X, 0.5X and 0.2X) for 20 min each, incubated in 0.2X SSC at 60°C for 1 h. Sections were dehydrated and exposed to Hyperfilm B-max for 68 h and then dipped in Kodak NTB2 nuclear emulsion and stored at 4°C for 2 weeks. Autoradiograms were developed in Kodak D19 for 4 min and fixed in Rapid Fix for 4 min. Sections were stained with cresyl violet and viewed under dark- and bright-field illuminations. Images were quantified using ImageJ, where background signal was subtracted from the signal intensity and divided by the area of the image.

Hormone measurement

All hormones were kindly measured by Dr. Refetoff and Xiao-Hui Liao (University of Chicago, Chicago, Il, USA) by radioimmunoassays (RIA) as described previously[182]. Briefly, T3 and T4 were first extracted from serum prior to RIA using chloroform-methanol 2:1, containing

1 mM PTU twice, where the final volume of chloroform-methanol extract was approximately 20 times the weight of serum. The iodothyronines were then back-extracted into an aqueous phase using 0.05% $CaCl_2$ added to the chloroform-methanol extract, followed by one extraction with 0.05% $CaCl_2$-MeOH-chloroform (48:49:3). A speed-vac was used to evaporate the pooled aqueous phases, which were then dissolved in RIA buffer. Three blank tubes and three tracer tubes were used for each assay. Blank tubes were used to assess assay background, and contained all reagents save for sample. Tracer tubes were used to assess the recovery of extracted iodothyronines, and contained 1500-2000 cpm of [^{125}I]-labeled T3 or T4 added to the sera. Based on the tracer output, recovery after extraction was 75-85%. The precision of measuring T3 and T4 by extraction and RIA assay was confirmed by liquid chromatography (LC, Shimadzu, Columbia, MD) followed by tandem mass spectrometry (MS/MS, API 4000 from Applied Biosystems) in 20 samples. Aliquots of the extracted serum were submitted to T3, T4 or TSH measurement by RIAs as follows. Serum total T4 concentration was measured by coated-tube RIA Kit according to manufacturer's instructions and modified for mouse using 25 µl serum. The limit of T4 detection in serum was 0.25 µg/dl and the assay sensitivity was 125 pg T4 per tube. Serum total T3 was measured by sensitive RIA[183] and the specific antibody against T3 was provided by Maria Jesus Obregon. Eight to 13 µl T3 was used for extraction, with an average recovery of 78%. The assay sensitivity was 1 pg T3 per tube and assay sensitivity was 10 ng/dl. Serum total TSH was measured using 10 µl serum in a sensitive, heterologous, disequilibrium, double-antibody precipitation RIA, as described in Pohlenz, J et al. (1999)[184].

Quantitative RT-PCR (qPCR)

Murine pituitary and hypothalamic RNA was extracted using TRIzol reagent, following the manufacturer's instructions. Approximately 1 µg of RNA was reverse transcribed into cDNA

using 50 ng random hexamer primers and Moloney murine leukemia virus reverse transcriptase (MMLV-RT). Contaminating DNA was removed prior to reverse transcription using RQ1 DNase and 2 µl cDNA was used for qPCR using EvaGreen and 0.4 pmol of *Trhr*, *Tshb*, *c-fos*, *Cga,* or *Rpl19* primers (Table 1.4) on a Corbett Rotor-Gene 6200 HRM (Corbett Life Science), according to the EvaGreen real-time cycling protocol. Transcript levels were normalized relative to the housekeeping gene ribosomal protein L19 (*Rpl19*) and results analyzed using the $2^{-\Delta\Delta Ct}$ method.

TRH stimulation

Eight-week old male mice were bled by submandibular venipuncture and 10-15 µl of blood was collected prior to injection with TRH (baseline). Mice were then injected with 10 µg/kg i.p. TRH (1 µg/ml, approximately 200 µl injected per animal) or 10 µl/kg D-PBS. Fifteen minutes post-injection, mice were sacrificed via CO_2 asphyxiation and blood collected via cardiac puncture. Blood was allowed to clot for 1-2 h at room temperature and centrifuged at 3000 rpm for 10 min at room temperature. Serum was collected for hormone measurement (as described above). Pituitaries were collected in 500 µl TRIzol and frozen on dry ice for RNA extraction and qPCR analysis (described above).

Statistical analysis

Statistical analysis of the qPCR and hormone data from the LoI/PTU and T3/T4 transport *in vivo*, and TRH stimulation studies consisted of 2-way ANOVA followed by post-hoc Bonferroni-corrected t-tests to compare the effects of treatment between genotypes. Results of 2-way ANOVA analysis are presented as an F-distribution (F) along with the degrees of freedom numerator (DFn) and degrees of freedom denominator (DFd) and the subsequent p-value associated with the ANOVA. Significant differences between genotypes under various

conditions are reported as a t-value and the degrees of freedom associated with the p-value as determined by the Bonferroni-corrected Student's t-test. T4 serum levels in T3/T4 replacement *in vivo* studies were analyzed by Student's t-test. Animals were only removed from studies post-analysis for genotyping errors as determined by *Igsf1-ex1* qPCR analysis. Some animals were removed from qPCR experiments prior to analysis due to low RNA concentrations (<100 ng/ul), and genotype and treatment was unknown at the time. The T3/T4 *in vitro* studies were analyzed using linear regression analysis and slopes were compared for significant difference. All statistical studies were conducted using GraphPad Prism 5.0. Significance was assessed relative to $p<0.05$.

Tables

Table 2.1 – Genotyping primers

Primer	Sequence
Igsf1^{+} forward	5'-TTTGCGGCATCTGGAGGAG-3'
Igsf1^{+} reverse	5'-GGGAGCAGTTTGATTTACGGC-3'
Igsf1$^{\Delta ex1}$ forward	5'-TGTTCTCCTCTTCCTCATCTCC-3'
Igsf1$^{\Delta ex1}$ reverse	5'-ACCCTTTCCAAATCCTCAGC-3'

Table 2.2 – Primers for generation of constructs

Gene	Sense	Antisense
Mct8	5'-ACTGGAATTCGCCGCGATGGCGCTGCCA-3'	5'-GCCGCTCGAGAATGGGCTCTTCAGGTGT-3'
Mct10	5'-CGGAATTCTCGGGACATGGTGCCGTCCCA-3'	5'-CCGCTCGAGCGGCATTAAATAATCGAGGCGGAG-3'
Crym	5'-CGGAATTCAAGGCAGGCGGCGAGATGAAGC-3'	5'-CCGCTCGAGCGGTTCCTTCAACTCACTTGC-3'

Table 2.3 – Mutagenesis primers

Mutation	Sense	Antisense
Mct10-HindIII Removal	5'-CTTCTCCAGGAGAAAGCTCAGTCCTCCAAAAAAAGTC-3'	5'-GACTTTTTTTGGAGGACTGAGCTTTCTCCTGGAGAAG-3'

Table 2.4 – RT-qPCR primers

Gene	Sense primer	Antisense primer
Trhr	5'-CTCCCCAACATAACCGACAG-3'	5'-GCAGAGAAACTGGGCTTTGA-3'
Tshb	5'-GAACGGTGGAAATACCAGGA-3'	5'-AGAAAGACTGCGGCTTGGTGCA-3'
Cga	5'-TCCCTCAAAAAGTCCAGAGC-3'	5'-GAAGAGAATGAAGAATATGCAG-3'

c-fos	5'-GGAGCTGACAGATACACTCCAA-3'	5'-GAGGCCACAGACATCTCCTC-3'
Rpl19	5'-CGGGAATCCAAGAAGATTGA-3'	5'-TTCAGCTTGTGGATCTGCTC-3'

Chapter 3: Results

IGSF1-CTD and MCT8 interact at the plasma membrane in vitro

Given that IGSF1-CTD and MCT8 are both expressed at the apical membrane of the CP of mice (Beata Bak, unpublished), and rats[171], and both proteins play a role in the HPT axis[127,157], we hypothesized that IGSF1-CTD and MCT8 might physically and/or functionally interact at the cell membrane. To test this hypothesis, we transfected HEK293 cells with human MCT8-GFP (Figure 3.3a, lane 2), human myc-IGSF1-HA (lane 3) or both MCT8-GFP and myc-IGSF1-HA (lane 4) and performed CSB/IP, with lysates analyzed via western blotting. As described previously[157,167], human IGSF1-HA migrated as a doublet of approximately 140 kDa (Figure 3.1a, lanes 2 and 4), similar to the doublet seen in the pituitaries of adult male mice (Figure 3.2, lane 4)[157]. Human MCT8-GFP protein migrated at approximately 95 kDa (Figure 3.1a, lanes 3 and 4) and MCT8-GFP was co-immunoprecipitated with IGSF1-HA (lane 4), indicating that the two proteins interact when co-expressed *in vitro*. Furthermore, as reflected in the results of the CSB, the mature IGSF1-HA glycoprotein was detected at the plasma membrane when expressed alone (lane 2), or with MCT8-GFP (lane 4). Moreover, biotinylated MCT8-GFP was co-precipitated with IGSF1, indicating that the proteins interact at the plasma membrane.

To confirm the specificity of the interaction and to determine whether this interaction also occurs between murine IGSF1-CTD and MCT8, we transfected HEK293 cells with either murine IGSF1-4 (Figure 3.1b, lane 2), murine MCT8-HA (lane 3), or murine MCT10-HA (lane 4) alone, or IGSF1-4 co-expressed with either MCT8-HA (lane 5) or MCT10-HA (lane 6). MCT10 is closely related to MCT8, sharing 49% amino acid identity, allowing us to observe the specificity of the interaction between IGSF1 and MCT8[185]. MCT8-HA migrated at 65 kDa (Figure 3.1b, lanes 3 and 5), whereas MCT10-HA migrated at 55 kDa (lanes 4 and 6) and

IGSF1-4 migrated as a doublet of approximately 140 kDa (lanes 2, 5 and 6). The mature IGSF1-CTD co-precipitated with MCT8-HA (lane 5), but not MCT10-HA (lane 6). These data confirm that murine IGSF1-4 interacts with murine MCT8-HA *in vitro* and this interaction is specific to MCT8.

IGSF1-CTD is expressed in the choroid plexus and pituitary of male Igsf1$^{+/y}$ mice

That IGSF1 and MCT8 are expressed in the CP relies on evidence from immunofluorescence (IF) conducted on embryonic mice (Bak, unpublished) and immunohistochemistry (IHC) on adult rats[186]; however, the antibody used in these analyses cross-reacts with other proteins in western blot analyses of brain homogenates (Robakis and Bak, unpublished). Therefore, to determine whether the signals detected in CP are authentic IGSF1, we used western blot analyses of deglycosylated CP protein lysates from adult mice (Figure 3.2). We observed a robust band of approximately 135 kDa in untreated CP lysates (lane 1), which was equivalent in size to the mature IGSF1 glycoform observed in the adult murine pituitary (lane 4). However, unlike the case in pituitary (lane 4), there was no distinguishable immature glycoform in the CP (lane 1). Treatment with EndoH to remove N-linked high mannose sugars resulted in a slight decrease in size of the IGSF1-CTD immunoreactive band in the CP (lane 2). A similar shift was observed for the mature glycoform in the pituitary (lane 5). In both cases, this shift suggests that the mature protein possesses hybrid glycosylation. EndoH also caused a shift of the immature glycoform down to about 90 kDa in the pituitary lysates (lane 5). No such protein is observed in CP, further indicating that IGSF1-CTD expressed in CP matures fully. Removal of immature, complex, and hybrid sugars with PNGaseF deglycosylated both the mature and immature IGSF1-CTD glycoproteins to reveal the unmodified size of approximately 90 kDa in both the CP and pituitary (lanes 3 and 6). These results indicate that IGSF1-CTD is

indeed expressed in adult murine CP as well as pituitary. Further confirmation came from the analysis of *Igsf1*$^{\Delta ex1/y}$ mice, which lack IGSF1-CTD expression in the CP (Figure 3.3).

IGSF1 is absent in adult male Igsf1$^{\Delta ex1/y}$ *mice, while MCT8 expression is similar in both genotypes*

The data in Figure 3.2 suggested that IGSF1-CTD is expressed to similar extents in the pituitary and CP of *Igsf1*$^{+/y}$ mice. MCT8 is robustly expressed in the CP (references, Figure 3.2). Here we examined the relative expression of MCT8 in the CP of *Igsf1*$^{+/y}$ and *Igsf1*$^{\Delta ex1/y}$ mice. MCT8 protein expression is expressed at a significantly higher level in CP than in pituitary, and extended exposures were required to detect an immunoreactive MCT8 signal in the pituitary. In addition, MCT8 expression in both tissues was similar in *Igsf1*$^{+/y}$ and *Igsf1*$^{\Delta ex1/y}$ mice. IGSF1 expression is similar in both the CP and pituitary of *Igsf1*$^{+/y}$ mice, but varies widely between individual animals. IGSF1 expression appears absent in the pituitary and CP of *Igsf1*$^{\Delta ex1/y}$ mice.

IGSF1-CTD does not affect MCT8 localization in the choroid plexus

Given the role of CD147 in basolateral sorting of MCT1, and the interaction between IGSF1 and MCT8, we hypothesized that IGSF1 might act as an ancillary protein to MCT8, directing its subcellular localization. If true, in the absence of IGSF1-CTD, MCT8 should be impaired in its apical membrane trafficking, resulting in a basolateral localization in the CP of *Igsf1*$^{\Delta ex1/y}$ mice. However, an MCT8 immunoreactive signal was detected in the apical membrane of the CP in both *Igsf1*$^{+/y}$ and *Igsf1*$^{\Delta ex1/y}$ mice (Figure 3.4a). The lack of an MCT8 signal in the CP of *Mct8*-ko mice confirmed the specificity of the antibody (Figure 3.4b).

IGSF1-CTD does not affect MCT8 transport of T3 or T4 in vitro

In order to elucidate the functional relevance, if any, of the IGSF1-CTD:MCT8 interaction, we next investigated whether co-expression of IGSF1-CTD impacts MCT8 influx of the iodothyronines T3 and T4 in HeLa cells. We examined MCT8-mediated transport of [^{125}I]-T3 into HeLa cells. Cells were transfected with IGSF1-HA and MCT8-GFP alone or in combination. Cells were co-transfected with the T3/T4 binding protein CRYM to prevent the efflux of imported hormone[187]. MCT8 potentiated [^{125}I]-T3 import (Figure 3.5a $F_{3,4}$=11.9775, p=0.01817); however, this effect was unchanged by co-expression of IGSF1. We observed a similar pattern of results with MCT8-mediated [^{125}I]-T4 influx (Figure 3.5b; $F_{3,4}$=61.396, p=0.0008411). Thus, IGSF1 does not appear to affect MCT8 mediated transport of either T3 or T4 in vitro. However, it is possible that a key interacting partner was missing from *in vitro* analyses, and thus we resolved to study the effects of IGSF1 on MCT8 transport in vivo.

MCT8 transport of T3 and T4 is not impaired at the level of the hypothalamus or pituitary in Igsf1$^{\Delta ex1/y}$ male mice

To address the potential effect of IGSF1 on MCT8 transport of T3 across the BCSF and into the hypothalamus, we investigated the ability of exogenous TH to negatively regulate TH-sensitive genes in *Igsf1*$^{+/y}$ mice compared to *Igsf1*$^{\Delta ex1/y}$. Experiments by Trajkovic et al. [2007] demonstrated that *Mct8*-ko mice had increased *Trh* expression in the PVN under control conditions, and that replacement with physiological doses of T3 were ineffective at suppressing *Trh* mRNA levels, while supraphysiological doses of T3 were able to suppress *Trh* levels, but to a lesser extent than in wild-type mice[188]. If IGSF1 affects MCT8-mediated transport of T3 into the PVN, we would expect that in *Igsf1*$^{\Delta ex1/y}$ mice the absence of IGSF1 would lead to a similar impairment in T3-mediated downregulation of *Trh* mRNA expression. However, while *Trh*

mRNA levels were significantly downregulated in response to iodothyronine treatment (Figure 3.6b $F_{3,19}$=76.28, p<0.0001), *Trh* mRNA levels in the PVN did not differ between genotypes (Figure 3.6b, $F_{1,19}$=0.03, p=0.8692). Interestingly, the TSH response to hypothyroidism was blunted in *Igsf1*$^{\Delta ex1/y}$ mice compared with controls (Figure 3.7a t=2.92, p<0.05). TSH serum levels were downregulated in response to iodothyronine treatment ($F_{3,62}$=59.61, p<0.0001) to equivalent extents in *Igsf1*$^{+/y}$ and *Igsf1*$^{\Delta ex1/y}$ across iodothyronine treatment conditions ($F_{1,62}$=2.04, p=0.1580). As expected, T3 serum levels were significantly higher in the supra-physiological dose compared to the physiological T3 dose (Figure 3.7b, $F_{1,24}$=27.3, p<0.0001). T3 serum levels did not differ between genotypes in either treatment condition ($F_{1,24}$=0.15, p=0.7012). Finally, there was no difference in serum T4 levels in *Igsf1*$^{+/y}$ and *Igsf1*$^{\Delta ex1/y}$ male mice in the T4 treatment group (Figure 3.7c, t=0.2108, df=17, p=0.8356).

Tshb mRNA levels were significantly downregulated by iodothyronine replacement (Figure 3.8a, $F_{3,49}$=24.66, p<0.0001); however, *Tshb* mRNA levels did not differ between genotypes ($F_{1,49}$=1.72, p=0.1962). *Cga* mRNA levels were negatively regulated by iodothyronines (Figure 3.8b, $F_{3,45}$=0.48, p=0.7012), but genotypes did not differ ($F_{1,45}$=0.35, p=0.5573). *Trhr* mRNA levels were downregulated by iodothyronine replacement (Figure 3.8c, $F_{3,49}$=8.19, p=0.0002), but there was no effect of genotype ($F_{1,49}$=0.34, p=0.5642). Interestingly, the early response gene to TRH signaling, *c-fos,* levels were not affected by treatment (Figure 3.8d, $F_{3,49}$=91.67, p=0.1870). Finally, *Igsf1* expression was significantly downregulated in the pituitaries of *Igsf1*$^{\Delta ex1/y}$ mice compared with *Igsf1*$^{+/y}$ mice in all treatment groups, confirming the genotyping of our animals (Figure 3.8e; $F_{1,49}$=207.43, p<0.0001), and there is a significant effect of treatment on expression of *Igsf1* ($F_{3,49}$=2.98, p=0.0403), suggesting that *Igsf1* is regulated by

THs. Additionally, while not significant, there appears to be increased suppression of pituitary TH-sensitive genes to low-T3 in *Igsf1*$^{\Delta ex1/y}$ mice.

Male Igsf1$^{\Delta ex1/y}$ *mice have a blunted TSH response to impaired iodothyronine production*

To investigate the effects of IGSF1-CTD protein absence on TSH, we examined the consequences of removing T3 and T4 negative feedback to the pituitary and hypothalamus by abolishing TH production using the LoI/PTU diet. T3 and T4 levels did not differ between genotypes in animals on the control diet (Figure 3.9a, t=0.1411, df=17, p=0.8894; Figure 3.9b, t=0.2617, df=18, p=0.7965), and the LoI/PTU diet effectively impaired TH production (Figure 3.9a, $F_{1,35}$=1597.33, p<0.0001; Figure 3.9b, $F_{1,36}$=574.23, p<0.0001). In both genotypes, circulating TSH levels, which did not differ on the control diet (Figure 3.9c, t=0.037, df=18, p>0.05), were significantly elevated in response to the LoI/PTU diet (Figure 3.9c, $F_{1,36}$=117.98 p<0.0001); however, the response was significantly blunted in *Igsf1*$^{\Delta ex1/y}$ compared with *Igsf1*$^{+/y}$ mice (t=4.385, df=18,p<0.001).

LoI/PTU treated animals showed significant increase in pituitary *Tshb* (Figure 3.10a, $F_{1,36}$=49.59, p<0.001), *Cga* (Figure 3.10b, $F_{1,35}$=20.05, p<0.001), and *Trhr* (Figure 3.10c, $F_{1,36}$= p<0.001) mRNA levels compared to controls, with no significant differences between genotypes. Impaired TSH release in the absence of differences in TSH subunit expression suggested impaired TRH release and/or signaling in these *Igsf1*$^{\Delta ex1/y}$ mice. However, the absence of a difference in TRH expression argues against the former possibility. To address the latter, we next examined the response of wild-type and knockout mice to exogenous TRH.

TSH response to TRH stimulation is blunted in Igsf1$^{\Delta ex1/y}$ male mice

When made hypothyroid, *Igsf1*$^{\Delta ex1/y}$ mice have a blunted TSH response compared to *Igsf1*$^{+/y}$ mice, which may be due to decreased TRH hormone expression by the hypothalamus, or insensitivity of the pituitary to increased TRH signaling. As in previous experiments, basal TSH levels did not differ between genotypes (Figure 3.11a and b, t=0.6563, df=11, p=0.5251). TRH treatment significantly increased TSH secretion in both *Igsf1*$^{+/y}$ and *Igsf1*$^{\Delta ex1/y}$ mice compared with saline treatment (Figure 3.11b and c, $F_{1,21}$=90.42, p<0.0001), and there was a significant difference between genotypes ($F_{1,21}$=13.59, p=0.0014). TSH response to exogenous TRH treatment was significantly blunted in *Igsf1*$^{\Delta ex1/y}$ mice compared with *Igsf1*$^{+/y}$ mice (t=5.108, df=21, p<0.001). Expression of *Tshb* (Figure 3.12a, genotype, $F_{1,17}$=0.79, p=0.5361; treatment, $F_{1,17}$=0.09, p=0.7733), and *Cga* (Figure 3.8b; genotype, $F_{1,16}$=0.34, p=0.5703; treatment, $F_{1,16}$=1.16, p=0.2973) were not significantly affected by either treatment or genotype. *Trhr* expression is not significantly affected by TRH treatment (Figure 3.12c; $F_{1,16}$=2.10, p=0.1670), however, *Trhr* mRNA expression is significantly downregulated in the pituitaries of control and TRH treated *Igsf1*$^{\Delta ex1/y}$ mice ($F_{1,16}$=11.45, p=0.0038). The blunted serum TSH levels observed in TRH treated *Igsf1*$^{\Delta ex1/y}$ mice may be the result of either a TRH signaling defect, or lower pituitary TSH protein content. To assess TRH signaling in the pituitary of *Igsf1*$^{\Delta ex1/y}$ mice, we analyzed *c-fos* mRNA expression and observed a significant effect of genotype on *c-fos* mRNA expression (Figure 3.12d, $F_{1,16}$=6.76, p=0.0193), with a significantly blunted *c-fos* response to TRH treatment in *Igsf1*$^{\Delta ex1/y}$ mice (t=3.182, df=16, p<0.05). There was an upward trend in *c-fos* mRNA expression in TRH-treated *Igsf1*$^{+/y}$ mice, but no effect of treatment overall (F=3.03, DFn=1, DFd=16, p=0.1008). Finally, *Igsf1* expression was significantly ablated in *Igsf1*$^{\Delta ex1/y}$ mice ($F_{1,15}$=181.36, p<0.0001), but no effect of treatment on *Igsf1*expression was observed

($F_{1,15}$=0.80, p=0.3857). TRH signaling appears impaired in *Igsf1*$^{\Delta ex1/y}$ mice and may be secondary to reduced *Trhr* expression in the pituitary.

Figure legends

Figure 3.1 – IGSF1-CTD and MCT8 interact *in vitro*. (A) HEK293 cells transfected with either pcDNA3 (lane 1), pcDNA3 and human myc-IGSF1-HA (lane 2, IGSF1-HA), pcDNA3 and human MCT8-GFP (lane 3, MCT8-GFP), or IGSF1-HA and MCT8-GFP (lane 4) were subjected to cell surface biotinylation and protein lysates were immunoprecipitated with anti-HA beads. Total lysates and immunoprecipitated lysates were run on SDS-PAGE and immunoblotted with anti-HA, anti-GFP or anti-BTUB antibody. The immunoprecipitated proteins were also probed with Streptavidin to detect immunoprecipitated cell surface proteins.**(B)** HEK293 cells transfected with either, pcDNA3 alone (lane 1), pcDNA3 and murine IGSF1 isoform 4 (lane 2, IGSF1-4), pcDNA3 and murine MCT8-HA (lane 3), pcDNA3 and murine MCT10-HA (lane 4), IGSF1-4 and MCT8-HA (lane 5) or IGSF1-4 and MCT10-HA (lane 6). Protein lysates were immunnoprecipitated with anti-HA beads and total lysates and immunoprecipitated lysates were run on SDS-PAGE. Membranes were probed with anti-HA, IGSF1-CTD antibody, and anti-BTUB as control. Data represents results from more than three independent experiments.

Figure 3.2 – IGSF1 is expressed in the choroid plexus and pituitary of male *Igsf1*$^{+/y}$ mice. Protein lysates from the CP and pituitary of three 12-week old male wild-type mice were pooled and deglycosylated with PNGaseF or EndoH. Lysates were run on SDS-PAGE and immunoblotted with IGSF1-CTD antibody and β-actin (ACTB) as control.

Figure 3.3 - IGSF1 is absent in the choroid plexus and pituitary of male *Igsf1*$^{\Delta ex1/y}$ mice while MCT8 is similarly expressed in both genotypes. Protein lysates from the CP and pituitary of three *Igsf1*$^{+/y}$ or *Igsf1*$^{\Delta ex1/y}$ (WT or KO)12-week old malemice. Lysates were run on SDS-PAGE and immunoblotted with IGSF1-CTD or MCT8 antibody and with β-tubulin (BTUB) as control.

Figure 3.4 – MCT8 protein localization in the choroid plexus is not altered in *Igsf1*$^{\Delta ex1/y}$ mice. Immunofluorescence of 10 μm coronal brain sections of *Igsf1*$^{+/y}$ and *Igsf1*$^{\Delta ex1/y}$ 8-week old littermate males and 12-week old male *Mct8*-ko probed with the anti-MCT8 antibody and DAPI was used as a cell marker.

Figure 3.5 – IGSF1-CTD does not affect MCT8 transport of radiolabeled iodothyronines *in vitro*. (A) Intracellular [^{125}I] levels from HeLa cells transfected with equivalent levels of *IGSF1, MCT8* and *Crym* cDNA treated with 1 nM [^{125}I]-T3 for 0, 15, and 30 min. **(B)** Intracellular [^{125}I] levels from transfected HeLa cells treated with 1 nM [^{125}I]-T4 for 0, 15 and 30 min.

Figure 3.6 – *Trh* expression in the PVN does not differ between *Igsf1*$^{+/y}$ and *Igsf1*$^{\Delta ex1/y}$ mice in response to hypothyroidism or exogenous TH replacement. Brains were collected and flash-frozen for ISH analysis of *Trh* mRNA expression in the paraventricular nucleus (PVN) of coronal brain sections (WT saline n=3, KO, n=3; WT low T3, n=4, KO, n=2; WT high T3 n=3, KO n=3; WT T4 n=4, KO n=5). **(A)** Representative images of *Trh* expression in WT and KO PVN under the various conditions **(B)** Quantification of average *Trh* ISH signal in WT and KO PVN in each condition. Bars with different letters are significantly different from one another.

Figure 3.7– Exogenous iodothyronine treatment suppresses TSH release similarly in *Igsf1*$^{+/y}$ and *Igsf1*$^{\Delta ex1/y}$ mice. Hypothyroid 8-week old male *Igsf1*$^{+/y}$ (WT) and *Igsf1*$^{\Delta ex1/y}$ (KO) mice, treated with either saline (WT, n=10; KO, n=10), low T3 (WT, n=8; KO, n=7), high T3 (WT, n=10; KO, n=7), or T4 (WT, n=9; KO, n=9) were sacrificed and blood collected 7 h after the final treatment for hormone analysis. Means + SEM of **(A)** TSH in all treatment groups, **(B)** T3 in both low T3 and high T3 treatment groups, and **(C)** T4 in the T4 treatment group are presented, (bars with the same letter do not differ significantly).

Figure 3.8– Exogenous iodothyronine treatment significantly decreases mRNA expression of TH-sensitive genes in the pituitary and PVN of hypothyroid *Igsf1*$^{+/y}$ and *Igsf1*$^{\Delta ex1/y}$ mice. Hypothyroid 8-week old male *Igsf1*$^{+/y}$ (WT) and *Igsf1*$^{\Delta ex1/y}$ (KO) mice either saline (WT, n=10; KO, n=8), low T3 (WT, n=7; KO, n=5), high T3 (WT, n=8; KO, n=6), or T4 (WT, n=8; KO, n=5) over the last 4 days of the LoI/PTU treatment. Pituitaries were collected for qPCR analysis of **(A)** *Tshb*, **(B)** *Cga,* **(C)** *Trhr* **(D)** *c-fos* and **(E)** *Igsf1-ex1* mRNA levels. Means +SEM are presented. Means and SEM of integrated signal intensity relative to background are presented. Bars with the same letter do not differ significantly.

Figure 3.9 – *Igsf1*$^{\Delta ex1/y}$ mice have a blunted TSH response to artificially-induced hypothyroidism. Serum from 12-week old male *Igsf1*$^{+/y}$ (WT) and *Igsf1*$^{\Delta ex1/y}$ (KO) mice fed either a control diet or a LoI/PTU diet (n=10 per genotype, per group) for 3 weeks was extracted for hormone analysis of **(A)** T3 and **(B)** T4 measured in control groups, and **(C)** TSH in both treatment groups. The means +SEM are presented and means with different letters differ significantly from one another.

Figure 3.10 – Artificially-induced hypothyroidism increases expression of genes expressed in the pituitary of both *Igsf1*$^{+/y}$ and *Igsf1*$^{\Delta ex1/y}$ mice. RNA from pituitaries and hypothalami of 12-week old male *Igsf1*$^{+/y}$ (WT) and *Igsf1*$^{\Delta ex1/y}$ (KO) mice fed either a control or LoI/PTU diet for three weeks was extracted (n=10 pituitaries per genotype per treatment) for qPCR analysis using primers in Table 2.4 to assess **(A)** *Tshb*; **(B)** *Cga*; and **(C)** *Trhr* mRNA levels in the pituitary and **(D)** *Trh* mRNA levels in the hypothalamus. Data are means +SEM and means with the same letter do not differ significantly

Figure 3.11 – TSH response to exogenous TRH treatment is blunted in *Igsf1*$^{\Delta ex1/y}$ mice. Blood was collected from 8-week old male *Igsf1*$^{+/y}$ (WT, n=12) and *Igsf1*$^{\Delta ex1/y}$ (KO, n=13) pre-treatment and 15 min post-treatment for measurement of serum TSH. Mice were treated with either saline (WT, n=6, KO, n=7), or TRH (WT, n=6, KO, n=6) and TSH serum levels for each group pre- and post-treatment are presented.

Figure 3.12 – TRH stimulation did not affect expression of selected genes in the pituitaries of *Igsf1*$^{+/y}$ *or Igsf1*$^{\Delta ex1/y}$ mice. Following TRH or saline treatment, 8-week old *Igsf1*$^{+/y}$ (WT; saline n=4, TRH n=5) and *Igsf1*$^{\Delta ex1/y}$ (KO; saline n=7, TRH n=5) male mice were sacrificed and pituitaries were collected for qPCR analysis of **(A)***Tshb*, **(B)** *Cga*, **(C)** *Trhr*, **(D)** *c-fos* and **(E)** *Igsf1-ex1*mRNA expression levels (n=7 per genotype, per condition). One animal from the WT saline group was not analyzed due to low RNA yield (less than 100 ng/µl). Data are presented as means +SEM, and means with the same letter do not differ significantly.

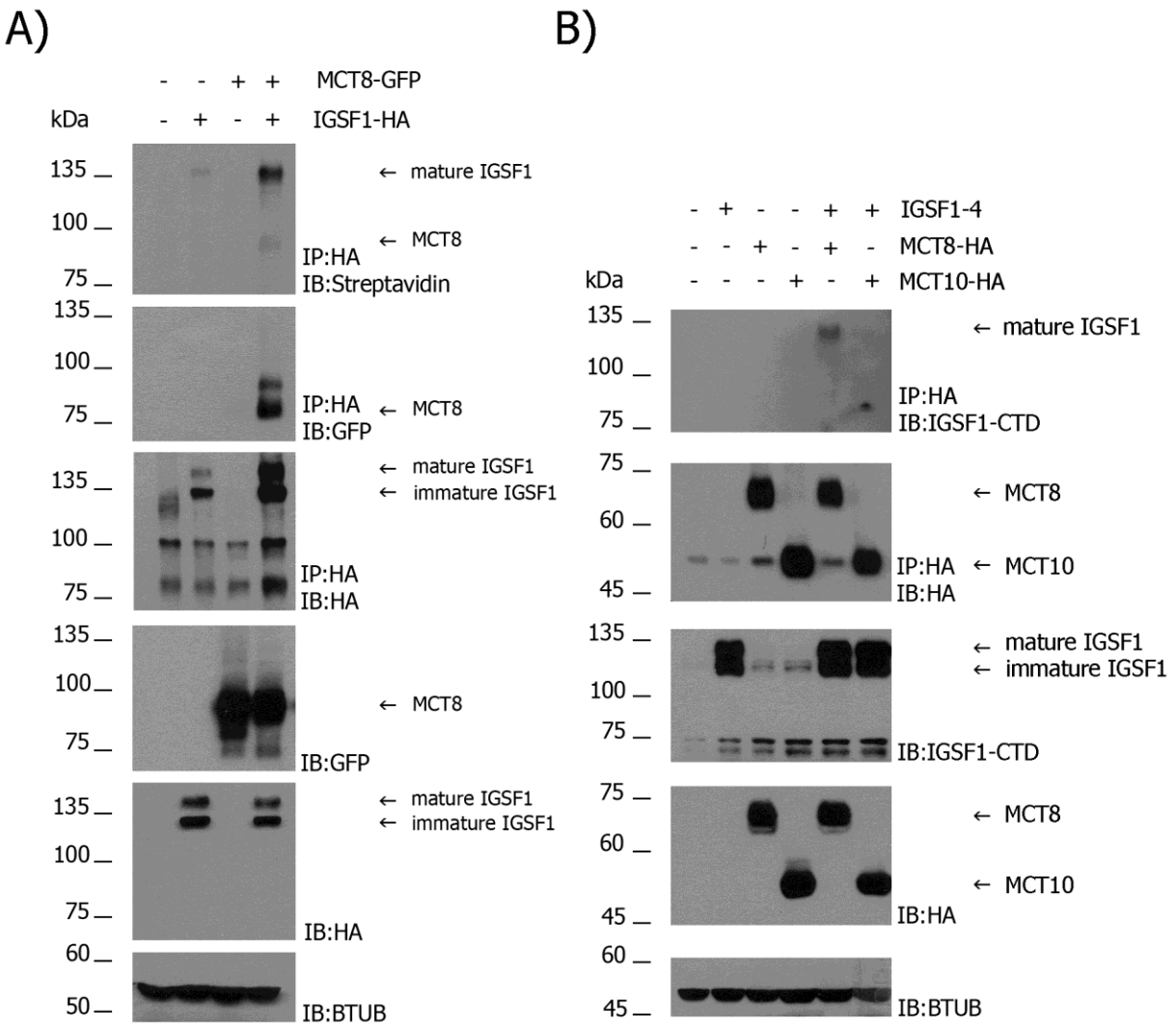
A)
- - + + MCT8-GFP
kDa - + - + IGSF1-HA
135
100
75
← mature IGSF1
← MCT8
IP:HA
IB:Streptavidin
135
100
75
IP:HA
IB:GFP
← MCT8
135
100
75
← mature IGSF1
← immature IGSF1
IP:HA
IB:HA
135
100
75
← MCT8
IB:GFP
135
100
75
← mature IGSF1
← immature IGSF1
IB:HA
60
50
IB:BTUB
B)
- + - - + + IGSF1-4
- - + - + - MCT8-HA
kDa - - - + - + MCT10-HA
135
100
75
← mature IGSF1
IP:HA
IB:IGSF1-CTD
75
60
45
← MCT8
IP:HA
IB:HA
← MCT10
135
100
75
← mature IGSF1
← immature IGSF1
IB:IGSF1-CTD
75
60
45
← MCT8
← MCT10
IB:HA
60
45
IB:BTUB

Figure 3.1

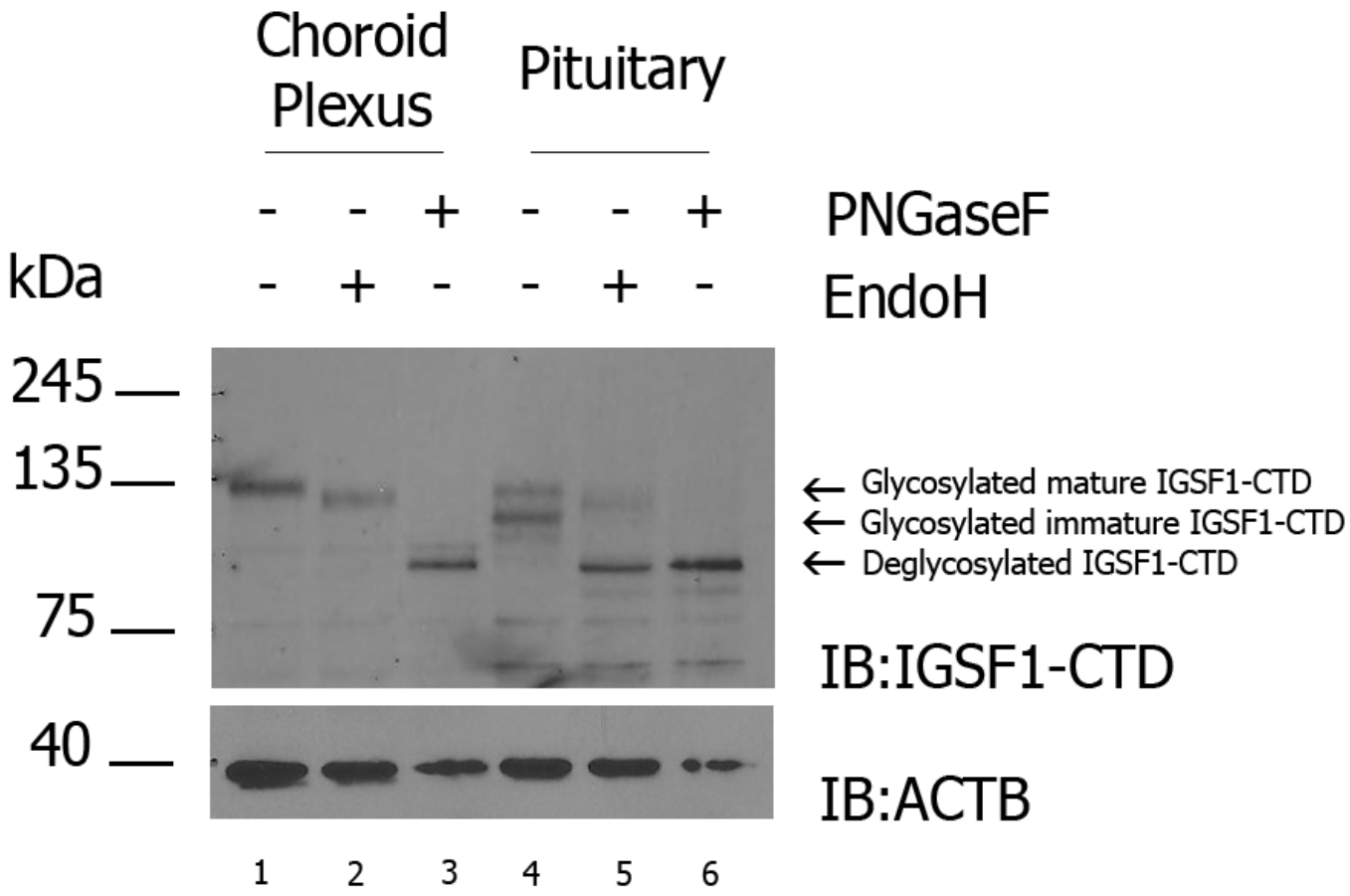
Choroid Plexus
Pituitary
- - + - - +
PNGaseF
kDa
- + - - + -
EndoH
245
135
75
40
← Glycosylated mature IGSF1-CTD
← Glycosylated immature IGSF1-CTD
← Deglycosylated IGSF1-CTD
IB:IGSF1-CTD
IB:ACTB
1 2 3 4 5 6

Figure 3.2

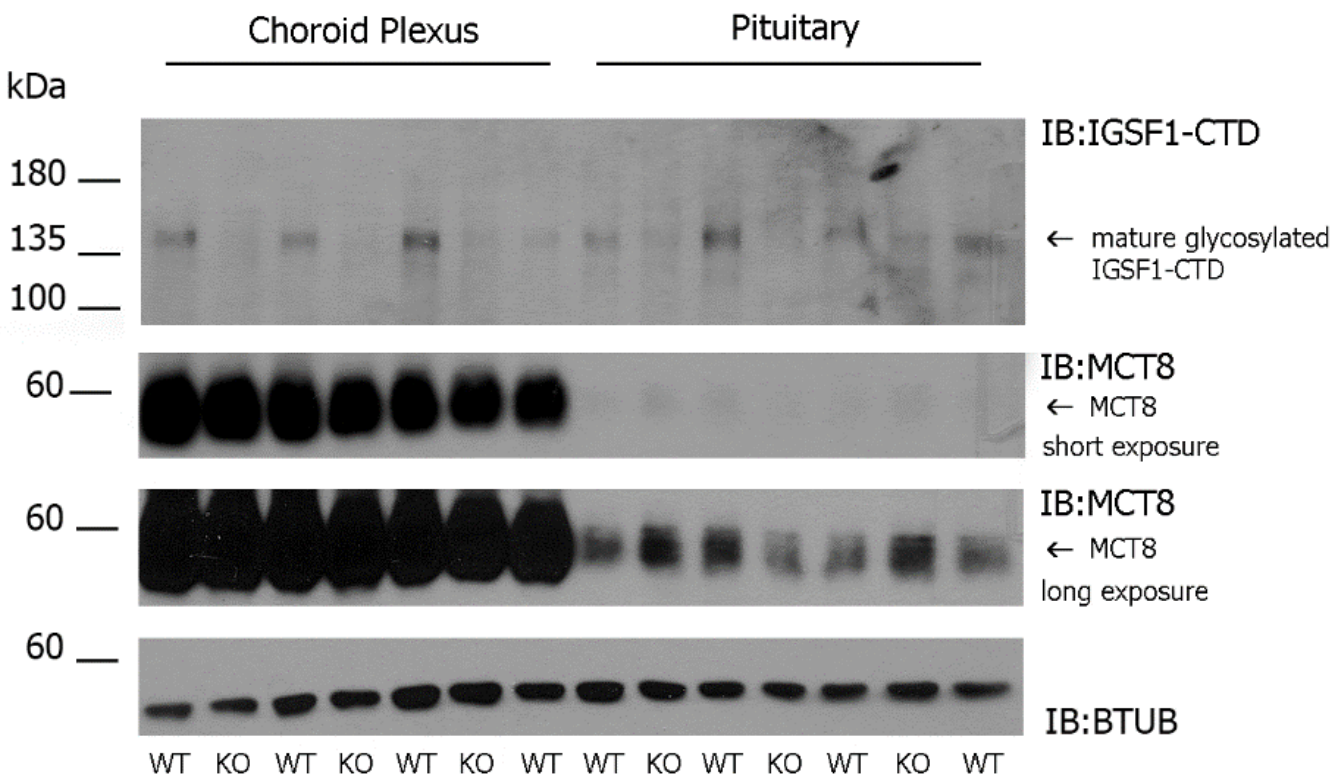
Choroid Plexus
Pituitary
kDa
180
135
100
60
60
60
IB:IGSF1-CTD
← mature glycosylated IGSF1-CTD
IB:MCT8
← MCT8
short exposure
IB:MCT8
← MCT8
long exposure
IB:BTUB
WT KO WT KO WT KO WT WT KO WT KO WT KO WT

Figure 3.3

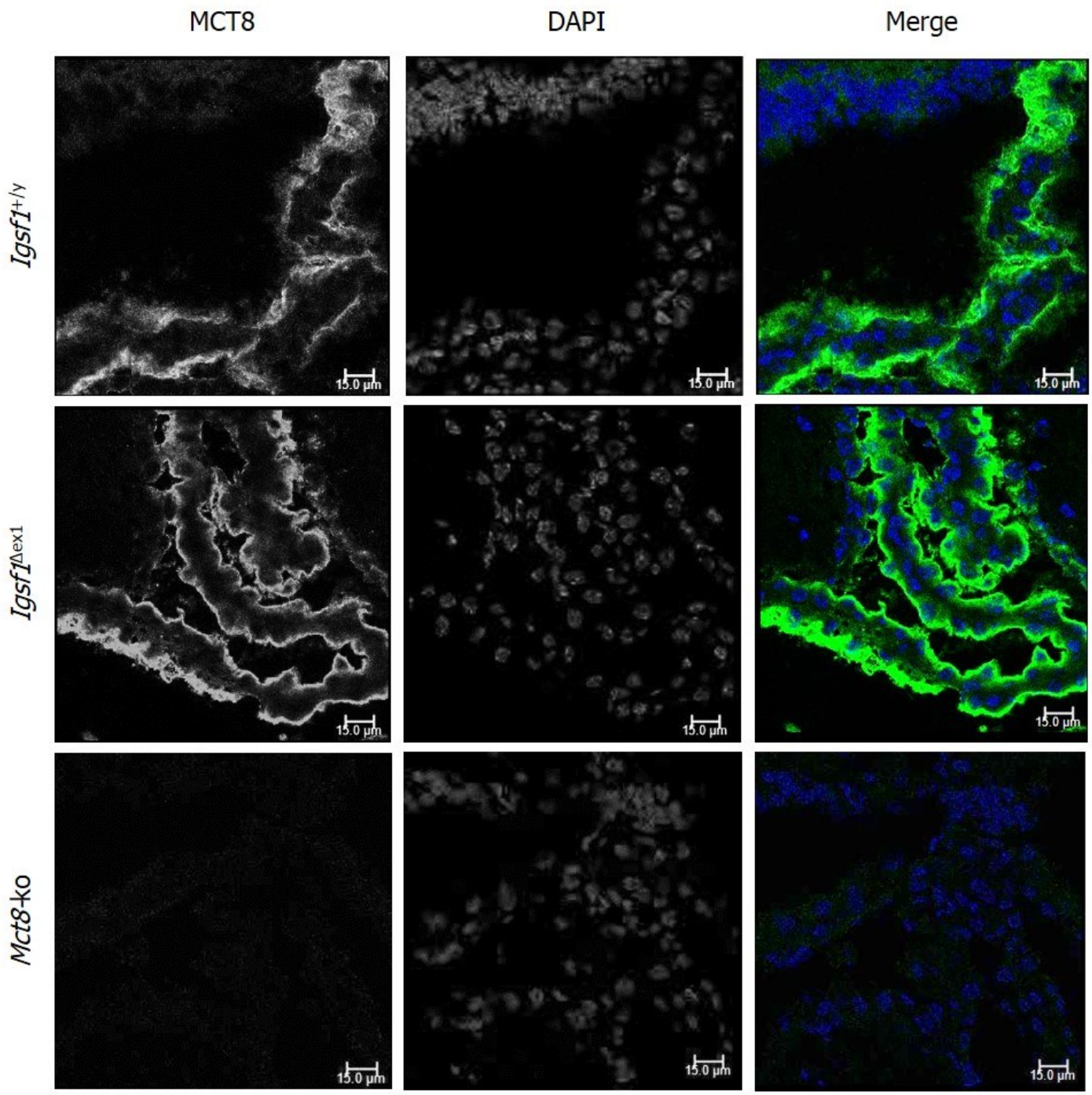

Figure 3.4

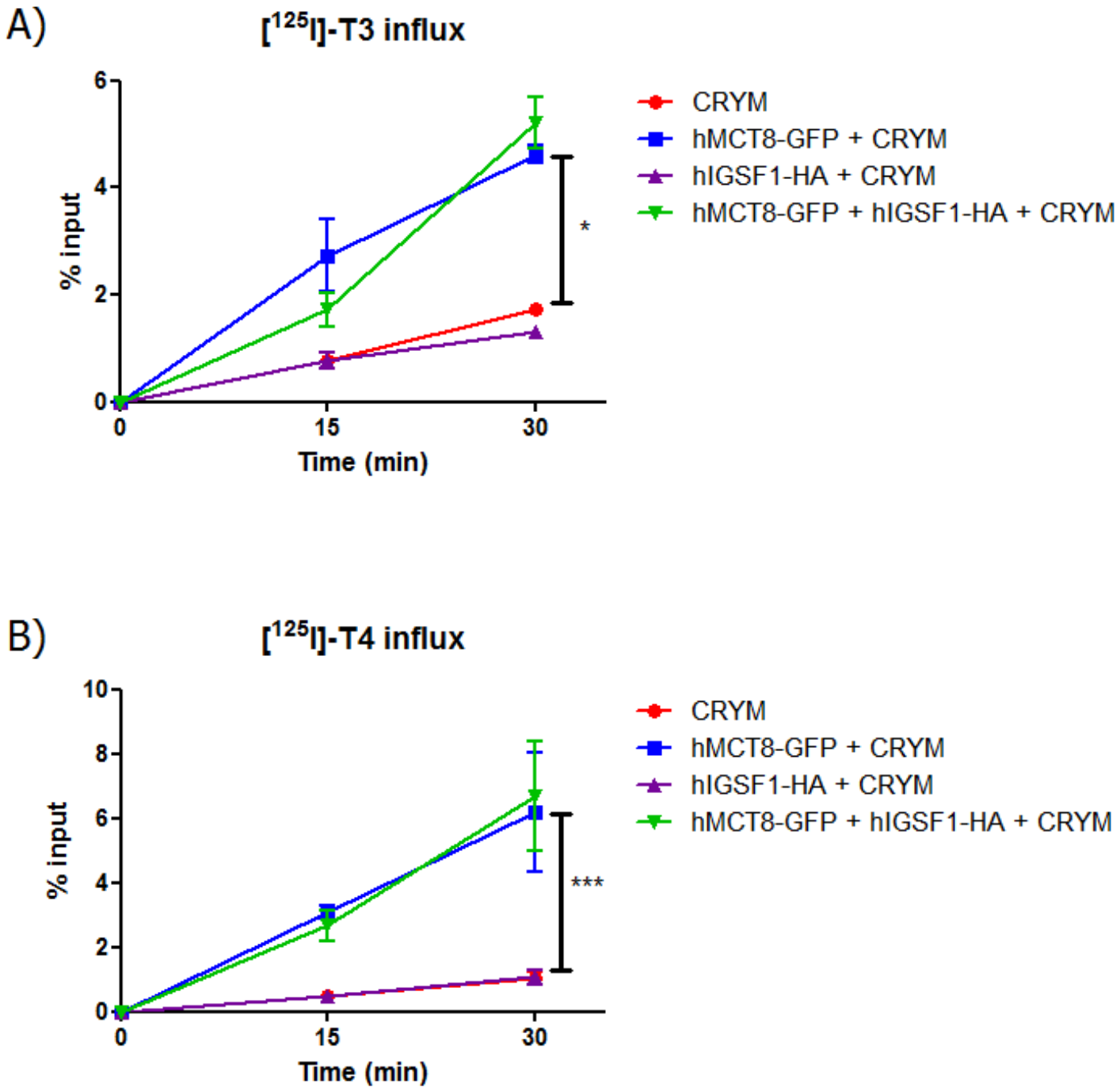
A)
[125I]-T3 influx
% input
Time (min)
0
15
30
2
4
6
*
CRYM
hMCT8-GFP + CRYM
hIGSF1-HA + CRYM
hMCT8-GFP + hIGSF1-HA + CRYM
B)
[125I]-T4 influx
% input
Time (min)
0
15
30
2
4
6
8
10
***
CRYM
hMCT8-GFP + CRYM
hIGSF1-HA + CRYM
hMCT8-GFP + hIGSF1-HA + CRYM

Figure 3.5

A)
Igsf1+/y
Igsf1Δex1/y
+ saline
+ low T3
+ high T3
+ high T4
3V
PVN
B)
Relative Trh integrated signal density
30
20
10
0
a a
b b
b b
b b
SALINE
LOW T3
HIGH T3
T4
Treatment
WT
KO

Figure 3.6

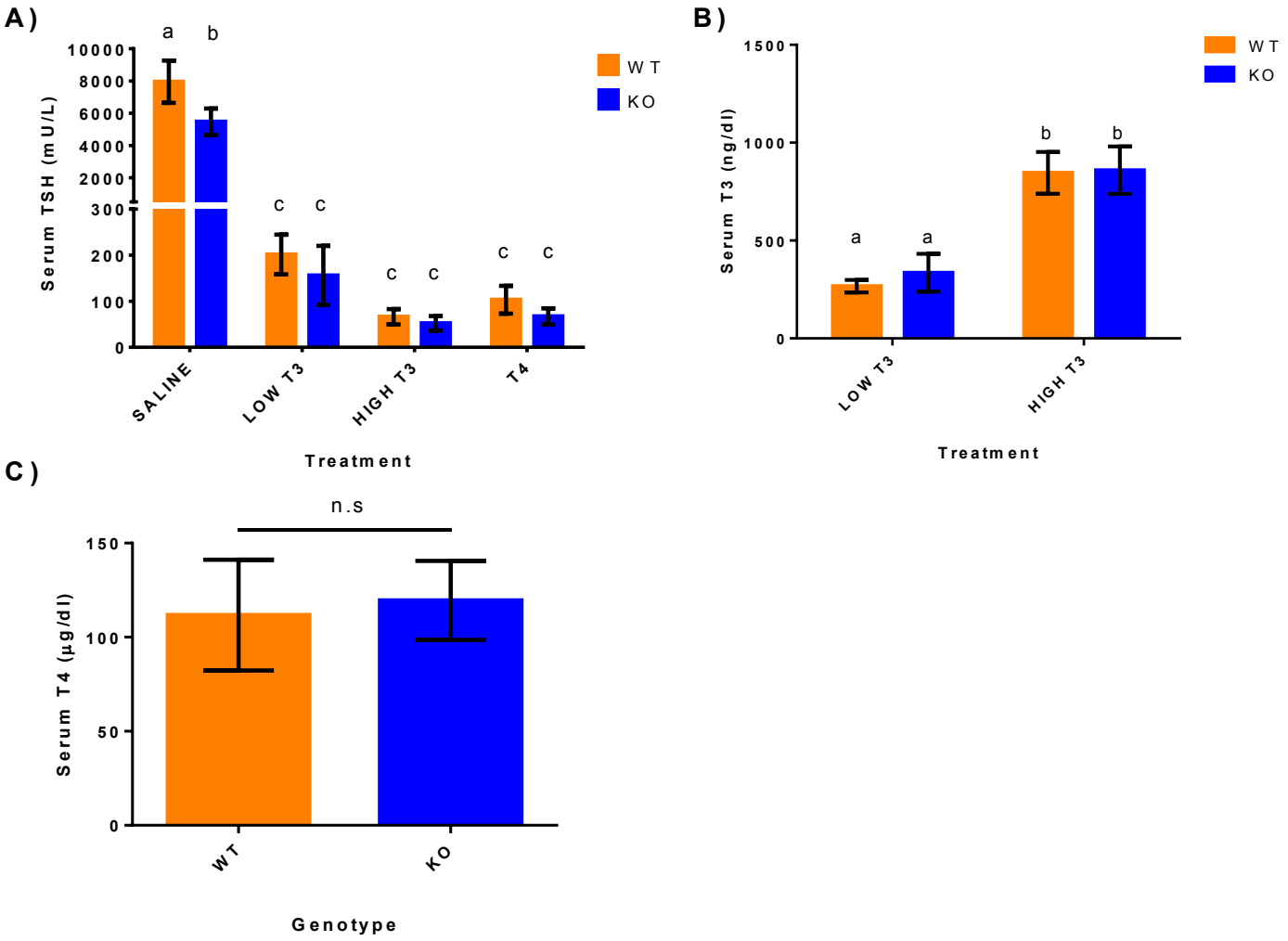
A)
Serum TSH (mU/L)
10000
8000
6000
4000
2000
300
200
100
0
a
b
c
c
c
c
c
c
WT
KO
SALINE
LOW T3
HIGH T3
T4
Treatment
B)
Serum T3 (ng/dl)
1500
1000
500
0
a
a
b
b
WT
KO
LOW T3
HIGH T3
Treatment
C)
Serum T4 (µg/dl)
150
100
50
0
n.s
WT
KO
Genotype

Figure 3.7

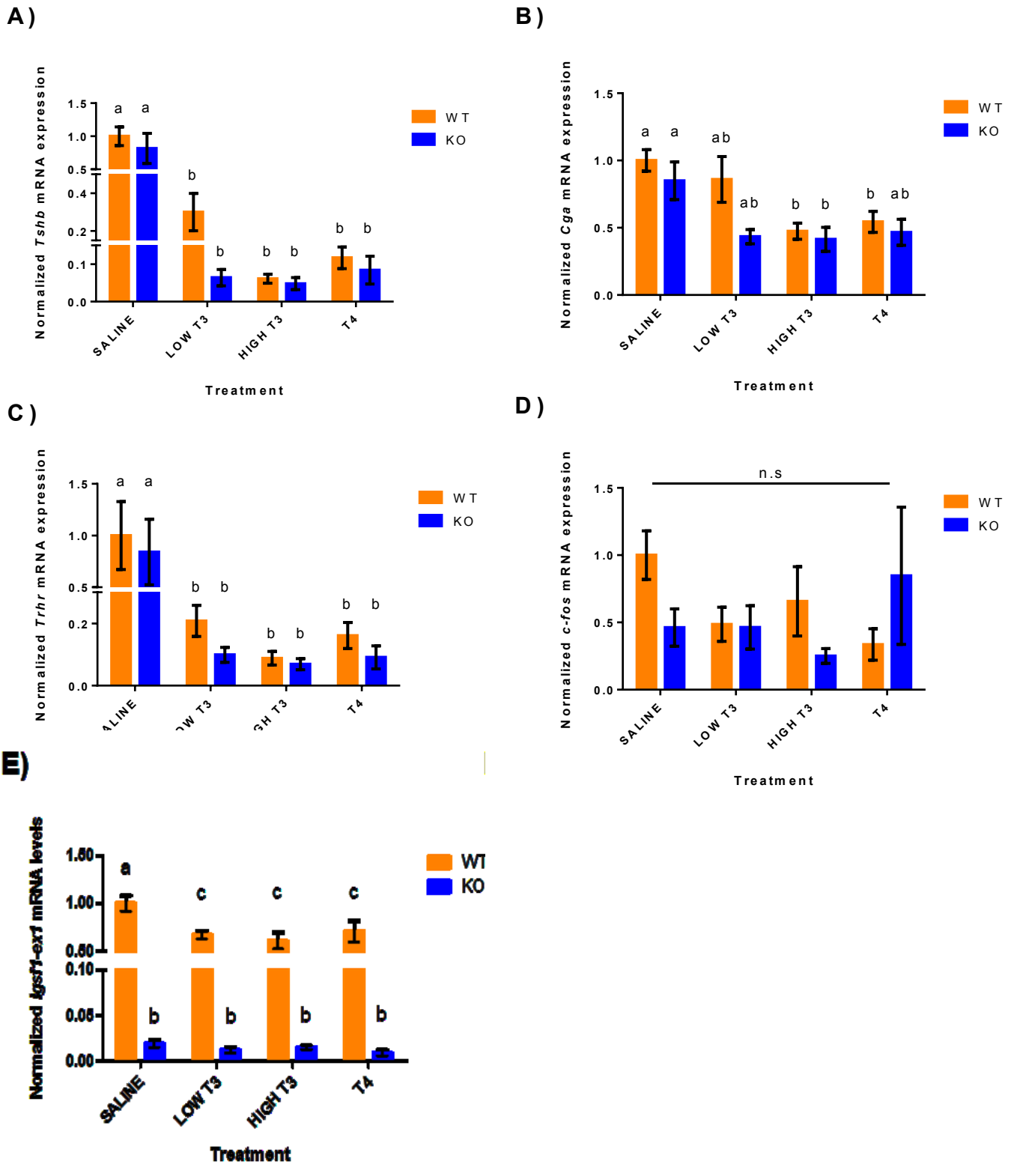
A)
Normalized Tshb mRNA expression
WT
KO
SALINE
LOW T3
HIGH T3
T4
Treatment
B)
Normalized Cga mRNA expression
C)
Normalized Trhr mRNA expression
D)
Normalized c-fos mRNA expression
n.s
E)
Normalized kgsf1-ex1 mRNA levels
WT
KO
SALINE
LOW T3
HIGH T3
T4
Treatment

Figure 3.8

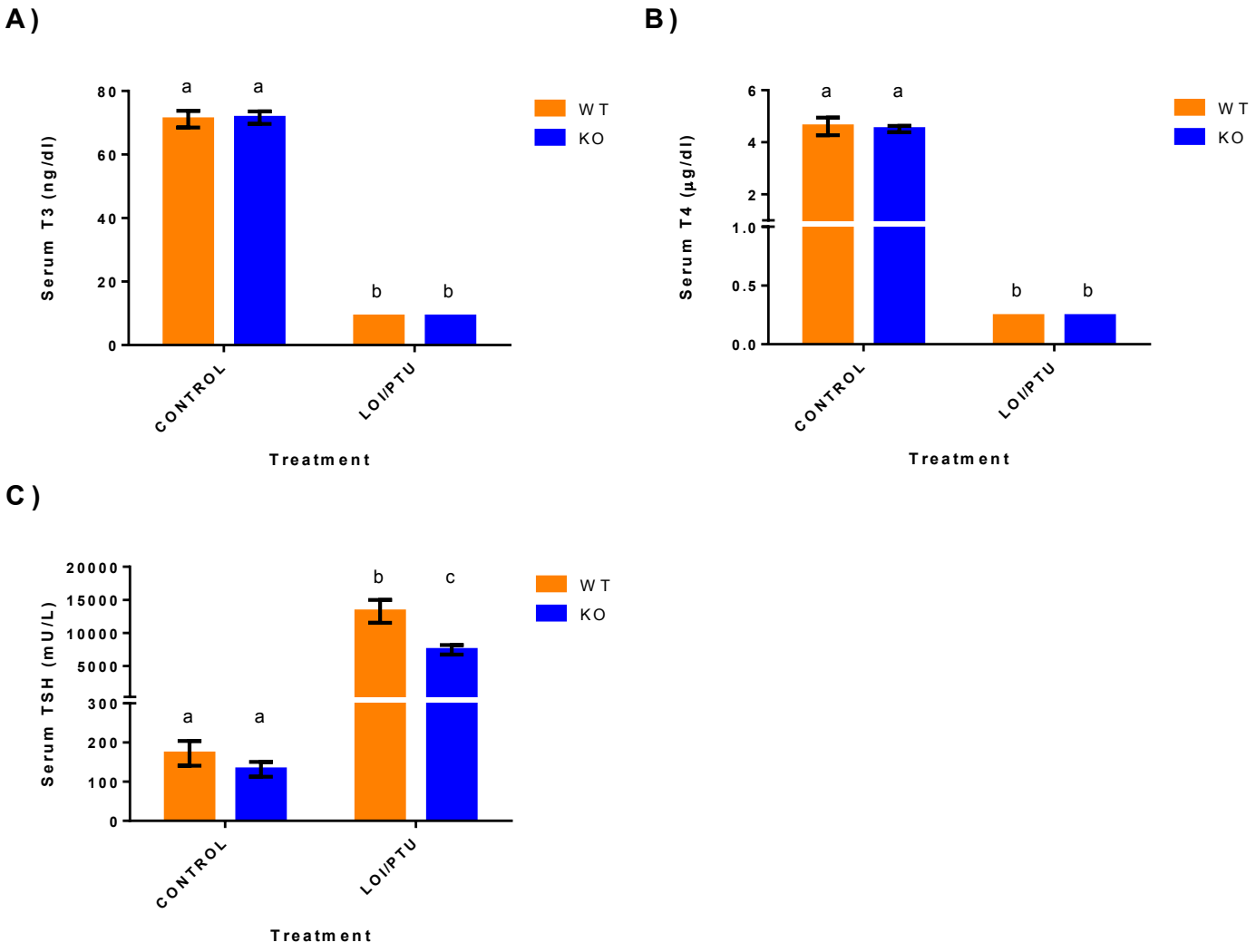
A)
Serum T3 (ng/dl)
80
60
40
20
0
a
a
b
b
CONTROL
LOI/PTU
Treatment
WT
KO
B)
Serum T4 (µg/dl)
6
4
2
1.0
0.5
0.0
a
a
b
b
CONTROL
LOI/PTU
Treatment
WT
KO
C)
Serum TSH (mU/L)
20000
15000
10000
5000
300
200
100
0
a
a
b
c
CONTROL
LOI/PTU
Treatment
WT
KO

Figure 3.9

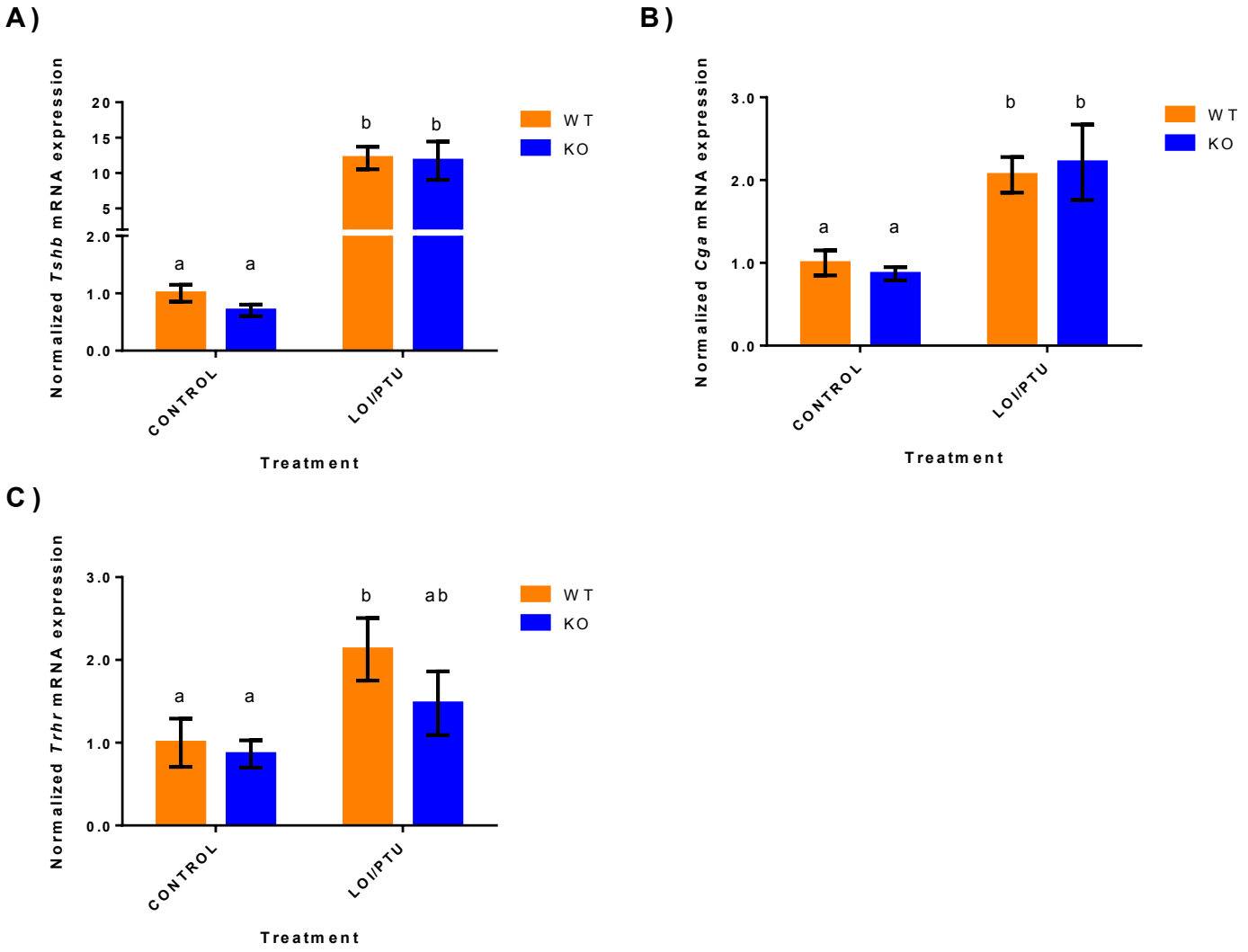
A)
Normalized Tshb mRNA expression
20
15
10
5
2.0
1.0
0.0
a
a
b
b
CONTROL
LOI/PTU
Treatment
WT
KO
B)
Normalized Cga mRNA expression
3.0
2.0
1.0
0.0
a
a
b
b
CONTROL
LOI/PTU
Treatment
WT
KO
C)
Normalized Trhr mRNA expression
3.0
2.0
1.0
0.0
a
a
b
ab
CONTROL
LOI/PTU
Treatment
WT
KO

Figure 3.10

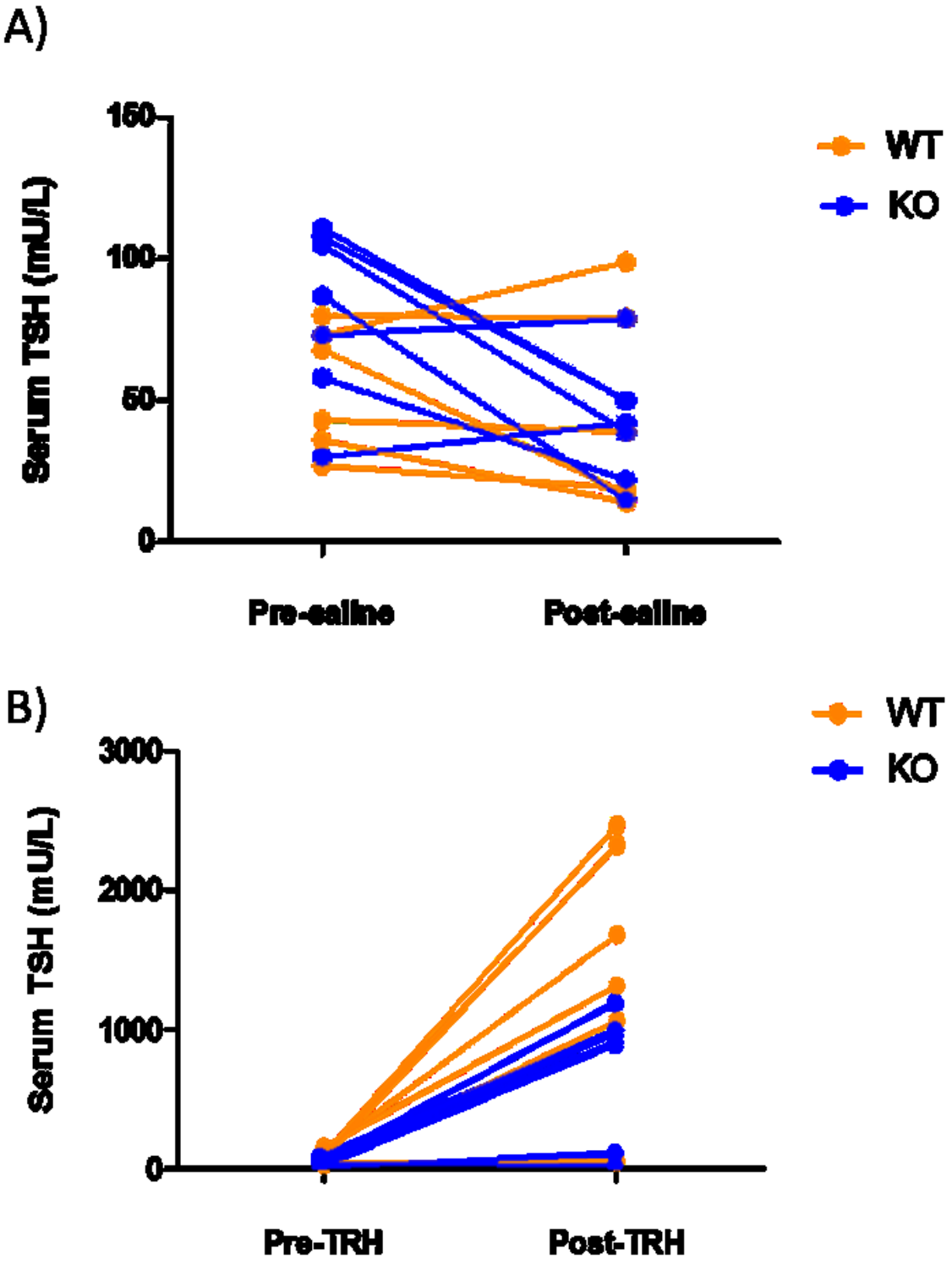
A)
Serum TSH (mU/L)
150
100
50
0
Pre-saline
Post-saline
WT
KO
B)
Serum TSH (mU/L)
3000
2000
1000
0
Pre-TRH
Post-TRH
WT
KO

Figure 3.11

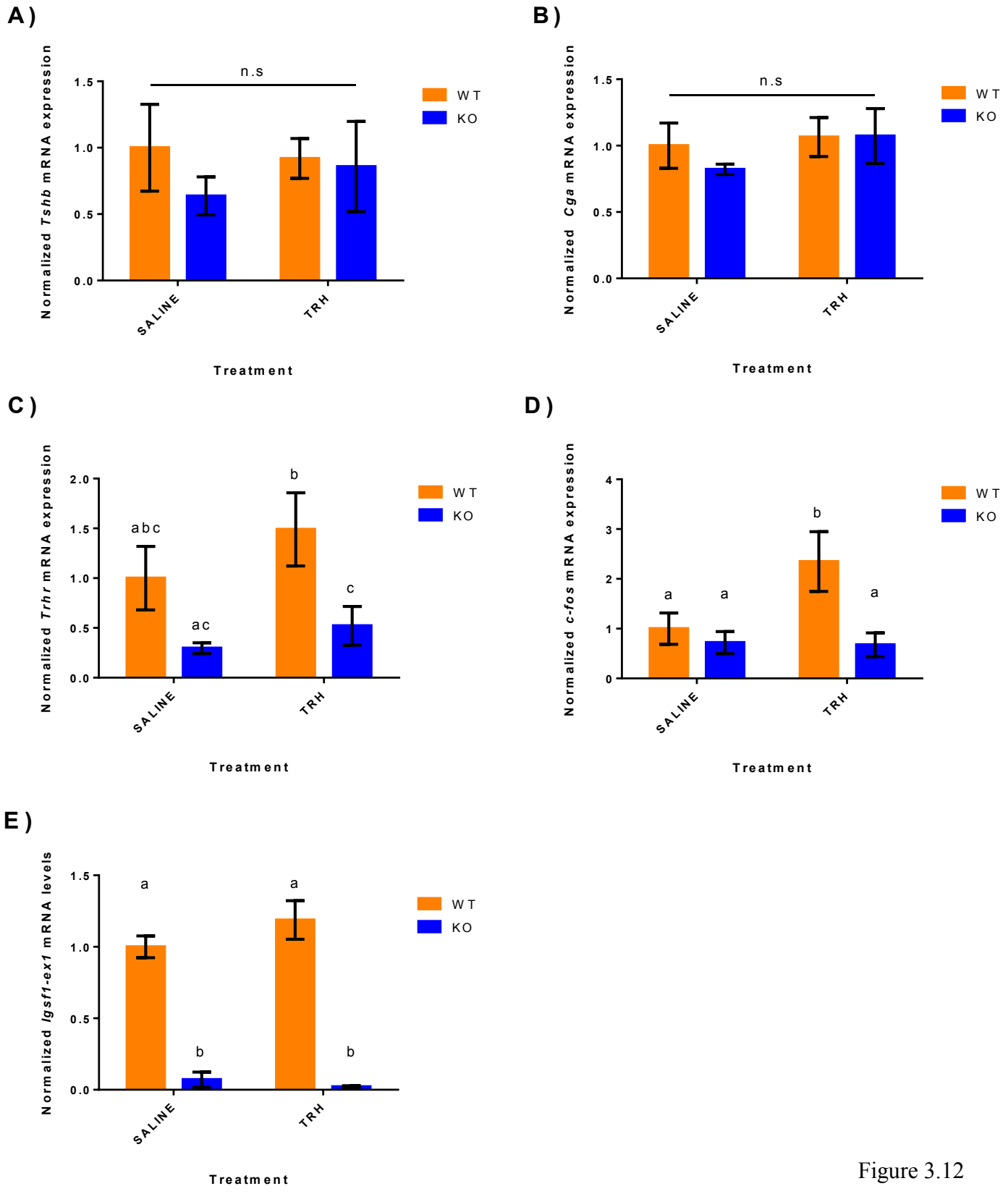
A)
Normalized Tshb mRNA expression
n.s
WT
KO
SALINE
TRH
Treatment
B)
Normalized Cga mRNA expression
n.s
WT
KO
SALINE
TRH
Treatment
C)
Normalized Trhr mRNA expression
abc
ac
b
c
WT
KO
SALINE
TRH
Treatment
D)
Normalized c-fos mRNA expression
a
a
b
a
WT
KO
SALINE
TRH
Treatment
E)
Normalized Igsf1-ex1 mRNA levels
a
b
a
b
WT
KO
SALINE
TRH
Treatment

Figure 3.12

Chapter 4: General Discussion

Pathogenic mutations in the *IGSF1* gene cause central hypothyroidism in humans, revealing a previously unappreciated role for IGSF1 in the regulation of the HPT axis[149,155–157]. The main focus of my thesis was to better define IGSF1's function in this context. To this end, I investigated a potential role for IGSF1 in TH transport and discovered that IGSF1 physically interacts with the THT, MCT8; however, I was unable to demonstrate a role for IGSF1 in TH transport *in vitro* or *in vivo*. Nonetheless, the results of my thesis clearly demonstrate that IGSF1-deficiency impairs TRH signaling in the murine pituitary.

4.1 Mature IGSF1 and MCT8 form a stable interaction at the plasma membrane

While the central hypothyroid phenotype of patients with pathogenic *IGSF1* mutations establishes a role for IGSF1 in HPT axis regulation, a specific function for IGSF1 remains unknown[149,155–157]. Based on evidence that the structurally similar IGSF protein, CD147, interacts with MCT family members directing their cell surface expression[178], we investigated the possibility that IGSF1 and the TH transporter, MCT8 interacted at the plasma membrane. To this end, we demonstrate a novel interaction between the mature glycoform of IGSF1 and MCT8 *in vitro* which we detect at the plasma membrane of HEK293 cells (Figure 3.1a). Interestingly, we do not detect an interaction between the immature glycoform of IGSF1 and MCT8, and experiments in our lab indicate that pathogenic mutations in IGSF1 which prevent acquisition of mature glycosylation impair the IGSF1:MCT8 interaction (Wang, unpublished). This suggests that the interaction between IGSF1 and MCT8 is either established post-ER, or that the interaction is less stable pre-Golgi and cannot be detected using co-immunoprecipitation assays. Discernment of the subcellular localization of the IGSF1:MCT8 interaction would establish

whether pathogenic *IGSF1* mutations that restrict IGSF1 protein maturation are capable of sequestering MCT8 in the ER, and can be achieved through pharmacological inhibition of protein trafficking from the ER to the Golgi using Brefeldin A[189] followed by co-immunoprecipitation or bioluminescence resonance energy transfer (BRET)[190,191] to evaluate IGSF1:MCT8 interaction. While IGSF1 interacts with MCT8, we do not detect an interaction between IGSF1 and MCT10, which shares 49% amino acid identity with MCT8[192], suggesting that this interaction is specific to MCT8 (Figure 3.1b). We have since mapped this interaction domain to the C-terminal region of MCT8; provided that the interaction between IGSF1 and MCT8 is significant, this interaction domain will be a useful bioinformatics tool in establishing additional IGSF1 interacting partners (Smith, Wang, Silander, unpublished).

In addition to the role of CD147 in cell surface expression of MCT family members, basolateral sorting signals (BLSSs) in the C-terminal region of CD147 direct MCT1 expression to the basolateral membrane in polarized tissues[178]. While IGSF1 does not appear to affect MCT8 subcellular localization in polarized cells *in vitro* (Silander, unpublished), the typically basolateral localization of MCT8 is altered to the apical membrane in the CP[37] where IGSF1 is similarly localized (Bak, unpublished)[186]. Previous *in vitro* studies on CD147-mediated trafficking of MCT1 to the basolateral membrane indicate that cell type influences basolateral localization by CD147[178], and we postulated that IGSF1 trafficking of MCT8 to the apical membrane may be influenced by additional protein partners present in the CP which are absent in *in vitro* cell systems. However, MCT8 effectively traffics to the CP apical membrane of *Igsf1*$^{\Delta ex1/y}$ mice (Figure 3.4), suggesting that IGSF1 is dispensable for MCT8 subcellular localization in the CP of adult mice, or that the IGSF1-4 isoform retained by *Igsf1*$^{\Delta ex1/y}$ mice[172] is capable of compensating for the loss of full-length IGSF1 isoforms. To differentiate between

these possibilities, we might first determine whether *Igsf1-4* mRNA expression is upregulated in the CP of *Igsf1*$^{\Delta ex1/y}$ mice compared with *Igsf1*$^{+/y}$ mice, which would likely be necessary given the low expression of *Igsf1-4* compared with the other *Igsf1* mRNA isoforms (Bak, unpublished). Dispersed primary CP cultures grown under polarizing conditions[193,194] could then be treated with short interfering RNA (siRNA) to knock-down all *Igsf1* mRNA isoforms[195] followed by examination of MCT8 subcellular localization by immunofluorescence or domain-specific CSB[196,197]. This method is limited in that one may alter expression of MCT8 or subcellular localization through the dispersion techniques utilized, thereby complicating analysis of these results[198]. The most appropriate experiment would be to generate a new murine model in which all isoforms encoding the IGSF1-CTD are deleted or impaired in their cell surface expression, which would be akin to the pathogenic mutations present in humans with IGSF1-deficiency syndrome. Appropriately, our lab has generated this murine model using CRISPR/Cas9 gene editing[199,200] to delete 312 bp in the CTD (*Igsf1*$^{\Delta 312bp}$ mice) resulting in an approximate 45-50 kDa reduction in protein mass and a loss of the mature form of IGSF1-CTD with presumably no effect on the NTD (Turgeon and Silander, unpublished). Provided IGSF1-CTD maturation is impaired in these mice, subcellular localization of MCT8 in the CP can be analyzed as described in this thesis. While IGSF1 clearly interacts with MCT8 at the plasma membrane *in vitro*, it does not appear to function as an ancillary protein to MCT8, leaving the function of this interaction elusive.

4.2 Absence of IGSF1 increases the pituitary sensitivity to exogenous low T3

Increased *Trh* transcription in the hypothalamus of *Igsf1*$^{\Delta ex1/y}$ mice suggests that IGSF1-deficiency may affect TH transport across the BCSFB, thereby inducing a hypothyroid state in the hypothalamus. Here we show that IGSF1 does not affect MCT8-mediated influx of T3 or T4

in HeLa cells (Figure 3.5a and b), and is dispensable for TH transport into the hypothalamus of *Igsf1*$^{\Delta ex1/y}$ mice (Figure 3.6-3.8). Unlike MCT8-deficient mice, whose *Trh* response to exogenous T3 is not significantly different from the hypothyroid state[188], *Trh* mRNA expression in *Igsf1*$^{\Delta ex1/y}$ mice was sufficiently suppressed in response to both low and high doses of T3 (Figure 3.6), suggesting that any IGSF1 effects on MCT8-mediated transport of T3 across the BCSFB are mild and expendable. Furthermore, *Trh* mRNA expression is not significantly different between genotypes under any of the experimental conditions (Figure 3.6b), indicating that increased *Trh* expression in the hypothalamus reported by Sun et al[157] is either a consequence of low circulating T4, not a TH transport defect, or is an artefact of experimental design. In the Sun et al study, crude hypothalamic dissections were obtained for qPCR assessment of *Trh*; however, TRH-expressing neurons not associated with the HPT axis are also present in these dissections[201], and may have skewed the initial results. Unfortunately, our TH replacement study does not include a control condition to assess *Trh* expression in the PVN via ISH and thus we cannot speculate on the endogenous state of *Trh* mRNA levels in this experiment. Reassessment of *Trh* mRNA expression via ISH under control conditions, where the TH status of the mice is known, would allow a definitive answer as to whether low circulating TH levels account for the upregulation of *Trh* mRNA in the absence of IGSF1.

Curiously, while *Tshb*, *Cga*, and *Trhr* mRNA are similarly upregulated in *Igsf1*$^{+/y}$ and *Igsf1*$^{\Delta ex1/y}$ mice under hypothyroid conditions, they appeared to be more sufficiently suppressed by low exogenous T3 (Figure 3.8a-c), suggesting that IGSF1-deficiency increases negative regulation by T3-bound THRs. If true, IGSF1 may decrease T3 transport into the pituitary, likely by interacting with a TH transporter other than MCT8 given the low expression of MCT8 in the pituitary (Figure 3.3). TH transport into the pituitary can be assessed by injecting radiolabeled

THs into hypothyroid *Igsf1*$^{+/y}$ and *Igsf1*$^{\Delta ex1/y}$ mice[188,202,203] and assessing TH levels in the thyrotropes by double-labeling with *Tshb*[204,205] and quantifying using autoradioagraphy. Alternatively, IGSF1 may act as a signaling molecule; binding to extracellular ligands and decreasing repression of TH-sensitive genes by T3-bound THRs. In the pituitary, T3-bound THRs bind TH response elements (TREs) in the promoter regions of *Tshb*, *Trhr*, and *Cga*[49]. THRs then form heterodimers with the co-regulator, retinoid X receptor-γ (RXR-γ), which binds RXR response elements (RREs) adjacent to TREs, and promotes histone deacetylase (HDAC)-mediated transcriptional repression[206]. Phosphorylation of serine residues in human RXR-α has been demonstrated to inhibit regulation of gene expression by RXR-α:THR, and may denote a general mechanism by which RXR-mediated regulation of TH-sensitive gene transcription is controlled[207,208]. Therefore, if IGSF1 generates intracellular signaling cascades leading to phosphorylation of RXR-γ, decreasing repression of TH-sensitive gene transcription, then loss of IGSF1 would increase repression of *Tshb*, *Trhr*, and *Cga* in the pituitary in response to T3-bound THRs. Decreased mRNA expression may also be attributable to increased mRNA degradation in the absence of IGSF1, where IGSF1 may repress transcription of micro RNAs (miRNAs) that target RNases to these RNAs[209]. Differentiation between decreased transcription and increased degradation in the absence of IGSF1 can easily be deduced by performing pre-mRNA qPCR[210,211], where primers are targeted to intron-exon junctions and allow quantification of unprocessed mRNA. If pre-mRNA transcript levels are not significantly different between genotypes, then the rate of transcription is likely unaffected and the difference attributed to increased mRNA degradation in the absence of IGSF1. Interestingly, *Igsf1* expression is significantly downregulated in response to exogenous TH replacement (Figure 3.8e), indicating

that *Igsf1* may contain TREs in the promoter region and subject to TH-mediated regulation of gene expression.

As IGSF1 has limited global tissue expression[157,172,186], circulating exogenous TH levels were expectedly similar between genotypes (Figure 3.7b and c), indicating that IGSF1 is dispensable for global influx of THs into target tissues. Interestingly, patients with IGSF1-deficiency exhibit macroorchidism, which may result from increased levels of circulating luteinizing hormone (LH), or decreased TH transport into the testes[212,213]. While IGSF1- deficiency does not increase LH levels in humans[214], TH transport in the testes may be impaired without affecting global circulating levels of TH. IGSF1 is not expressed in murine testes (Silander, unpublished), and we were unable to test this hypothesis; however, IGSF1 is expressed in the testes of rats[186] and an IGSF1 knock-out rat model could be generated using a similar strategy as that used to create the *Igsf1*$^{\Delta 312bp}$ mice for the purposes of studying the macroorchidism phenotype.

Despite greater apparent suppression of *Tshb* and *Cga* mRNA expression in *Igsf1*$^{\Delta ex1/y}$ mice treated with low T3, there did not appear to be a reciprocally larger suppression of circulating TSH under these conditions (Figure 3.7a). This is largely due to negative regulation of secretion of stored TSH in a TH- and neuromedin B (NB)-dependent fashion[215,216]; a pathway which does not appear to be impaired in *Igsf1*$^{\Delta ex1/y}$ mice as TSH is secreted normally in the face of exogenous TH. However, circulating TSH levels are significantly lower in *Igsf1*$^{\Delta ex1/y}$ mice in response to primary hypothyroidism (Figure 3.7a), despite normally upregulated *Tshb* and *Cga* mRNA expression (Figure 3.8a and b), suggesting that TRH-mediated stimulation of TSH secretion is impaired. Measurement of TRH in the median eminence of mice is very difficult and therefore, one cannot eliminate the possibility that TRH protein production or release is impaired

in *Igsf1*$^{\Delta ex1/y}$ mice despite appropriately upregulated *Trh* in response to hypothyroidism (Figure 3.6). In order to measure TRH release, one would require a larger animal model such as the *Igsf1*-deficient rats suggested earlier, on which one could perform push-pull perfusions followed by RIA for TRH[217–222]. TRH production can be assessed using an antibody for murine TRH developed by the Fekete lab, and conducting immunofluorescence on the PVN of *Igsf1*$^{+/y}$ and *Igsf1*$^{\Delta ex1/y}$ mice as previously described[11]. Pituitary *Trhr* mRNA expression levels are likewise a poor readout of TRHR protein levels, which may be downregulated in the thyrotropes of *Igsf1*$^{\Delta ex1/y}$ mice. Lacking an appropriate antibody for TRHR, one can assess TRHR expression *in vivo* by injecting *Igsf1*$^{+/y}$ and *Igsf1*$^{\Delta ex1/y}$ mice with [^{125}I]-TRH, extracting pituitaries 15 min post-injection, double-labeling with *Tshb* and quantifying TRHR bound to TRH on thyrotrope cells of the anterior pituitary[204,205,223]. While this would not differentiate between TRHR expression and effective TRH binding to the TRHR, if TRH binding to TRHRs on thyrotropes were significantly different between *Igsf1*$^{\Delta ex1/y}$ and *Igsf1*$^{+/y}$ mice it would necessitate investigations of IGSF1 on TRHR expression and function.

These experiments do not differentiate between TSH bioactivity and TSH secretion, where TRH is dispensable for TSH secretion, but not TSH bioactivity[17,148]. Circulating TH levels are a typical read-out of TSH bioactivity, where impaired TRH signaling results in normal-to-elevated circulating TSH without a concurrent increase in circulating TH levels. In our current study, we cannot assess the bioactivity of TSH via TH levels as we deliberately abolished their production. Therefore, we sought to determine the bioactivity of TSH under physiological conditions and to further assess the impaired TSH secretion in response to hypothyroidism. We also looked at the TSH response to exogenous TRH and found that while TSH bioactivity does not appear impaired

under physiological conditions, TSH secretion in response to exogenous TRH and hypothyroidism is blunted in *Igsf1*$^{\Delta ex1/y}$ mice.

4.3 Impaired TRH signaling in *Igsf1*$^{\Delta ex1/y}$ mice may be secondary to reduced TRHR expression

Basal circulating TSH was not significantly altered in *Igsf1*$^{\Delta ex1/y}$ mice compared with *Igsf1*$^{+/y}$ controls (Figure 3.9c), nor was circulating TH noticeably diminished (Figure 3.9a and b). This is contrary to previous results obtained by Sun et al, who observed markedly decreased circulating TSH as well as low circulating T3 under basal conditions[157]. This may be the result of variability in the IGSF1-deficient phenotype, which is observed in both mice and man, and may be attributable to either environmental conditions or age[149,156,157,214]. Indeed, the IGSF1-deficient phenotype appears to wane with age, and may also reflect maternal thyroidal states, as the fetus is reliant on maternal TH during early fetal development, setting the HPT axis set-point[2,157,224]. Normal circulating TH in the face of normal TSH indicates that TSH bioactivity is not affected in this cohort of *Igsf1*$^{\Delta ex1/y}$ mice, arguing against a TRH signaling defect under physiological conditions. However, a pilot experiment to investigate the *Igsf1*$^{\Delta ex1/y}$ response to hypothyroidism detected a significant decrease in circulating T4 levels in the face of normal circulating TSH (Silander, unpublished). This study was conducted on *Igsf1*$^{\Delta ex1/y}$ and *Igsf1*$^{+/y}$ mice of mixed backgrounds born to *Igsf1*$^{+/+}$ or *Igsf1*$^{\Delta ex1/\Delta ex1}$ dams, and were thus not littermates. While circulating TH levels were not measured in these dams, it is probable that *Igsf1*$^{\Delta ex1/y}$ mice derived from *Igsf1*$^{\Delta ex1/\Delta ex1}$ dams were subject to lower maternal TH during embryonic development, which may have altered their HPT axis set-point. To determine whether the variability in IGSF1-deficiency phenotype is resultant from differential maternal TH levels, circulating TH levels in

pregnant *Igsf1*$^{\Delta ex1/+}$ mice should be established, and the circulating TH and TSH levels measured in the resultant offspring. One might also consider normalizing maternal TH status by abolishing TH production using the LoI/PTU diet during pregnancy and exogenously replacing TH with daily physiological doses of T4, which would alleviate the potential for maternal thyroid status to disrupt the HPT axis of offspring and provide a clearer understanding of the direct effects of IGSF1-deficiency on the HPT axis[225]. Under hypothyroid conditions, TSH levels were again blunted in *Igsf1*$^{\Delta ex1/y}$ mice (Figure 3.9c); a consequence of either impaired TSH protein production or release, which may be a direct consequence of impaired TRH signaling or an intrinsic pituitary defect. Knowledge of the bioactivity of TSH in the hypothyroid condition would allow indirect assessment of TRH signaling, and can be assessed using a bioassay developed by the Inada lab which measures cAMP levels produced by FRTL-5 cells in response to bioactive TSH[226]. While *Trh* mRNA levels would be a valuable addition to this data set, they were not analyzed via ISH and we were not confident in the qPCR results as *Trh* mRNA expression was not apparently upregulated in the hypothyroid condition. The immediate early gene of TRH signaling, *c-fos*[80], has not been measured in this data set, but would be a useful read-out of TRH signaling in the pituitary in both the basal and hypothyroid conditions. Neither *Tshb* nor *Cga* expression was significantly altered in the *Igsf1*$^{\Delta ex1/y}$ mice (Figure 3.10a and b), and differences in TSH levels cannot be readily explained by impaired TH-mediated transcriptional regulation in the pituitary. *Trhr* expression tends to be lower in *Igsf1*$^{\Delta ex1/y}$ mice, though not significantly, and may be the primary cause for deficient TRH signaling (Figure 3.10c). Since TRHR is expressed in lactotropes and somatotropes, as well as thyrotrope cell types of the anterior pituitary[70,72], with thyrotropes being the least abundant of the three[227], it is possible that *Trhr* is downregulated in thyrotropes and not the other two cell types, resulting in

relatively normal *Trhr* expression when the pituitary is looked at on the whole. To discern thyrotrope specific decreases in *Trhr* expression, one could employ fluorescence-activated cell sorting (FACS)[228,229] of thyrotrope cells of *Igsf1*$^{+/y}$ and *Igsf1*$^{\Delta ex1/y}$ mice and perform qPCR to assess *Trhr* levels in the thyrotropes. This can be accomplished by crossing *Tshb*-cre mice[230] with ROSA-26 yellow fluorescent protein (YFP) mice[231] (*Tshb*-YFP mice), allowing expression of YFP specifically in the thyrotropes, and subsequently crossing these mice to *Igsf1*$^{\Delta ex1/y}$ mice. If IGSF1 affects transcription of *Trhr*, then it is reasonable to assume that IGSF1 plays a role in regulating transcription of some TH-regulated genes of the pituitary through an as-yet unknown signaling cascade. RNA sequencing[232,233] conducted on these FACS derived thyrotropes would allow identification of additional genes regulated by IGSF1, and analysis of response elements present in their promoter regions would provide information on transcription factors and co-regulators affected by IGSF1 signaling. Without knowing *Trh* mRNA expression or the levels of *c-fos* mRNA expression as a result of downstream TRH signaling effects in the hypothyroid condition, as well as apparently normal TSH bioactivity, we had not yet garnered conclusive evidence of a TRH signaling defect, as TRH production and signaling through the TRHR may be unobstructed and TSH production and secretion impaired instead. Treatment with exogenous TRH allowed us to discern whether impaired TSH secretion was indeed the result of impaired TRH signaling at the level of the pituitary.

While basal TSH levels were normal in *Igsf1*$^{\Delta ex1/y}$ mice (Figure 3.11a), their TSH response to exogenous TRH administration was blunted (Figure 3.11b). Indeed, this may be secondary to decreased TRHR expression as *Trhr* mRNA levels were significantly reduced in both the saline and TRH stimulated cohorts of *Igsf1*$^{\Delta ex1/y}$ mice (Figure 3.12c). While reduced *Trhr* levels are sufficient to maintain basal levels of TSH, they appear inadequate for mounting a response to

hypothyroidism. Repetition of this experiment using radiolabeled TRH as described earlier would allow direct quantification of TRH binding to the TRHR under tertiary hypothyroid conditions (TRH is in excess). If *Trhr* downregulation is a direct effect of IGSF1-deficiency, then IGSF1 must promote *Trhr* transcription via signaling. There are various fashions in which IGSF1 may signal, namely through phosphorylation of the serine/threonine residues in the intracellular C-terminal tail upon binding of an unknown ligand to the extracellular Ig domains. This would lead to phosphorylation of downstream effector proteins, ultimately resulting in transcriptional regulation of IGSF1-sensitive genes, which may account for alterations in *Trhr* mRNA expression in *Igsf1*$^{\Delta ex1/y}$ mice. Modifications of protein phosphorylation profiles in the absence of IGSF1 can be detected by isolating phosphorylated proteins from the pituitaries of *Igsf1*$^{\Delta ex1/y}$ mice and identifying the proteins via mass spectrometry for comparison with the phosphoproteome of *Igsf1*$^{+/y}$ pituitaries[234,235]. As thyrotrope cells are the least abundant cell type of the anterior pituitary, if IGSF1 affects phosphorylation of different proteins in the lactotropes and somatotropes in which it is also expressed, or if the effects of IGSF1 on the phosphoproteome are restricted to the thyrotrope cells, then differences in the phosphoproteome of *Igsf1*$^{\Delta ex1/y}$ mice compared with *Igsf1*$^{+/y}$ mice may be difficult to detect. Ideally, one would utilize the *Tshb*-YFP mice to isolate thyrotrope cells from *Igsf1*$^{\Delta ex1/y}$ and *Igsf1*$^{+/y}$ mice prior to analysis of the phosphoproteomes. While changes in the phosphoproteome of *Igsf1*$^{\Delta ex1/y}$ mice may indeed be present, this would not directly implicate IGSF1 in the signaling cascade, where IGSF1 may instead bind another receptor in the plasma membrane upon ligand binding, resulting in phosphorylation of this interacting partner rather than IGSF1 itself. Indeed, the IGSF membrane protein, osteoclast-associated receptor (OSCAR), binds extracellular matrix proteins and associates with an ITAM receptor, which activates downstream signaling events[236]. Like

IGSF1, OSCAR contains a positively charged amino acid in the TMD, and this amino acid is necessary for OSCAR binding to this receptor[237]. If, like OSCAR, IGSF1 signaling occurs through an interacting receptor, then IGSF1 may be absent from the initial phosphoproteomic analysis in wild-type mice, either due to inefficient separation of plasma membrane proteins in these screens, or because IGSF1 is not phosphorylated. To determine whether IGSF1 itself is phosphorylated, one could enrich for plasma membrane proteins in the *in vivo* screens or for IGSF1 itself using immunoprecipitation techniques to pull down endogenous IGSF1[235,238–240],. Alternatively, one could attempt these studies in vitro using SILAC enrichment techniques and immunoprecipitation of HA-tagged IGSF1[241]. Unfortunately, without knowledge of the potential IGSF1 ligand, *in vitro* techniques may be of little informative value as IGSF1 may not signal in its absence. Identification of potential ligands for IGSF1 would be best achieved by ascertaining *in vitro* protein-protein interactions between the extracellular domain of murine IGSF1 and extracellular proteins of the murine pituitary. These analyses could be conducted using yeast 2-hybrid, with the murine pituitary cDNA library as prey and the extracellular domain of IGSF1 as bait, which would allow detection of both transient and stable protein interactions[242–244]. However, yeast 2-hybrid assays are limited to detecting interactions between soluble proteins, and are not capable of identifying interactions with integral membrane proteins[245], which limits the scope of potential binding partners. Identifying binding partners via tandem affinity purification (TAP)-tag might be another alternative; however this assay is stringent and often unable to identify transient interactions[246,247]. Ideally, interactions would be identified *in vivo* rather in an *in vitro* system, a task which could be achieved by creating a knock-in mouse line which expresses a TAP-tag at the C-terminus of IGSF1 (*Igsf1*^{TAP})[200,248–250], a system which has the advantage of identifying protein interacting partners under endogenous conditions, as well as

under various physiological conditions and developmental time points within the various tissues in which IGSF1 is expressed.

Blunted TSH response to exogenous TRH stimulation identifies an intrinsic pituitary defect in *Igsf1*$^{\Delta ex1/y}$ mice, but does not eliminate a possible defect in the hypothalamus, nor have we addressed the effect of IGSF1-deficiency on TRH signaling in the somatotropes or lactotropes. Examination of the thyrotrope-specific effect of IGSF1-deficiency on the HPT axis, one would require an animal model in which IGSF1 expression is specifically eliminated in the thyrotropes of the pituitary. These mice could be generated using the *Tshb*-cre mouse line[230] crossed to mice with loxp sites flanking the TMD or C-terminal tail of IGSF1 (*Tshb-Igsf1*$^{fl/y}$), elimination of either having been shown to abolish plasma membrane expression of IGSF1 (Turgeon and Wang, unpublished). By crossing these two mouse lines, one would generate mice in which the IGSF1-CTD is rendered effectively non-functional in the thyrotropes of the anterior pituitary, yet maintains wild-type expression elsewhere. These mice would address whether the variable PRL deficiency and transient GH deficiency seen in patients with IGSF1-deficiency syndrome[157,214] were an effect of intrinsic lack of IGSF1-deficiency in lactotropes and somatotropes or were the result of impaired pituitary crosstalk[251] between lactotropes, somatotropes and thyrotropes. As the nature of IGSF1 signaling is not yet known, it is possible that IGSF1 interacts with ligands expressed on neighbouring cell types and, like Notch[252,253], is cleaved upon binding, resulting in endocytosis of the extracellular domain of IGSF1 in the ligand-expressing cell and the C-terminal domain in the IGSF1-expressing cell, directly affecting gene expression in an autocrine/paracrine manner. Indeed, experiments designed to analyze the cleavage of IGSF1 at the internal signal peptide in the ER[167] have shown that blocking SP and SPP cleavage of IGSF1 results in recruitment of a rhomboid-4 protease, which is then capable of cleaving IGSF1

(Turgeon, unpublished). Rhomboid-4 proteases have been detected at the plasma membrane[254,255] and may be capable of cleaving IGSF1 in a similar manner to Notch, resulting in autocrine/paracrine signaling. While we have never detected IGSF1 in the nucleus of cells, our antibody detects an epitope expressed in the TMD of IGSF1[157,167], which would remain in the plasma membrane in this model, obfuscating our ability to detect IGSF1 in the nucleus. Detection of IGSF1 in the nucleus of pituitary cell types would thus require the development of a novel antibody which detects either the extracellular portion of IGSF1 or the C-terminal tail followed by immunofluorescence analysis of IGSF1 subcellular localization in pituitary sections of *Igsf1*$^{+/y}$ mice.

Conclusion

While IGSF1 appears dispensable for TH transport into the hypothalamus, as well as MCT8-mediated influx of THs in vitro, IGSF1-deficiency clearly affects the thyrotrope response to TRH, likely secondary to reduced TRHR expression. Given that *Trhr* expression is downregulated in the absence of IGSF1, it seems plausible that IGSF1 acts as a signaling protein, binding an extracellular ligand and initiating a signaling cascade that enhances transcription of *Trhr*. Future studies aimed at identifying the extracellular ligand of IGSF1, as well as the nature of the signaling cascade may unravel the function of IGSF1 and its subsequent contribution to central hypothyroidism in IGSF1-deficient patients.

References

1. Ahmed OM, El-Gareib a. W, El-bakry a. M, Abd El-Tawab SM, Ahmed RG. Thyroid hormones states and brain development interactions. *Int J Dev Neurosci*. 2008;26(2):147-209. doi:10.1016/j.ijdevneu.2007.09.011.

2. Ausó E, Lavado-Autric R, Cuevas E, Escobar Del Rey F, Morreale De Escobar G, Berbel P. A moderate and transient deficiency of maternal thyroid function at the beginning of fetal neocorticogenesis alters neuronal migration. *Endocrinology*. 2004;145(9):4037-4047. doi:10.1210/en.2004-0274.

3. Yen PM. Physiological and molecular basis of thyroid hormone action. *Physiol Rev*. 2001;81(3):1097-1142.

4. Aizenman Y, de Vellis J. Brain neurons develop in a serum and glial free environment: effects of transferrin, insulin, insulin-like growth factor-I and thyroid hormone on neuronal survival, growth and differentiation. *Brain Res*. 1987;406(1-2):32-42. doi:10.1016/0006-8993(87)90766-9.

5. Robson H, Siebler T, Stevens D a., Shalet SM, Williams GR. Thyroid hormone acts directly on growth plate chondrocytes to promote hypertrophic differentiation and inhibit clonal expansion and cell proliferation. *Endocrinology*. 2000;141(10):3887-3897. doi:10.1210/endo.141.10.7733.

6. Chiamolera MI, Wondisford FE. Minireview: Thyrotropin-releasing hormone and the thyroid hormone feedback mechanism. *Endocrinology*. 2009;150(3):1091-1096. doi:10.1210/en.2008-1795.

7. Costa-e-Sousa RH, Hollenberg AN. Minireview: The neural regulation of the hypothalamic-pituitary-thyroid axis. *Endocrinology*. 2012;153(9):4128-4135. doi:10.1210/en.2012-1467.

8. Fekete C, Lechan RM. Central regulation of hypothalamic-pituitary-thyroid axis under physiological and pathophysiological conditions. *Endocr Rev*. 2014;35(2):159-194. doi:10.1210/er.2013-1087.

9. Fliers E, Unmehopa U a, Alkemade A. Functional neuroanatomy of thyroid hormone feedback in the human hypothalamus and pituitary gland. *Mol Cell Endocrinol*. 2006;251(1-2):1-8. doi:10.1016/j.mce.2006.03.042.

10. Lechan RM, Jackson IM. Immunohistochemical localization of thyrotropin-releasing hormone in the rat hypothalamus and pituitary. *Endocrinology*. 1982;111(1):55-65.

11. Kádár A, Sánchez E, Wittmann G, et al. Distribution of hypophysiotropic thyrotropin-releasing hormone (TRH)-synthesizing neurons in the hypothalamic paraventricular nucleus of the mouse. *J Comp Neurol*. 2010;518(19):3948-3961. doi:10.1002/cne.22432.

12. Zoeller RT, Tan SW, Tyl RW. General background on the hypothalamic-pituitary-thyroid (HPT) axis. *Crit Rev Toxicol*. 2007;37(1-2):11-53. doi:10.1080/10408440601123446.

13. Hollenberg AN, Monden T, Flynn TR, Boers M-E, Cohen O, Wondisford FE. The Human Thyrotropin-Releasing Hormone Gene Is Regulated by Thyroid Hormone through Two Distinct Classes of Negative Thyroid Hormone Response Elements. *Mol Endocrinol*. 1995;9:540-550.

14. Perello M, Friedman T, Paez-Espinosa V, Shen X, Stuart RC, Nillni E a. Thyroid hormones selectively regulate the posttranslational processing of prothyrotropin-releasing hormone in the paraventricular nucleus of the hypothalamus. *Endocrinology*. 2006;147(6):2705-2716. doi:10.1210/en.2005-1609.

15. Gershengorn MC. Mechanism of thyrotropin releasing hormone stimulation of pituitary hormone secretion. *Annu Rev Physiol*. 1986;48:515-526.

16. Visser TJ. Effects of hypothyroidism on hypothalamic release of thyrotropin-releasing hormone in rats. *Endocrinology*. 1992;130(2):651-656.

17. Rabeler R, Mittag J, Geffers L, et al. Generation of thyrotropin-releasing hormone receptor 1-deficient mice as an animal model of central hypothyroidism. *Mol Endocrinol*. 2004;18(6):1450-1460. doi:10.1210/me.2004-0017.

18. Taylor T, Weintraub BD. Thyrotropin (TSH)-releasing hormone regulation of TSH subunit biosynthesis and glycosylation in normal and hypothyroid rat pituitaries. *Endocrinology*. 1985;116(5):1968-1976. doi:10.1210/endo-116-5-1968.

19. Faglia G, Bitensky L, Pinchera a., et al. Thyrotropin secretion in patients with central hypothyroidism: Evidence for reduced biological activity of immunoreactive thyrotropin. *J Clin Endocrinol Metab*. 1979;48(6):989-998.

20. Magner J a., Papagiannes E. Structures of high-mannose oligosaccharides of mouse thyrotropin: Differential processing of alpha- versus beta-subunits of the heterodimer. *Endocrinology*. 1987;120(1):10-17.

21. Hsieh K-P, Martin TFJ. Thyrotropin-Releasing Hormone and Gonadotropin-Releasing Hormone Receptors Activate Phospholipase C by Coupling to the Guanosine Triphosphate-Binding Proteins Gq and G11. *Mol Endocrinol*. 1992;6(10):1673-1681.

22. Straub RE, Gershengorn C. Thyrotropin-releasing Hormone and GTP Activate Inositol Trisphosphate Formation in Membranes Isolated from Rat Pituitary Cells*. *J Biol Chem*. 1986;261(6):2712-2717.

23. Ponsin G, Mornex R. Control of Thyrotropin Glycosylation in Normal Rat Pituitary Cells in Culture: Effect of Thyrotropin- Releasing Hormone. *Endocrinology*. 2015;113(2):549-556.

24. Larsen CC, Karaviti LP, Seghers V, Weiss RE, Refetoff S, Dumitrescu AM. A new family with an activating mutation (G431S) in the TSH receptor gene: a phenotype discussion and review of the literature. *Int J Pediatr Endocrinol*. 2014;2014:23. doi:10.1186/1687-9856-2014-23.

25. Narumi S, Muroya K, Abe Y, et al. TSHR mutations as a cause of congenital hypothyroidism in Japan: a population-based genetic epidemiology study. *J Clin Endocrinol Metab*. 2009;94(4):1317-1323. doi:10.1210/jc.2008-1767.

26. Tonacchera M, Agretti P, Pinchera a., et al. Congenital hypothyroidism with impaired thyroid response to thyrotropin (TSH) and absent circulating thyroglobulin: Evidence for a new inactivating mutation of the TSH receptor gene. *J Clin Endocrinol Metab*. 2000;85(3):1001-1008. doi:10.1210/jc.85.3.1001.

27. Van Sande J, Dequanter D, Lothaire P, Massart C, Dumont JE, Erneux C. Thyrotropin stimulates the generation of inositol 1,4,5-trisphosphate in human thyroid cells. *J Clin Endocrinol Metab*. 2006;91(3):1099-1107. doi:10.1210/jc.2005-1324.

28. Grossmann M, Weintraub BD, Szkudlinski MW. Novel insights into the molecular mechanisms of human thyrotropin action: Structural, physiological, and therapeutic implications for the glycoprotein hormone family. *Endocr Rev*. 1997;18(4):476-501. doi:10.1210/er.18.4.476.

29. Van Sande J, Dequanter D, Lothaire P, Massart C, Dumont JE, Erneux C. Thyrotropin stimulates the generation of inositol 1,4,5-trisphosphate in human thyroid cells. *J Clin Endocrinol Metab*. 2006;91(3):1099-1107. doi:10.1210/jc.2005-1324.

30. Yamashita K, Field JB. Effects of long-acting thyroid stimulator on thyrotropin stimulation of adenyl cyclase activity in thyroid plasma membranes. *J Clin Invest*. 1972;51(3):463-472. doi:10.1172/JCI106834.

31. Laurent E, Mockel J, Van Sande J, Graff I, Dumont JE. Dual activation by thyrotropin of the phospholipase C and cyclic AMP cascades in human thyroid. *Mol Cell Endocrinol*. 1987;52(3):273-278. doi:10.1016/0303-7207(87)90055-4.

32. Szkudlinski MW, Fremont V, Ronin C, Weintraub BD, Fremont V, Ronin C. Thyroid-Stimulating Hormone and Thyroid-Stimulating Hormone Receptor Structure-Function Relationships. *Physiol Rev*. 2001;82:473-502.

33. Schomburg L, Köhrle J. On the importance of selenium and iodine metabolism for thyroid hormone biosynthesis and human health. *Mol Nutr Food Res*. 2008;52(11):1235-1246. doi:10.1002/mnfr.200700465.

34. Magner JA. Thyroid-Stimulating Hormone: Biosynthesis, Cell Biology, and Bioactivity. *Endocr Rev*. 1990;11(2):354-385.

35. Roef GL, Rietzschel ER, De Meyer T, et al. Associations between single nucleotide polymorphisms in thyroid hormone transporter genes (MCT8, MCT10 and OATP1C1) and circulating thyroid hormones. *Clin Chim Acta*. 2013;425:227-232. doi:10.1016/j.cca.2013.08.017.

36. Heuer H, Visser TJ. The pathophysiological consequences of thyroid hormone transporter deficiencies: Insights from mouse models. *Biochim Biophys Acta - Gen Subj*. 2013;1830(7):3974-3978. doi:10.1016/j.bbagen.2012.04.009.

37. Roberts LM, Woodford K, Zhou M, et al. Expression of the thyroid hormone transporters monocarboxylate transporter-8 (SLC16A2) and organic ion transporter-14 (SLCO1C1) at the blood-brain barrier. *Endocrinology*. 2008;149(12):6251-6261. doi:10.1210/en.2008-0378.

38. Friesema ECH, Kuiper GGJM, Jansen J, Visser TJ, Kester MH a. Thyroid hormone transport by the human monocarboxylate transporter 8 and its rate-limiting role in intracellular metabolism. *Mol Endocrinol*. 2006;20(11):2761-2772. doi:10.1210/me.2005-0256.

39. Visser WE, Friesema ECH, Jansen J, Visser TJ. Thyroid hormone transport in and out of cells. *Trends Endocrinol Metab*. 2008;19(2):50-56. doi:10.1016/j.tem.2007.11.003.

40. Arjona FJ, De Vrieze E, Visser TJ, Flik G, Klaren PHM. Identification and functional characterization of zebrafish solute carrier Slc16a2 (Mct8) as a thyroid hormone membrane transporter. *Endocrinology*. 2011;152(12):5065-5073. doi:10.1210/en.2011-1166.

41. Friesema ECH, Ganguly S, Abdalla A, Manning Fox JE, Halestrap AP, Visser TJ. Identification of monocarboxylate transporter 8 as a specific thyroid hormone transporter. *J Biol Chem*. 2003;278(41):40128-40135. doi:10.1074/jbc.M300909200.

42. Mayerl S, Müller J, Bauer R, et al. Transporters MCT8 and OATP1C1 maintain murine brain thyroid hormone homeostasis. *J Clin Invest*. 2014;124(5):1987-1999. doi:10.1172/JCI70324.

43. Núñez B, Martínez De Mena R, Obregon MJ, et al. Cerebral cortex hyperthyroidism of newborn Mct8-deficient mice transiently suppressed by Lat2 inactivation. *PLoS One*. 2014;9(5):3-9. doi:10.1371/journal.pone.0096915.

44. Müller J, Mayerl S, Visser TJ, et al. Tissue-specific alterations in thyroid hormone homeostasis in combined Mct10 and Mct8 deficiency. *Endocrinology*. 2014;155(1):315-325. doi:10.1210/en.2013-1800.

45. St Germain DL, Galton V a. The deiodinase family of selenoproteins. *Thyroid*. 1997;7(4):655-668. doi:10.1089/thy.1997.7.655.

46. Köhrle J. Local activation and inactivation of thyroid hormones: The deiodinase family. *Mol Cell Endocrinol*. 1999;151(1-2):103-119. doi:10.1016/S0303-7207(99)00040-4.

47. Behne D, Kyriakopoulos a, Meinhold H, Köhrle J. Identification of type I iodothyronine 5'-deiodinase as a selenoenzyme. *Biochem Biophys Res Commun*. 1990;173(3):1143-1149. doi:10.1016/S0006-291X(05)80905-2.

48. Wagner RL, Apriletti JW, McGrath ME, West BL, Baxter JD, Fletterick RJ. A structural role for hormone in the thyroid hormone receptor. *Nature*. 1995;378(6558):690-697. doi:10.1038/378690a0.

49. Umesono K, Murakami KK, Thompson CC, Evans R. Direct repeats as selective response elements for the thyroid hormone, retinoic acid, and vitamin D3 receptors. *Cell*. 1991;65(7):1255-1266. doi:10.1016/0092-8674(91)90020-Y.

50. Yu VC, Delsert C, Andersen B, et al. RXR beta: a coregulator that enhances binding of retinoic acid, thyroid hormone, and vitamin D receptors to their cognate response elements. *Cell*. 1991;67(6):1251-1266. doi:10.1016/0092-8674(91)90301-E.

51. Damm K, Thompson CC, Evans RM. Protein encoded by v-erbA functions as a thyroid-hormone receptor antagonist. *Nature*. 1989;339:593-597.

52. Glass CK, Holloway JM, Devary O V, Rosenfeld MG. The thyroid hormone receptor binds with opposite transcriptional effects to a common sequence motif in thyroid hormone and estrogen response elements. *Cell*. 1988;54(3):313-323. doi:10.1016/0092-8674(88)90194-8.

53. Glass CK, Lipkin SM, Devary O V, Rosenfeld MG. Positive and negative regulation of gene transcription by a retinoic acid-thyroid hormone receptor heterodimer. *Cell*. 1989;59(4):697-708.

54. Fondell JD, Ge H, Roeder RG. Ligand induction of a transcriptionally active thyroid hormone receptor coactivator complex. *Proc Natl Acad Sci U S A*. 1996;93(16):8329-8333. doi:10.1073/pnas.93.16.8329.

55. Fondell JD, Roy a. L, Roeder RG. Unliganded thyroid hormone receptor inhibits formation of a functional preinitiation complex: Implications for active repression. *Genes Dev*. 1993;7(7 B):1400-1410. doi:10.1101/gad.7.7b.1400.

56. Baniahmad a, Ha I, Reinberg D, Tsai S, Tsai MJ, O'Malley BW. Interaction of human thyroid hormone receptor beta with transcription factor TFIIB may mediate target gene derepression and activation by thyroid hormone. *Proc Natl Acad Sci U S A*. 1993;90(19):8832-8836.

57. Cheng SY. Multiple mechanisms for regulation of the transcriptional activity of thyroid hormone receptors. *Rev Endocr Metab Disord*. 2000;1(1-2):9-18. doi:10.1023/A:1010052101214.

58. Bargi-Souza P, Romano RM, Goulart-Silva F, Brunetto EL, Nunes MT. T3 rapidly regulates several steps of alpha subunit glycoprotein (CGA) synthesis and secretion in the pituitary of male rats: Potential repercussions on TSH, FSH and LH secretion. *Mol Cell Endocrinol*. 2015;409:73-81. doi:10.1016/j.mce.2015.04.002.

59. Franklyn JA, Sheppard MC. Regulation of TSH gene transcription. *Eur J Clin Invest*. 1986;16:452-454.

60. Chatterjee VKK, Lee J-K, Rentoumis A, Jameson JL. Negative regulation of the thyroid-stimulating hormone alpha gene by thyroid hormone: receptor interaction adjacent to the TATA box. *Proc Natl Acad Sci U S A*. 1989;86(December):9114-9118. http://www.pubmedcentral.nih.gov/articlerender.fcgi?artid=298444&tool=pmcentrez&rendertype=abstract.

61. Nikrodhanond A a, Ortiga-Carvalho TM, Shibusawa N, et al. Dominant role of thyrotropin-releasing hormone in the hypothalamic-pituitary-thyroid axis. *J Biol Chem*. 2006;281(8):5000-5007. doi:10.1074/jbc.M511530200.

62. Bulant M, Delfour a., Vaudry H, Nicolas P. Processing of thyrotropin-releasing hormone prohormone (pro-TRH) generates Pro-TRH-connecting peptides. Identification and characterization of prepro-TRH-(160-169) and prepro-TRH-(178-199) in the rat nervous system. *J Biol Chem*. 1988;263(32):17189-17196.

63. Satoh T, Yamada M, Monden T, Iizuka M, Mori M. Cloning of the mouse hypothalamic preprothyrotropin-releasing hormone (TRH) cDNA and tissue distribution of its mRNA. *Brain Res Mol Brain Res*. 1992;14(1-2):131-135. doi:10.1016/0169-328X(92)90020-C.

64. Bulant M, Roussel JP, Astier H, Nicolas P, Vaudry H. Processing of thyrotropin-releasing hormone prohormone (pro-TRH) generates a biologically active peptide, prepro-TRH-(160-169), which regulates TRH-induced thyrotropin secretion. *Proc Natl Acad Sci U S A*. 1990;87(12):4439-4443. doi:10.1073/pnas.87.12.4439.

65. Yamada M, Radovick S, Wondisford FE, Nakayama Y, Weintraub BD, Wilber JF. Cloning and structure of human genomic DNA and hypothalamic cDNA encoding human prepro thyrotropin-releasing hormone. *Mol Endocrinol*. 1990;4(4):551-556.

66. Lee SL, Stewart K, Goodman RH. Structure of the gene encoding rat thyrotropin releasing hormone. *J Biol Chem*. 1988;263(32):16604-16609.

67. Schaner P, Todd RB, Seidah NG, Nillni E a. Processing of prothyrotropin-releasing hormone by the family of prohormone convertases. *J Biol Chem*. 1997;272(32):19958-19968. doi:10.1074/jbc.272.32.19958.

68. Nillni EA, Sevarino K. The Biology of pro-Thyrotropin-Releasing Hormone- Derived Peptides. *Endocr Rev*. 1999;20(5):599-648.

69. Loudes C, Faivre-Bauman a, Barret a, Grouselle D, Puymirat J, Tixier-Vidal a. Release of immunoreactive TRH in serum-free cultures of mouse hypothalamic cells. *Brain Res*. 1983;285(2):231-234. doi:10.1016/0165-3806(83)90057-3.

70. Yu R, Ashworth R, Hinkle PM. Receptors for thyrotropin-releasing hormone on rat lactotropes and thyrotropes. *Thyroid*. 1998;8(10):887-894. doi:10.1089/thy.1998.8.887.

71. Aragayl AM, Katz A, Simon MI. The G alpha q, and G alpha 11 Proteins Couple the Thyrotropin-releasing Hormone Receptor to Phospholipase C in GH3 Rat Pituitary Cells. *J Biol Chem*. 1992;267(35):24983-24988.

72. Konaka S, Yamada M, Satoh T, et al. Expression of thyrotropin-releasing hormone (TRH) receptor mRNA in somoatotrophs in the rat anterior pituitary. *Endocrinology*. 1997;138(2):827-830.

73. Yamada M, Shibusawa N, Ishii S, et al. Prolactin secretion in mice with thyrotropin-releasing hormone deficiency. *Endocrinology*. 2006;147(5):2591-2596. doi:10.1210/en.2005-1326.

74. Collu R, Tang J, Castagné J, et al. A novel mechanism for isolated central hypothyroidism: Inactivating mutations in the thyrotropin-releasing hormone receptor gene. *J Clin Endocrinol Metab*. 1997;82(5):1561-1565. doi:10.1210/jc.82.5.1561.

75. Duthie SM, Taylor PL, Anderson L, Cook J, Eidne K a. Cloning and functional characterisation of the human TRH receptor. *Mol Cell Endocrinol*. 1993;95(1-2):R11-R15.

76. Cohen LE, Wondisford FE, Radovick S. Role of Pit-1 in the gene expression of growth hormone, prolactin, and thyrotropin. *Endocrinol Metab Clin North Am*. 1996;25(3):523-540.

77. Matre V, Høvring PI, Ørstavik S, et al. Structural and Functional Organization of the Gene Encoding the Human Thyrotropin-Releasing Hormone Receptor. *J Neurochem*. 2002;72(1):40-50. doi:10.1046/j.1471-4159.1999.0720040.x.

78. Naor Z. Signaling by G-protein-coupled receptor (GPCR): Studies on the GnRH receptor. *Front Neuroendocrinol*. 2009;30(1):10-29. doi:10.1016/j.yfrne.2008.07.001.

79. Howard PW, Maurersn RA. Thyrotropin Releasing Hormone Stimulates Transient Phosphorylation of the Tissue-specific Transcription Factor, Pit-1. *J Biol Chem*. 1994;269(46):28662-28669.

80. Carr FE, Fisher CU, Fein HG, Smallridge RC. Thyrotropin-Releasing Hormone Stimulates c-jun and c-fos Messenger Ribonucleic Acid Levels: Implications for Calcium Mobilization and Protein Kinase-C Activation. *Endocrinology*. 1993;133(4):1700-1707.

81. Kim DS, Ahn SK, Yoon JH, et al. Involvement of a cAMP-Responsive DNA Element in Mediating TRH Responsiveness of the Human Thyrotropin alpha-Subunit Gene. *Mol Endocrinol*. 1994;8:528-536.

82. Kim MK, McClaskey JH, Bodenner DL, Weintraub BD. An AP-1-like Factor and the Pituitary-specific Factor Pit-1 Are Both Necessary to Mediate Hormonal Induction of Human Thyrotropin-Beta Gene Expression. *J Biol Chem*. 1993;268(31):23366-23375.

83. Yang J, Tashjian AH. Regulation of Endogenous Hormone (TRH) Receptor Messenger RNA by TRH in GH4C1 cells. *Mol Endocrinol*. 1993;7:753-758.

84. Hinkle PM, Gehret AU, Jones BW. Desensitization, trafficking, and resensitization of the pituitary thyrotropin-releasing hormone receptor. *Front Neurosci*. 2012;6(December):180. doi:10.3389/fnins.2012.00180.

85. Yu R, Hinkle PM. Signal Transduction, Desensitization, and Recovery of Responses to Thyrotropin- Releasing Hormone after Inhibition of Receptor Internalization. *Mol Endocrinol*. 1998;12:737-749.

86. Heuer H, Schäfer MK-H, Bauer K. The Thyrotropin-Releasing Hormone-Degrading Ectoenzyme: The Third Element of the Thyrotropin-Releasing Hormone-Signaling System. *Thyroid*. 1998;8(10):915-920. doi:10.1089/thy.1998.8.915.

87. Grasberger H, Van Sande J, Hag-Dahood Mahameed A, Tenenbaum-Rakover Y, Refetoff S. A familial thyrotropin (TSH) receptor mutation provides in vivo evidence that the inositol phosphates/Ca2+ cascade mediates TSH action on thyroid hormone synthesis. *J Clin Endocrinol Metab*. 2007;92(7):2816-2820. doi:10.1210/jc.2007-0366.

88. Alberti L, Proverbio MC, Costagliola S, et al. Germline mutations of TSH receptor gene as cause of nonautoimmune subclinical hypothyroidism. *J Clin Endocrinol Metab*. 2002;87(6):2549-2555. doi:10.1210/jc.87.6.2549.

89. Vassart G, Dumont JE. The Thyrotropin Receptor and the Regulation of Thyrocyte Function and Growth. *Endocr Rev*. 1992;13(3):596-611.

90. Larsen CC, Karaviti LP, Seghers V, Weiss RE, Refetoff S, Dumitrescu AM. A new family with an activating mutation (G431S) in the TSH receptor gene: a phenotype discussion and review of the literature. *Int J Pediatr Endocrinol*. 2014;2014(1):23. doi:10.1186/1687-9856-2014-23.

91. Wondisford FE, Usala SJ, DeCherney GS, et al. Cloning of the human thyrotropin beta-subunit gene and transient expression of biologically active human thyrotropin after gene transfection. *Mol Endocrinol*. 1988;2(1):32-39.

92. Fiddes JC, Goodman HM. Isolation, cloning and sequence analysis of the cDNA for the alpha-subunit of human chorionic gonadotropin. *Nature*. 1979;281:351-356.

93. Nilsson BO, Rosen SW, Weintraub BD, Zopf DA. Differences in the Carbohydrate Moieties of the Common alpha-subunits of Human Chorionic Gonadotropin, Luteinizing Hormone, Follicle-Stimulating Hormone, and Thyrotropin: Preliminary Structural Inferences from Direct Methylation Analysis. *Endocrinology*. 1986;119(6):2737-2743.

94. Tumor P, Influence C, Units O, Weintraub BD, Stannard BS, Meyers L. Glycosylation of Thyroid-Stimulating Hormone in Pituitary Tumor Cells: Influence of High Mannose Oligosaccharide Units on Subunit Aggregation, Combination and Intracellular Degradation. *Endocrinology*. 1983;112(4):1331-1345.

95. Chin WW, Habener JF. Thyroid-stimulating hormone subunits: Evidence from endoglycosidase-H cleavage for late presecretory glycosylation. *Endocrinology*. 1981;108(5):1628-1633.

96. Taylor T, Gesundheit N, Weintraub BD. Effects of in vivo bolus versus continuous TRH administration on TSH secretion, biosynthesis, and glycosylation in normal and hypothyroid rats. *Mol Cell Endocrinol*. 1986;46:253-261.

97. Weintraub BD, Gesundheit N, Taylor T, Gyves PW. Effect of TRH on TSH glycosylation and biological action. *Ann N Y Acad Sci*. 1989;553:205-213.

98. Taylor T, Weintraub BD. Differential regulation of thyrotropin subunit apoprotein and carbohydrate biosynthesis by thyroid hormone. *Endocrinology*. 1985;116(4):1535-1542. doi:10.1210/endo-116-4-1535.

99. Marians RC, Ng L, Blair HC, Unger P, Graves PN, Davies TF. Defining thyrotropin-dependent and -independent steps of thyroid hormone synthesis by using thyrotropin receptor-null mice. *Proc Natl Acad Sci U S A*. 2002;99(24):15776-15781. doi:10.1073/pnas.242322099.

100. Deme D, Pommier J, Nunez J. Specificity of thyroid hormone synthesis. The role of thyroid peroxidase. *Biochim Biophys Acta*. 1978;540(1):73-82.

101. Cosmo C Di, Liao X, Dumitrescu AM, Philp NJ, Weiss RE, Refetoff S. Mice deficient in MCT8 reveal a mechanism regulating thyroid hormone secretion. *J Clin Invest*. 2010;120(9):3377-3388. doi:10.1172/JCI42113.thyroacetic.

102. Gavaret J, Cahnmann HJ, Nunez J. Thyroid Hormone Synthesis in Thyroglobulin. *J Biol Chem*. 1981;256(17):9167-9173.

103. Larsen PR, Silva JE, Kaplan MM. Relationships between circulating and intracellular thyroid hormones: physiological and clinical implications. *Endocr Rev*. 1981;2(1):87-102. doi:10.1210/edrv-2-1-87.

104. Nilsson SF, Peterson PA. Studies on Thyroid Hormone-binding proteins. *J Biol Chem*. 1975;250(21):8543-8553.

105. Galton VA. The roles of the iodothyronine deiodinases in mammalian development. *Thyroid*. 2005;15(8):823-834. doi:10.1089/thy.2005.15.823.

106. Flamant F, Samarut J. Thyroid hormone receptors: lessons from knockout and knock-in mutant mice. *Trends Endocrinol Metab*. 2003;14(2):85-90. doi:10.1016/S1043-2760(02)00043-7.

107. Schomburg L, Bauer K. Thyroid hormones rapidly and stringently regulate the messenger RNA levels of the thyrotropin-releasing hormone (TRH) receptor and the TRH-degrading ectoenzyme. *Endocrinology*. 1995;136(8):3480-3485.

108. Wu Y, Koenig RJ. Gene regulation by thyroid hormone. *Trends Endocrinol Metab*. 2000;11(6):207-211. doi:10.1016/S1043-2760(00)00263-0.

109. Hollenberg AN, Monden T, Flynn TR, Boers ME, Cohen O, Wondisford FE. The human thyrotropin-releasing hormone gene is regulated by thyroid hormone through two distinct classes of negative thyroid hormone response elements. *Mol Endocrinol*. 1995;9(5):540-550. doi:10.1210/mend.9.5.7565802.

110. Lazar MA. Thyroid hormone receptors: Multiple forms, multiple possibilities. *Endocr Rev*. 1993;14(2):184-193. doi:10.1210/er.14.2.184.

111. Tagami T, Madison LD, Nagaya T, Jameson JL. Nuclear receptor corepressors activate rather than suppress basal transcription of genes that are negatively regulated by thyroid hormone. *Mol Cell Biol*. 1997;17(5):2642-2648.

112. Bonen A, Heynen M, Hatta H. Distribution of monocarboxylate transporters MCT1-MCT8 in rat tissues and human skeletal muscle. *Appl Physiol Nutr Metab*. 2006;31(1):31-39. doi:10.1139/h05-002.

113. Muzzio AM, Noyes PD, Stapleton HM, Lema SC. Tissue distribution and thyroid hormone effects on mRNA abundance for membrane transporters Mct8, Mct10, and organic anion-transporting polypeptides (Oatps) in a teleost fish. *Comp Biochem Physiol - A Mol Integr Physiol*. 2014;167:77-89. doi:10.1016/j.cbpa.2013.09.019.

114. Friesema ECH, Visser TJ, Borgers AJ, et al. Thyroid hormone transporters and deiodinases in the developing human hypothalamus. *Eur J Endocrinol*. 2012;167(3):379-386. doi:10.1530/EJE-12-0177.

115. Dumitrescu AM, Liao XH, Weiss RE, Millen K, Refetoff S. Tissue-specific thyroid hormone deprivation and excess in monocarboxylate transporter (Mct) 8-deficient mice. *Endocrinology*. 2006;147(9):4036-4043. doi:10.1210/en.2006-0390.

116. Alkemade A, Friesema EC, Unmehopa U a., et al. Neuroanatomical pathways for thyroid hormone feedback in the human hypothalamus. *J Clin Endocrinol Metab*. 2005;90(7):4322-4334. doi:10.1210/jc.2004-2567.

117. Heuer H, Maier MK, Iden S, et al. The monocarboxylate transporter 8 linked to human psychomotor retardation is highly expressed in thyroid hormone-sensitive neuron populations. *Endocrinology*. 2005;146(4):1701-1706. doi:10.1210/en.2004-1179.

118. Trajkovic-Arsic M, Müller J, Darras VM, et al. Impact of monocarboxylate transporter-8 deficiency on the hypothalamus-pituitary-thyroid axis in mice. *Endocrinology*. 2010;151(10):5053-5062. doi:10.1210/en.2010-0593.

119. Schweizer U, Köhrle J. Function of thyroid hormone transporters in the central nervous system. *Biochim Biophys Acta - Gen Subj*. 2013;1830(7):3965-3973. doi:10.1016/j.bbagen.2012.07.015.

120. Zlokovic B V., Jovanovic S, Miao W, Samara S, Verma S, Farrell CL. Differential regulation of leptin transport by the choroid plexus and blood-brain barrier and high affinity transport systems for entry into hypothalamus and across the blood-cerebrospinal fluid barrier. *Endocrinology*. 2000;141(4):1434-1441. doi:10.1210/en.141.4.1434.

121. Mullier A, Bouret SG, Prevot V, Dehouck B. Differential distribution of tight junction proteins suggests a role for tanycytes in blood-hypothalamus barrier regulation in the adult mouse brain. *J Comp Neurol*. 2010;518(7):943-962. doi:10.1002/cne.22273.

122. Langlet F, Mullier A, Bouret SG, Prevot V, Dehouck B. Tanycyte-like cells form a blood-cerebrospinal fluid barrier in the circumventricular organs of the mouse brain. *J Comp Neurol*. 2013;521(15):3389-3405. doi:10.1002/cne.23355.

123. Dickson PW, Aldred a. R, Menting JG, Marley PD, Sawyer WH, Schreiber G. Thyroxine transport in choroid plexus. *J Biol Chem*. 1987;262(29):13907-13915.

124. Richardson SJ, Wijayagunaratne RC, D'Souza DG, Darras VM, Van Herck SLJ. Transport of thyroid hormones via the choroid plexus into the brain: the roles of transthyretin and thyroid hormone transmembrane transporters. *Front Neurosci*. 2015;9(March):1-8. doi:10.3389/fnins.2015.00066.

125. Schwartz CE, Stevenson RE. The MCT8 thyroid hormone transporter and Allan-Herndon-Dudley syndrome. *Best Pract Res Clin Endocrinol Metab*. 2007;21(2):307-321. doi:10.1016/j.beem.2007.03.009.

126. Kobayashi S, Onuma A, Inui T, et al. Clinical Course and Images of Four Familial Cases of Allan-Herndon-Dudley Syndrome With a Novel Monocarboxylate Transporter 8 Gene Mutation. *Pediatr Neurol*. 2014;51(3):414-416. doi:10.1016/j.pediatrneurol.2014.05.004.

127. Namba N, Etani Y, Kitaoka T, et al. Clinical phenotype and endocrinological investigations in a patient with a mutation in the MCT8 thyroid hormone transporter. *Eur J Pediatr*. 2008;167(7):785-791. doi:10.1007/s00431-007-0589-6.

128. Spaulding SW. The Allan–Herndon–Dudley Syndrome: How Common Is It, and Does Normalizing Thyroid Function Tests in Such Patients Improve Any Clinical Parameters? *ThyroidOrg*. 2012;24(12):12-14. doi:10.1111/cen.12023.SUMMARY.

129. Di Cosmo C, Liao XH, Ye H, et al. Mct8-deficient mice have increased energy expenditure and reduced fat mass that is abrogated by normalization of serum T3 levels. *Endocrinology*. 2013;154(12):4885-4895. doi:10.1210/en.2013-1150.

130. Hollingsworth DR, Mabry CC. Congenital Graves Disease. *Am J Dis Child*. 1976;130:148-155.

131. Volpe R, Farid NR, Von Westarp C, Row V V. The pathogenesis of Graves' disease and Hashimoto's thyroiditis. *Clin Endocrinol (Oxf)*. 1974;3:239-261.

132. Wood AJJ. The management of hyperthyroidism. *Drug Ther (NY)*. 1994;330(24):1731-1738.

133. Toft AD. Subclinical hyperthyroidism. *N Engl J Med*. 2011;170(7):821-829. doi:10.1007/s00431-011-1451-4.

134. Clague R, Mukhtar ED, Pyle G a, et al. Thyroid-stimulating immunoglobulins and the control of thyroid function. *J Clin Endocrinol Metab*. 1976;43(3):550-556.

135. Smith BR, Hall R. Thyroid-stimulating immunoglobulins in Graves' disease. *Lancet*. 1973:427-430.

136. Weetman A. Graves' disease. *N Engl J Med*. 2000;343(17):1236-1248. http://www.nejm.org/doi/full/10.1056/NEJM200010263431707.

137. Surks MI, Chopra IJ, Mariash CN, Nicoloff JT, Solomon DH. American Thyroid Association guidelines for use of laboratory tests in thyroid disorders. *JAMA*. 1990;263(11):1529-1532. doi:10.1001/jama.1990.03440110095035.

138. Monaco F. Clinical perspective: Classification of thyroid diseases: Suggestions for a revision. *J Clin Endocrinol Metab*. 2003;88(4):1428-1432. doi:10.1210/jc.2002-021260.

139. Ladenson PW, Singer P a, Ain KB, et al. American Thyroid Association guidelines for detection of thyroid dysfunction. *Arch Intern Med*. 2000;160(11):1573-1575. doi:10.1001/archinte.160.11.1573.

140. Hetzel BS. Iodine deficiency disorders (IDD) and their eradication. *Lancet*. 1983;2(8359):1126-1129. doi:10.1016/S0140-6736(83)90636-0.

141. Vanderpas JB, Contempré B, Duale NL, et al. Iodine and selenium deficiency associated with cretinism in northern Zaire. *Am J Clin Nutr*. 1990;52(6):1087-1093.

142. Canaris GJ, Manowitz NR, Mayor G, Ridgway EC. The Colorado thyroid disease prevalence study. *Arch Intern Med*. 2000;160(4):526-534. doi:10.1001/archinte.160.4.526.

143. De Groot LJ, Hall R, McDermott W V., Davis AM. Hashimoto's thyroiditis. *N Engl J Med*. 1962;267(6):267-273.

144. Fisher DA, Oddie TH, Johnson DE, Nelson JC. The Diagnosis of Hashimoto's Thyroiditis. 2015;(September).

145. Duprez L, Parma J, Van Sande J, et al. TSH Receptor Mutations and Thyroid Disease. *Trends Endocrinol Metab*. 1998;9(4):133-140. doi:10.1016/S1043-2760(98)00036-8.

146. Kapell D, Nightingale B, Rodriguez a, Lee JH, Zigman WB, Schupf N. Prevalence of chronic medical conditions in adults with mental retardation: comparison with the general population. *Ment Retard*. 1998;36(4):269-279. doi:10.1352/0047-6765(1998)036<0269:pocmci>2.0.co;2.

147. Rabeler R, Mittag J, Geffers L, et al. Generation of thyrotropin-releasing hormone receptor 1-deficient mice as an animal model of central hypothyroidism. *Mol Endocrinol*. 2004;18(6):1450-1460. doi:10.1210/me.2004-0017.

148. Yamada M, Shibusawa N, Ishii S, et al. Prolactin secretion in mice with thyrotropin-releasing hormone deficiency. *Endocrinology*. 2006;147(5):2591-2596. doi:10.1210/en.2005-1326.

149. Joustra SD, van Trotsenburg a. SP, Sun Y, et al. IGSF1 deficiency syndrome: A newly uncovered endocrinopathy. *Rare Dis*. 2013;1(2):e24883. doi:10.4161/rdis.24883.

150. Persani L. Central hypothyroidism: Pathogenic, diagnostic and therapeutic challenges. *J Clin Endocrinol Metab*. 2012;97(9):3068-3078. doi:10.1210/jc.2012-1616.

151. Bonomi M, Busnelli M, Beck-Peccoz P, et al. A family with complete resistance to thyrotropin-releasing hormone. *N Engl J Med*. 2009;360(7):731-734. doi:10.1056/NEJMc0808557.

152. Bonomi M, Proverbio MC, Weber G, Chiumello G, Beck-Peccoz P, Persani L. Hyperplastic pituitary gland, high serum glycoprotein hormone alpha-subunit, and variable circulating thyrotropin (TSH) levels as hallmark of central hypothyroidism due to mutations of the TSH?? gene. *J Clin Endocrinol Metab*. 2001;86(4):1600-1604. doi:10.1210/jc.86.4.1600.

153. McDermott MT, Haugen BR, Black JN, Wood WM, Gordon DF, Ridgway EC. Congenital isolated central hypothyroidism caused by a "hot spot" mutation in the thyrotropin-beta gene. *Thyroid*. 2002;12(12):1141-1146. doi:10.1089/105072502321085252.

154. Dacou-Voutetakis C, Feltquate DM, Drakopoulou M, Kourides I a, Dracopoli NC. Familial hypothyroidism caused by a nonsense mutation in the thyroid-stimulating hormone beta-subunit gene. *Am J Hum Genet*. 1990;46(5):988-993.

155. Joustra SD, Wehkalampi K, Oostdijk W, et al. IGSF1 variants in boys with familial delayed puberty. *Eur J Pediatr*. October 2014. doi:10.1007/s00431-014-2445-9.

156. Joustra SD, Schoenmakers N, Persani L, et al. The IGSF1 Deficiency Syndrome: Characteristics of Male and Female Patients. *J Clin Endocrinol Metab*. 2013;98(12):4942-4952. doi:10.1210/jc.2013-2743.

157. Sun Y, Bak B, Schoenmakers N, et al. Loss-of-function mutations in IGSF1 cause an X-linked syndrome of central hypothyroidism and testicular enlargement. *Nat Genet*. 2012;44(12):1375-1381. doi:10.1038/ng.2453.

158. Barclay AN. Membrane proteins with immunoglobulin-like domains—a master superfamily of interaction molecules. *Semin Immunol*. 2003;15(4):215-223. doi:10.1016/S1044-5323(03)00047-2.

159. Fusaoka E, Inoue T, Mineta K, Agata K, Takeuchi K. Structure and function of primitive immunoglobulin superfamily neural cell adhesion molecules: a lesson from studies on planarian. *Genes Cells*. 2006;11(5):541-555. doi:10.1111/j.1365-2443.2006.00962.x.

160. Rougon G, Hobert O. New insights into the diversity and function of neuronal immunoglobulin superfamily molecules. *Annu Rev Neurosci*. 2003;26:207-238. doi:10.1146/annurev.neuro.26.041002.131014.

161. Yap E-H, Rosche T, Almo S, Fiser A. Functional clustering of immunoglobulin superfamily proteins with protein-protein interaction information calibrated hidden Markov model sequence profiles. *J Mol Biol*. 2014;426(4):945-961. doi:10.1016/j.jmb.2013.11.009.

162. Ioerger TR, Du C, Linthicum DS. Conservation of cys–cys trp structural triads and their geometry in the protein domains of immunoglobulin superfamily members. *Mol Immunol*. 1999;36(6):373-386. doi:10.1016/S0161-5890(99)00032-2.

163. Williams AF, Barclay NA. The immunoglobulin superfamily - domains for cell surface recognition. *Annu Rev Immunol*. 1988;6:381-405.

164. Williams AF. A year in the life of the immunoglobulin superfamily. *Immunol Today*. 1987;8(10):298-303. doi:10.1016/0167-5699(87)90016-8.

165. Iacono KT, Brown AL, Greene MI, Saouaf SJ. CD147 immunoglobulin superfamily receptor function and role in pathology. *Exp Mol Pathol*. 2007;83(3):283-295. doi:10.1016/j.yexmp.2007.08.014.

166. Nakayama M, Kikuno R, Ohara O. Protein-protein interactions between large proteins: two-hybrid screening using a functionally classified library composed of long cDNAs. *Genome Res*. 2002;12(11):1773-1784. doi:10.1101/gr.406902.

167. Robakis T, Bak B, Lin S, Bernard DJ, Scheiffele P. An internal signal sequence directs intramembrane proteolysis of a cellular immunoglobulin domain protein. *J Biol Chem*. 2008;283(52):36369-36376. doi:10.1074/jbc.M807527200.

168. Mazzarella R, Pengue G, Jones J, Jones C, Schlessinger D. Cloning and expression of an immunoglobulin superfamily gene (IGSF1) in Xq25. *Genomics*. 1998;48(2):157-162. doi:10.1006/geno.1997.5156.

169. Frattini A, Faranda S, Redolfi E, Allavena P, Vezzoni P. Identification and genomic organization of a gene coding for a new member of the cell adhesion molecule family mapping to Xq25. *Gene*. 1998;214(1-2):1-6. doi:10.1016/S0378-1119(98)00253-4.

170. Bernard DJ, Woodruff TK. Inhibin Binding Protein in Rats: Alternative Transcripts and Regulation in the Pituitary across the Estrous Cycle. *Mol Endocrinol*. 2001;15(4):654-667.

171. Joustra SD, Meijer OC, Heinen C a, et al. Spatial and temporal expression of immunoglobulin superfamily member 1 in the rat. *J Endocrinol*. 2015;226(3):181-191. doi:10.1530/JOE-15-0204.

172. Bernard DJ, Burns KH, Haupt B, Matzuk MM, Woodruff TK. Normal Reproductive Function in InhBP/p120-Deficient Mice. *Mol Cell Biol*. 2003;23(14):4882-4891. doi:10.1128/MCB.23.14.4882-4891.2003.

173. States DJ, Omenn GS, Blackwell TW, et al. Challenges in deriving high-confidence protein identifications from data gathered by a HUPO plasma proteome collaborative study. *Nat Biotechnol*. 2006;24(3):333-338. doi:10.1038/nbt1183.

174. Nakamura A, Bak B, Silander TLR, et al. Three novel IGSF1 mutations in four Japanese patients with X-linked congenital central hypothyroidism. *J Clin Endocrinol Metab*. 2013;98(10):E1682-E1691. doi:10.1210/jc.2013-1224.

175. Tajima T, Nakamura A, Ishizu K. A novel mutation of IGSF1 in a Japanese patient of congenital central hypothyroidism without macroorchidism. *Endocr J*. 2013;60(2):245-249.

176. Asakura Y, Abe K, Muroya K, et al. Combined Growth Hormone and Thyroid-Stimulating Hormone Deficiency in a Japanese Patient with a Novel Frameshift Mutation in IGSF1. *Horm Res Paediatr*. 2015.

177. Walters DK, Arendt BK, Jelinek DF. CD147 regulates the expression of MCT1 and lactate export in multiple myeloma cells. *Cell Cycle*. 2013;12(19):3175-3183. doi:10.4161/cc.26193.

178. Castorino JJ, Deborde S, Deora A, et al. Basolateral Sorting Signals Regulating Tissue-Specific Polarity of Heteromeric Monocarboxylate Transporters in Epithelia. *Traffic*. 2011;12(4):483-498. doi:10.1111/j.1600-0854.2010.01155.x.

179. Deora A a, Philp N, Hu J, Bok D, Rodriguez-Boulan E. Mechanisms regulating tissue-specific polarity of monocarboxylate transporters and their chaperone CD147 in kidney and retinal epithelia. *Proc Natl Acad Sci U S A*. 2005;102(45):16245-16250. doi:10.1073/pnas.0504419102.

180. Heuer H, Schäfer MKH, O'Donnell D, Walker P, Bauer K. Expression of thyrotropin-releasing hormone receptor 2 (TRH-R2) in the central nervous system of rats. *J Comp Neurol*. 2000;428(2):319-336. doi:10.1002/1096-9861(20001211)428:2<319::AID-CNE10>3.0.CO;2-9.

181. Bustin S a. Absolute quantification of mrna using real-time reverse transcription polymerase chain reaction assays. *J Mol Endocrinol*. 2000;25(2):169-193. doi:JME00927 [pii].

182. Ferrara AM, Liao XH, Gil-Ibáñez P, et al. Changes in thyroid status during perinatal development of MCT8-deficient male mice. *Endocrinology*. 2013;154(7):2533-2541. doi:10.1210/en.2012-2031.

183. Obregon MJ, Pascual a., Morreale De Escobar G, Escobar Del Rey F. Pituitary and plasma thyrotropin, thyroxine, and triiodothyronine after hyperthyroidism. *Endocrinology*. 1979;104(5):1467-1473.

184. Pohlenz J, Maqueem a, Cua K, Weiss RE, Van Sande J, Refetoff S. Improved radioimmunoassay for measurement of mouse thyrotropin in serum: strain differences in thyrotropin concentration and thyrotroph sensitivity to thyroid hormone. *Thyroid*. 1999;9(12):1265-1271. doi:10.1089/thy.1999.9.1265.

185. Van Der Deure WM, Peeters RP, Visser TJ. Molecular aspects of thyroid hormone transporters, including MCT8, MCT10, and OATPs, and the effects of genetic variation in these transporters. *J Mol Endocrinol*. 2010;44(1):1-11. doi:10.1677/JME-09-0042.

186. Joustra SD, Meijer OC, Heinen C, et al. Spatial and temporal expression of immunoglobulin superfamily member 1 (IGSF1) in the rat. *J Endocrinol* . July 2015. doi:10.1530/JOE-15-0204.

187. Choi J, Moskalik C, Ng A, Matter SF, Buchholz DR. Regulation of thyroid hormone-induced development in vivo by thyroid hormone transporters and cytosolic binding proteins. *Gen Comp Endocrinol*. 2015;3. doi:10.1016/j.ygcen.2015.07.006.

188. Trajkovic M, Visser T, Mittag J. Abnormal thyroid hormone metabolism in mice lacking the monocarboxylate transporter 8. *J Clin Invest*. 2007;117(3):627-635. doi:10.1172/JCI28253.A.

189. Orci L, Tagaya M, Amherdt M, et al. Brefeldin A, a drug that blocks secretion, prevents the assembly of non-clathrin-coated buds on golgi cisternae. *Cell*. 1991;64(6):1183-1195. doi:10.1016/0092-8674(91)90273-2.

190. Lippincott-Schwartz J, Snapp E, Kenworthy a. Studying protein dynamics in living cells. *Nat Rev Mol Cell Biol*. 2001;2(6):444-456. doi:10.1038/35073068.

191. Herrick-Davis K, Weaver B a., Grinde E, Mazurkiewicz JE. Serotonin 5-HT2C Receptor Homodimer Biogenesis in the Endoplasmic Reticulum: REAL-TIME VISUALIZATION WITH CONFOCAL FLUORESCENCE RESONANCE ENERGY TRANSFER. *J Biol Chem*. 2006;281(37):27109-27116. doi:10.1074/jbc.M604390200.

192. Friesema ECH, Jansen J, Jachtenberg J-W, Visser WE, Kester MH a, Visser TJ. Effective cellular uptake and efflux of thyroid hormone by human monocarboxylate transporter 10. *Mol Endocrinol*. 2008;22(6):1357-1369. doi:10.1210/me.2007-0112.

193. Monnot AD, Zheng W. Culture of choroid plexus epithelial cells and in vitro model of blood-CSF barrier. *Methods Mol Biol*. 2013;945:13-29. doi:10.1007/978-1-62703-125-7.

194. Menheniott TR, Charalambous M, Ward A. Derivation of Primary Choroid Plexus Epithelial Cells from the Mouse. *Methods Mol Biol*. 2010;633:207-220. doi:10.1007/978-1-59745-019-5.

195. Boassa D, Stamer WD, Yool a. J. Ion Channel Function of Aquaporin-1 Natively Expressed in Choroid Plexus. *J Neurosci*. 2006;26(30):7811-7819. doi:10.1523/JNEUROSCI.0525-06.2006.

196. Gottardi CJ, Caplan MJ. Cell surface biotinylation in the determination of epithelial membrane polarity. *J Tissue Cult Methods*. 1992;14:173-180.

197. Gottardi CJ, Dunbar L a, Caplan MJ. Biotinylation and assessment of membrane polarity: caveats and methodological concerns. *Am J Physiol*. 1995;268(2 Pt 2):F285-F295.

198. Bargi-Souza P, Kucka M, Bjelobaba I, et al. Loss of Basal and TRH-Stimulated Tshb Expression in Dispersed Pituitary Cells. *Endocrinology*. 2015;156(1):242-254. doi:10.1210/en.2014-1281.

199. Sander JD, Joung JK. CRISPR-Cas systems for editing, regulating and targeting genomes. *Nat Biotechnol*. 2014;32(4):347-355. doi:10.1038/nbt.2842.

200. Ran F, Hsu P, Wright J, Agarwala V. Genome engineering using the CRISPR-Cas9 system. *Nat Protoc*. 2013;8(11):2281-2308. doi:10.1038/nprot.2013.143.

201. Wittmann G, Füzesi T, Singru PS, Liposits Z, Lechan RM, Fekete C. Efferent projections of thyrotropin-releasing hormone-synthesizing neurons residing in the anterior parvocellular subdivision of the hypothalamic paraventricular nucleus. *J Comp Neurol*. 2009;330(December 2008):NA - NA. doi:10.1002/cne.22017.

202. Pardridge WM. Carrier-mediated transport of thyroid hormones through the blood-brain barrier: primary role of albumin-bound hormone. *Endocrinology*. 1979;105(3):605-612.

203. Pardridge WM, Mietus LJ. Influx of Thyroid Hormones into Rat Liver In Vivo - Differential availability of thyroxine and triiodothyronine bound by plasma proteins. *J Clin Invest*. 1980;66:367-374.

204. Christoffolete M a., Ribeiro R, Singru P, et al. Atypical Expression of Type 2 Iodothyronine Deiodinase in Thyrotrophs Explains the Thyroxine-Mediated Pituitary Thyrotropin Feedback Mechanism. *Endocrinology*. 2006;147(4):1735-1743. doi:10.1210/en.2005-1300.

205. Japón M a, Rubinstein M, Low MJ. In situ hybridization analysis of anterior pituitary hormone gene expression during fetal mouse development. *J Histochem Cytochem*. 1994;42(8):1117-1125.

206. Haugen BR, Brown NS, Wood WM, Gordon DF, Ridgway EC. The thyrotrope-restricted isoform of the retinoid-X-receptor-gamma1 mediates 9-cis-retinoic acid suppression of thyrotropin-b promoter activity. *Mol Endocrinol*. 1997;11(September):481-489.

207. Macoritto M, Nguyen-Yamamoto L, Huang DC, et al. Phosphorylation of the Human Retinoid X Receptor at Serine 260 Impairs Coactivator(s) Recruitment and Induces Hormone Resistance to Multiple Ligands. *J Biol Chem*. 2008;283(8):4943-4956. doi:10.1074/jbc.M707517200.

208. Rochette-Egly C, Oulad-Abdelghani M, Staub a, et al. Phosphorylation of the retinoic acid receptor-alpha by protein kinase A. *Mol Endocrinol*. 1995;9(7):860-871. doi:10.1210/me.9.7.860.

209. Hobert O. Gene regulation by transcription factors and microRNAs. *Science*. 2008;319(5871):1785-1786. doi:10.1126/science.1151651.

210. Iype T, Francis J, Garmey JC, et al. Mechanism of insulin Gene Regulation by the Pancreatic Transcription Factor Pdx-1: APPLICATION OF PRE-mRNA ANALYSIS AND CHROMATIN IMMUNOPRECIPITATION TO ASSESS FORMATION OF FUNCTIONAL TRANSCRIPTIONAL COMPLEXES. *J Biol Chem*. 2005;280(17):16798-16807. doi:10.1074/jbc.M414381200.

211. Zeisel A, Kostler WJ, Molotski N, et al. Coupled pre-mRNA and mRNA dynamics unveil operational strategies underlying transcriptional responses to stimuli. *Mol Syst Biol*. 2014;7(1):529-529. doi:10.1038/msb.2011.62.

212. Palmero S, de Marchis M, Gallo G, Fugassa E. Thyroid hormone affects the development of Sertoli cell function in the rat. *J Endocrinol*. 1989;123(1):105-111.

213. Wagner MS, Wajner SM, Maia AL. Is there a role for thyroid hormone on spermatogenesis? *Microsc Res Tech*. 2009;72(11):796-808. doi:10.1002/jemt.20759.

214. Joustra SD, Roelfsema F, Endert E, et al. Pituitary Hormone Secretion Profiles in IGSF1 Deficiency Syndrome. *Neuroendocrinology*. 2015:1-24. doi:10.1159/000439433.

215. Rettori V, Milenkovic L, Fahim a M, Polak J, Bloom SR, McCann SM. Role of neuromedin B in the control of the release of thyrotropin in the rat. *Proc Natl Acad Sci U S A*. 1989;86(12):4789-4792. doi:10.1073/pnas.86.12.4789.

216. Oliveira KJ. Disruption of neuromedin B receptor gene results in dysregulation of the pituitary-thyroid axis. *J Mol Endocrinol*. 2006;36(1):73-80. doi:10.1677/jme.1.01892.

217. De Greef WJ, Neill JD. Dopamine levels in hypophysial stalk plasma of the rat during surges of prolactin secretion induced by cervical stimulation. *Endocrinology*. 1979;105(5):1093-1099. doi:10.1210/endo-105-5-1093.

218. Visser TJ, Klootwijk W, Docter R, Hennemann G. A new radioimmunoassay of thyrotropin-releasing hormone. *FEBS Lett*. 1977;83(1):37-40.

219. Rondeel JMM, De Greef WJ, Van Der Schoot P, Karels B, Klootwijk W, Visser TJ. Effect of thyroid status and paraventricular area lesions on the release of thyrotropin-releasing hormone and catecholamines into hypophysial portal blood. *Endocrinology*. 1988;123(1):523-527.

220. Gibbs DM, Neill JD. Dopamine levels in hypophysial stalk blood in the rat are sufficient to inhibit prolactin secretion in vivo. *Endocrinology*. 1978;102(6):1895-1900. http://www.ncbi.nlm.nih.gov/entrez/query.fcgi?cmd=Retrieve&db=PubMed&dopt=Citation&list_uids=570492.

221. Oliver C, Mical RS, Porter JC. Hypothalamic-pituitary vasculature: evidence for retrograde blood flow in the pituitary stalk. *Endocrinology*. 1977;101(2):598-604. doi:10.1210/endo-101-2-598.

222. Kottegoda S, Shaik I, Shippy S a. Demonstration of low flow push-pull perfusion. *J Neurosci Methods*. 2002;121:93-101. doi:10.1016/S0165-0270(02)00245-5.

223. Mantyh PW, Hunt SP. Thyrotropin-releasing hormone (TRH) receptors - Localization by light microscopic autoradiography in rat brain using [3H][3-Me-His2]TRH as the radioligand. *J Neurosci*. 1985;5(2):551-561.

224. De Escobar GM, Obregón MJ, del Rey FE. Maternal thyroid hormones early in pregnancy and fetal brain development. *Best Pract Res Clin Endocrinol Metab*. 2004;18(2):225-248. doi:10.1016/j.beem.2004.03.012.

225. Astapova I, Vella KR, Ramadoss P, et al. The Nuclear Receptor Corepressor (NCoR) Controls Thyroid Hormone Sensitivity and the Set Point of the Hypothalamic-Pituitary-Thyroid Axis. *Mol Endocrinol*. 2011;25(2):212-224. doi:10.1210/me.2010-0462.

226. Yoshikawa N, Nishikawa M, Horimoto M, Uno C, Taniguchi N, Inada M. Activity of thyroid stimulating antibody and thyroid stimulation blocking antibody determined by radioiodine uptake into FRTL-5 cells. *Endocrinol Jpn*. 1989;36(1):55-63.

227. Villalobos C, Núñez L, García-Sancho J. Anterior pituitary thyrotropes are multifunctional cells. *Am J Physiol Endocrinol Metab*. 2004;287(6):E1166-E1170. doi:10.1152/ajpendo.00194.2004.

228. Fortin J, Boehm U, Deng C-X, Treier M, Bernard DJ. Follicle-stimulating hormone synthesis and fertility depend on SMAD4 and FOXL2. *FASEB J*. 2014;28(8):3396-3410. doi:10.1096/fj.14-249532.

229. Birnbaum K, Jung JW, Wang JY, et al. Cell type-specific expression profiling in plants via cell sorting of protoplasts from fluorescent reporter lines. *Nat Methods*. 2005;2(8):615-619. doi:10.1038/nmeth0805-615.

230. Castinetti F, Brinkmeier ML, Gordon DF, et al. PITX2 AND PITX1 regulate thyrotroph function and response to hypothyroidism. *Mol Endocrinol*. 2011;25(11):1950-1960. doi:10.1210/me.2010-0388.

231. Srinivas S, Watanabe T, Lin CS, et al. Cre reporter strains produced by targeted insertion of EYFP and ECFP into the ROSA26 locus. *BMC Dev Biol*. 2001;1:4. doi:10.1186/1471-213X-1-4.

232. Wang Z, Gerstein M, Snyder M. RNA-Seq: a revolutionary tool for transcriptomics. *Nat Rev Genet*. 2009;10(1):57-63. doi:10.1038/nrg2484.

233. Mortazavi A, Williams B a, McCue K, Schaeffer L, Wold B. Mapping and quantifying mammalian transcriptomes by RNA-Seq. *Nat Methods*. 2008;5(7):621-628. doi:10.1038/nmeth.1226.

234. Gafken PR, Lampe PD. Methodologies for characterizing phosphoproteins by mass spectrometry. *Cell Commun Adhes*. 2006;13(5-6):249-262.

235. Villén J, Beausoleil S a, Gerber S a, Gygi SP. Large-scale phosphorylation analysis of mouse liver. *Proc Natl Acad Sci U S A*. 2007;104(5):1488-1493. doi:10.1073/pnas.0609836104.

236. Barrow AD, Raynal N, Andersen TL, et al. OSCAR is a collagen receptor that costimulates osteoclastogenesis in DAP12-deficient humans and mice. *J Clin Invest*. 2011;121(9):3505-3516. doi:10.1172/JCI45913DS1.

237. Ishikawa S, Arase N, Suenaga T, et al. Involvement of FcR-gamma in signal transduction of osteoclast-associated receptor (OSCAR). *Int Immunol*. 2004;16(7):1019-1025. doi:10.1093/intimm/dxh103.

238. Thingholm TE, Jørgensen TJD, Jensen ON, Larsen MR. Highly selective enrichment of phosphorylated peptides using titanium dioxide. *Nat Protoc*. 2006;1(4):1929-1935. doi:10.1038/nprot.2006.185.

239. Olsen J V., Blagoev B, Gnad F, et al. Global, In Vivo, and Site-Specific Phosphorylation Dynamics in Signaling Networks. *Cell*. 2006;127(3):635-648. doi:10.1016/j.cell.2006.09.026.

240. Gronowskis AM, Rotweins P. Rapid Changes in Nuclear Protein Tyrosine Phosphorylation after Growth Hormone Treatment in vivo. *J Biol Chem*. 1994;269(11):7874-7878.

241. Ibarrola N, Kalume DE, Gronborg M, Iwahori a, Pandey a. A proteomic approach for quantitation of phosphorylation using stable isotope labelling in cell culture. *Anal Chem*. 2003;75(22):6043-6049. C:\documents and settings\phains\my documents\journals\AnalChem_75_6043-6049.pdf.

242. Fields S, Song O. A novel genetic system to detect protein-protein interactions. *Nature*. 1989;340(6230):245-246. doi:10.1038/340245a0.

243. Gietz RD, Triggs-Raine B, Robbins A, Graham KC, Woods R a. Identification of proteins that interact with a protein of interest: Applications of the yeast two-hybrid system. *Mol Cell Biochem*. 1997;172(1-2):67-79. doi:10.1023/A:1006859319926.

244. Joung JK, Ramm EI, Pabo CO. A bacterial two-hybrid selection system for studying protein-DNA and protein-protein interactions. *Proc Natl Acad Sci U S A*. 2000;97(13):7382-7387. doi:10.1073/pnas.110149297.

245. Chen Y-C, Rajagopala SV, Stellberger T, Uetz P. Exhaustive benchmarking of the yeast two-hybrid system. *Nat Methods*. 2010;7(9):667-668. doi:10.1038/nmeth0910-667.

246. Rigaut G, Shevchenko a, Rutz B, Wilm M, Mann M, Séraphin B. A generic protein purification method for protein complex characterization and proteome exploration. *Nat Biotechnol*. 1999;17(10):1030-1032. doi:10.1038/13732.

247. Puig O, Caspary F, Rigaut G, et al. The Tandem Affinity Purification (TAP) Method: A General Procedure of Protein Complex Purification. *Methods*. 2001;24(3):218-229. doi:10.1006/meth.2001.1183.

248. Inui M, Miyado M, Igarashi M, et al. Rapid generation of mouse models with defined point mutations by the CRISPR/Cas9 system. *Sci Rep*. 2014;4:5396. doi:10.1038/srep05396.

249. Cong L, Ran F, Cox D, Lin S, Barretto R. Multiplex Genome Engineering Using CRISPR / Cas Systems. *Science (80-)*. 2013;819(January). doi:10.1038/nbt1319.

250. Wang H, Yang H, Shivalila CS, et al. One-step generation of mice carrying mutations in multiple genes by CRISPR/cas-mediated genome engineering. *Cell*. 2013;153(4):910-918. doi:10.1016/j.cell.2013.04.025.

251. Denef C. Paracrinicity: the story of 30 years of cellular pituitary crosstalk. *J Neuroendocrinol*. 2008;20(1):1-70. doi:10.1111/j.1365-2826.2007.01616.x.

252. Baron M. An overview of the Notch signalling pathway. *Semin Cell Dev Biol*. 2003;14(2):113-119. doi:10.1016/S1084-9521(02)00179-9.

253. Kopan R, Ilagan MXG. The Canonical Notch Signaling Pathway: Unfolding the Activation Mechanism. *Cell*. 2009;137(2):216-233. doi:10.1016/j.cell.2009.03.045.

254. Brossier F, Jewett TJ, Sibley LD, Urban S. A spatially localized rhomboid protease cleaves cell surface adhesins essential for invasion by Toxoplasma. *Proc Natl Acad Sci U S A*. 2005;102(11):4146-4151. doi:10.1073/pnas.0407918102.

255. Urban S. Rhomboid proteins: Conserved membrane proteases with divergent biological functions. *Genes Dev*. 2006;20(22):3054-3068. doi:10.1101/gad.1488606.